UNIVERSIDADE FEDERAL DE SANTA CATARINA
PROGRAMA DE PÓS-GRADUAÇÃO EM ENGENHARIA
DE AUTOMAÇÃO E SISTEMAS

Vitor Mateus Moraes

DELAY-DEPENDENT OUTPUT FEEDBACK
COMPENSATORS FOR A CLASS OF NETWORKED
CONTROL SYSTEMS

Florianópolis

2014

Vitor Mateus Moraes

DELAY-DEPENDENT OUTPUT FEEDBACK COMPENSATORS FOR A CLASS OF NETWORKED CONTROL SYSTEMS

A Thesis submitted to the Departament of Automation and Systems Engineering in partial fulfillment of the requirements for the degree of Doctor of Philosophy in Automation and Systems Engineering.
Supervisor: Dr. Eugênio de Bona Castelan Neto
Co-Supervisor: Dr. Ubirajara Franco Moreno

Florianópolis

2014

ABSTRACT

Networked control system (NCS) is a special class of sampled-data system where control systems devices are interconnected through a communication network. Despite the advantages, such as lower cost, flexibility and easy of maintenance compared to a more traditional implementation, some undesired effects may be induced by the use of a shared medium in the feedback loop, for instance, time-varying sampling intervals and delays.

Due to the multidisciplinary nature of an NCS, the analysis and design of such systems also demand a more comprehensive approach. Thus, the main objective of this thesis is to propose some strategies for the synthesis of dynamic output feedback compensators, assuming an industrial network control system environment with temporal behavior features and requirements.

Throughout this document, the NCS is modeled considering unknown time-varying delays, which leads to an uncertain system representation, later overapproximated by a convex polytope with additional norm-bounded uncertainty. Based on parameter dependent Lyapunov functions, closed-loop stability conditions are provided, which can be verified in terms of feasibility of a set of linear matrix inequalities (LMIs). The control designs are then promptly derived from the stability conditions, leading to delay-dependent compensators.

Furthermore, an integrated control design and resource management strategy is proposed, taking into account the controller design while also addressing the shared nature of the communication network. This co-design strategy assumes that a supervisor task has the knowledge of all devices that access the network, as well as their allocated bandwidths. Numerical examples and simulations are provided to illustrate the effectiveness of the proposed design methodologies.

Keywords: networked control system, parameter-dependent output feedback, switching control, co-design strategy.

RESUMO EXPANDIDO

**COMPENSADORES DINÂMICOS DE SAÍDA
DEPENDENTES DE ATRASO PARA UMA CLASSE DE
SISTEMAS DE CONTROLE VIA REDE**

Palavras-chave: sistema de controle via rede, realimentação de saída dependente de parâmetro, controle comutado, estratégia para co-design.

Introdução

Sistemas de controle via rede (NCS, do inglês *Networked Control Systems*) são uma classe especial de sistemas amostrados digitalmente, nos quais os dispositivos do sistema de controle se comunicam através de uma rede de comunicação (como mostrado na Fig. I). Significantes avanços tecnológicos tem levado a um maior interesse tanto na utilização de NCS em ambiente industrial (MOYNE; TILBURY, 2007), quanto em pesquisas relacionadas ao assunto (HESPANHA; NAGHSHTABRIZI; XU, 2007; HEEMELS; WOUW, 2010; ZHANG; GAO; KAYNAK, 2013).

Algumas das vantagens oferecidas por tais sistemas, com relação a sistemas de controle tradicionais, compreendem menor custo de implementação, flexibilidade e facilidade de manutenção. Apesar disso, inerentemente alguns efeitos indesejados também podem ocorrer, tais como atrasos na comunicação e intervalos de amostragem variantes, ocasionando degradação no desempenho do sistema em malha fechada. Devido a esses efeitos, a análise de estabilidade e também o projeto de controladores para NCS tornam-se mais desafiadores (TANG; YU, 2007).

De modo geral, os estudos sobre NCS podem ser divididos em duas grandes áreas: *controle da rede* e *controle via rede* (GUPTA; CHOW, 2010). A primeira está mais interessada em proporcionar uma melhor qualidade no serviço de transmissão de dados realizado pela rede de comunicação, enquanto a segunda objetiva uma melhor qualidade do desempenho dos sistemas de controle sob determinadas condições induzidas pelos efeitos da utilização da rede.

Embora tipicamente tratadas de forma separada, recentemente alguns esforços têm sido empreendidos de modo a integrar algumas características de ambas as áreas em fase de projeto, as chamadas estratégias de *co-design* (TORNGREN et al., 2006). Uma abordagem integrada é necessária de modo a se obter uma maior compreensão do
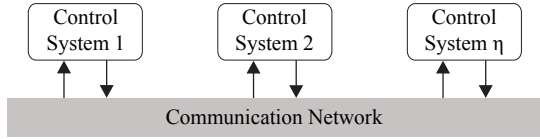
Figure I – Rede de comunicação compartilhada por diversos sistemas de controle.

funcionamento de um NCS, podendo assim obter um melhor desempenho geral do sistema.

Neste contexto, especialmente levando em consideração que o uso rede de comunicação é limitado, tal recurso deve ser corretamente distribuído entre os sistemas de controle de modo a garantir um funcionamento adequado. Além disso, requisitos de desempenho individuais de cada planta também devem ser cumpridos, mesmo sujeitos a tais restrições de limites de recursos.

Objetivos

O principal objetivo desta tese é propor algumas estratégias para síntese de compensadores dinâmicos de saída dependentes de parâmetro, assumindo um ambiente de implementação industrial com requerimentos e características de funcionamento que respeitem alguns requisitos temporais.

Neste escopo, uma importante motivação consiste no fato de que na prática nem sempre todos os estados da planta estão disponíveis para amostragem. Além disso, devido a multidisciplinaridade de um projeto de sistema de controle via rede, que tem como base teorias de controle e sistemas de tempo-real além de redes de comunicação, devem ser levados em consideração para obtenção de um desempenho adequado.

Como objetivos específicos, as estratégias apresentadas neste documento tem como próposito:

- investigar a utilização de informações referentes aos atrasos na estrutura do controlador;

- utilizar técnicas de projeto baseadas em ferramentas da teoria de controle robusto, híbrido e amostrado;

- delinear um projeto mais abrangente no que diz respeito à natureza multidisciplinar de um NCS.

Fundamentos Básicos

Nesta tese, considera-se como principal interesse a aplicação de NCS em ambiente industrial. Portanto, a utilização de redes de comunicação, que possam prover algumas características de sistemas de tempo-real (e.g., transmissão de dados confiáveis cumprindo com requisitos temporais (WITTENMARK; ÅSTRÖM; ÅRZÉN, 2002)), são requeridas. Alguns exemplos de redes industriais que satisfazem este requerimento são: Foundation Fieldbus, ControlNet, CAN, DeviceNet, TTP, entre outras.

De modo geral, considera-se a utilização de mensagens contendo estampas de tempo dos instantes de medição e atuação. Esta hipótese permite ao controlador utilizar o valor real dos atrasos para o cálculo do sinal de controle. Outrossim, a utilização de estimativas dos atrasos também é abordada a partir de uma extensão do modelo discretizado. No entanto, devido a incertezas nos modelos induzidas pelo atraso, em ambos os casos, representações politópicas adicionadas de uma incerteza por norma (HETEL; DAAFOUZ; IUNG, 2006) são utilizadas para efetivamente representar o sistema em tempo discreto durante as análises de estabilidade e projetos de controladores.

Ademais, uma outra extensão para o modelo também é apresentada, na qual são considerados múltiplos modos de operação com relaçao a taxa de amostragem, i.e., o sensor pode operar com diferentes intervalos de amostragem, comutando arbitrariamente entre eles.

Contribuições da Tese

Dentre as contribuições da pesquisa realizada, no Capítulo 3 é apresentado um método para síntese de compensador dinâmico de saída, dependente do atraso variante. Tal compensador assume a possibilidade de obtenção do valor real do atraso em tempo de execução. Partindo da utilização de uma função de Lyapunov dependente de parâmetro para definir uma condição de estabilidade para o sistema em malha fechada, obtém-se ferramentais baseados em desigualdades matriciais lineares, as quais são utilizadas para o projeto de controladores. Uma alternativa, para quando não há possiblidade da obtenção do valor real do atraso em tempo de execução, é discutida no Capítulo 4. Com uma modificação na modelagem do sistema em tempo discreto, é obtido então um método para projeto de compensadores dependentes de estimativas dos atrasos.
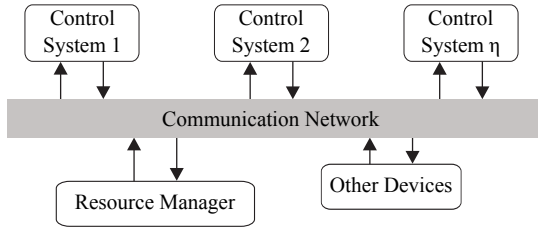
Figure II – NCS com acesso à rede controlado por um gerenciador de recursos (RM).

Além disso, uma extensão para estes métodos é proposta no capítulo 5, na qual assume-se que o sistema de controle pode funcionar com diversos valores diferentes de intervalos de amostragem, arbitrariamente comutando entre eles. Esta hipótese está relacionada com o compartilhamento da rede por diversos sistemas de controle e possivelmente outros dispositivos relacionados ao processo de produção, o que implica em eventuais alterações na largura de banda disponível ao sistema de controle. Embora apresentado como extensão ao compensador dependente do valor real do atraso, um procedimento similiar pode ser utilizado para a utilização de estimativas do atraso.

Complementarmente, no Capítulo 6 um projeto mais abrangente, com relação a multidisciplinaridade de um sistema de controle via rede, é considerado. Com base em uma restrição de utilização do recurso compartilhado e no projeto de compensadores comutados, uma estratégia integrada de síntese de controladores e gestão da rede é proposta. Assume-se a utilização de um gerenciador de recursos, vide Fig. II, que coordena o acesso à rede, e portanto pode controlar a distribuição de banda de acordo com alguma condição arbitrária.

Conclusão

Nesta tese, novas abordagens para projeto de compensadores dinâmicos de saída dependentes de parâmetro são apresentadas. Considera-se uma classe de sistemas de controle na qual o valor real do atraso variante, ou uma estimativa do atraso, pode ser obtida em tempo de execução, permitindo assim ao controlador a utilização dessa informação para o cálculo do sinal de controle.

Essencialmente, dois casos gerais são tratados. De início, apenas uma planta controlada via rede é considerada para análise de estabilidade

e síntese de controlador, assumindo certas condições de funcionamento proporcionadas pela rede de comunicação. Posteriormente, estende-se a ideia para um procedimento de projeto mais abrangente, considerando um conjunto de plantas e sistemas de controle compartilhando um recurso de comunicação limitado. Exemplos são apresentados ao longo do documento, de modo a ilustrar as técnicas propostas.

LIST OF FIGURES

LIST OF TABLES

ABBREVIATIONS

NOTATIONS

$\forall$	For all
$\in$	Included
$\mathcal{N}$	Set of natural numbers
$\Re$	Set of real numbers
$\Re^+$	Set of nonnegative real numbers
$\Re^n$	n-dimensional real vector space
$I\ (0)$	Identity (zero) matrix with appropriate dimension
$I_n\ (0_n)$	n-dimensional identity (zero) matrix
$A'\ (a')$	Transpose of a matrix (vector) $A\ (a)$
A^{-1}	Inverse of a matrix A
$\|A\|$	Euclidean norm of a matrix A
$A > B$	for two matrices, $A - B$ is positive definite
$A \geq B$	for two matrices, $A - B$ is positive semi-definite
$He(A)$	Hermitian matrix given by $A + A'$
diag$\{A, B\}$	Block diagonal matrix, with main diagonal blocks A and B
$*$	Symmetric block with respect to the main diagonal of a matrix
$(\bullet)$	Element that has no influence on the development

CONTENTS

1 INTRODUCTION

The technological advances, that have been occurring specially since the middle of the last century, led to a fast improvement in terms of computational tools, causing great impact in several fields, including process control engineering. Nowadays, most of the control systems exploit the usage of digital devices, which characterize the so-called sampled-data systems (sometimes, also known as computer-controlled systems). For this reason, the study and development of new theories and techniques for analysis and design of digital control systems are essential.

A sampled-data control system is distinguished by being composed of a continuous-time process (or plant), a sensor, an analog-to-digital converter device, a digital controller, a digital-to-analog converter device and an actuator. A simplified interpretation of this classical configuration is depicted in Fig. 1. Basically, in this sort of systems, the plant is periodically or sporadically sampled by the sensor and the controller use the provided sampled-data to compute a control signal to be applied to the plant by the actuator.
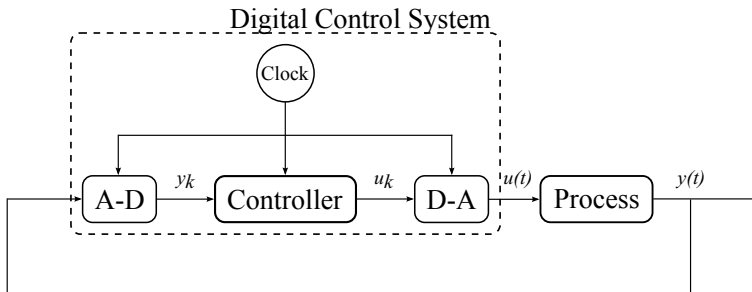
Figure 1 – Classical sampled-data control system.

Due to the hybrid nature of such a system, the stability analysis and control synthesis are more complex than those of continuous- or discrete-time systems. In this context, several approaches have been developed to deal with sampled-data control systems, such as (LAILA; NEŠIĆ; ASTOLFI, 2006):

***emulation*:** a control design is performed in continuous-time, and later the controller is discretized for digital implementation. Due to this approximation (discretization), this approach is typically valid

only for small sampling intervals. Advanced emulation techniques may be used for controller redesign, allowing larger sampling intervals.

discrete-time: a control design is performed using the discrete-time model of the plant, which typically exploit an approximation (discretization) of the continuous-time plant model. This method is usually less conservative than the previous one, in terms that it doesn't require fast sampling intervals to guarantee stability. Still, its implementation depends on a closed-loop performance analysis, once the inter-sampled behavior may be unacceptable.

Another significant improvement in terms of technology was the rise of communication networks, which, as well as it happened with digital devices, has been quickly introduced and is one of the technologies that most evolved recently in the field of industrial control (MOYNE; TILBURY, 2007). The so-called Networked Control System (NCS) is a system characterized by the interconnection among control system devices through a communication network, i.e., the information among control system devices is exchanged using a communication network (GUPTA; CHOW, 2010).

It is important to highlight that the physical channel, used for transmission in the network, is typically shared among several control systems, as shown in Fig. 2, or even with other devices or tasks. This feature leads to some of the main advantages arising from the usage of such systems, such as ease of deployment and maintenance, flexibility, lower costs and increased management of the information flows (YANG, 2006).
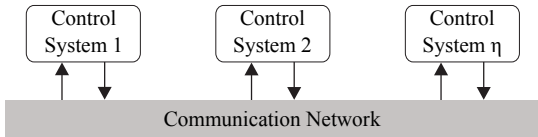
Figure 2 – Several NCS sharing a communication network.

Although the aforementioned benefits largely justify the usage of NCSs, the introduction of a communication network in the control loop may also bring some undesired effects, such as time-varying delays, uncertain sampling intervals and data losses. The occurrence of such issues may cause some performance degradation, occasionally leading

to stability loss, rendering the stability analysis and control design even more challenging (TANG; YU, 2007).

Due to these characteristics, industrial NCSs typically have as a requirement the usage of communication networks that can grant some real-time system features, e.g., data flow reliability within specific deadlines (WITTENMARK; ÅSTRÖM; ÅRZÉN, 2002). This means that the messages sent through the communication network can be properly scheduled using a deterministic Medium Access Control (MAC) protocol, as well as data losses are not likely to happen. Some examples of industrial networks that satisfy these requirements are: Foundation Fieldbus, ControlNet, CAN, DeviceNet, TTP, among others (HRISTU-VARSAKELIS; LEVINE, 2005).

Some issues related to NCSs may be handled by the improvement of communication and network technology. Still, it is also important to develop better control techniques that can deal with network induced undesired effects (MOYNE; TILBURY, 2007). Thus, in broader terms, researches related to NCSs can be categorized into the following two parts, which typically are handled separately by the scientific community (GUPTA; CHOW, 2010):

*control of network***:** study and research on communication and networks to make them suitable for real-time NCSs, dealing with routing control, congestion reduction, efficient data communication, networking protocol, etc,

*control over network***:** stability analysis and control synthesis strategies for NCSs aiming to minimize the effect of adverse network parameters on the system performance, such as network delays, packet losses, etc.

Basically, researches related to the *control of network* are more interested on medium access policies, improving the network Quality of Service (QoS), but not always verifying the impact of these modified strategies on the plant performances. On the other side, the *control over network* literature mainly deals with the Quality of Control (QoC) and, even considering some network effects, it is not usually concerned about how to guarantee some assumptions related to the communication network usage.

Although most of the work found in the literature follow this separation, recently some techniques have been proposed in the sense of integrating design, the so-called *co-design strategies* (TORNGREN et al., 2006), taking into account some aspects from both parts. This integrated approach perspective is required in order to have a better

understanding of the whole system, and thus definitely improve the overall performance, once the multidisciplinarity in networked control systems is actually related to at least three main scientific communities (see Fig. 3).
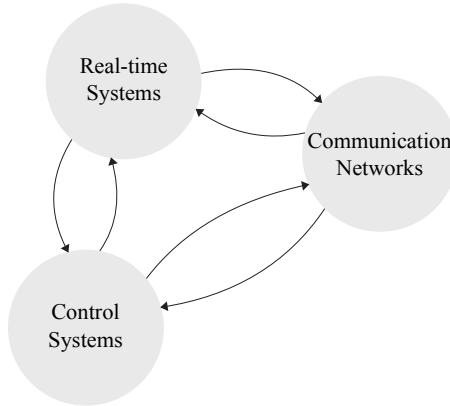
Figure 3 – Multidisciplinarity in networked control systems.

In this context, i.e., given a set of plants and controllers and shared resources (central processing unities and communication networks), two issues of interest are often investigated in the co-design literature (SALA et al., 2010):

- Given a required plant performance, obtain the lowest level of resource utilization needed;

- Given an allowable resource utilization level, obtain the best possible closed-loop performance.

Despite being different in a certain level, both of them are actually concerned that the shared resource should be optimally and efficiently used in order to obtain a suitable system performance. This is provided by an incorporation of the availability of the shared resources into the control system design by using the results of real-time scheduling theory.

Co-design strategies may also be distinguished by allowing (online strategies) or not (off-line strategies) some system parameters to be modified at runtime, according to an arbitrary rule. In this regard, although off-line methods can handle application requirements, they cannot easily deal with timing uncertainties due to, e.g., workload variation (BOUYSSOUNOUSE; SIFAKIS, 2005). Thus it can be useful to

consider a more dynamical solution, i.e., an online co-design strategy of feedback control and real-time scheduling.

To provide some QoC guarantee even in dynamic resource constrained environments, the control algorithms should be adapted for flexible scheduling of available resources, so that online tradeoffs between control performance and resources requirements are achieved (XIA; SUN, 2006; GUPTA; CHOW, 2010). Still, it is intuitive that an integrated off-line design of control algorithms (plant performance) and scheduling algorithms (shared resource management) is a prerequisite for online co-design of control and scheduling (ÅRZÉN et al., 1999).

1.1 OBJECTIVES

In the aforementioned context, the goal of this thesis is to provide strategies for the usage of dynamic output feedback compensators (DOFC) for a class of linear systems, assuming an industrial network control system environment. In this scope, a major motivation is that in practice not all plant states are always available for sampling, and also, due to the multidisciplinary nature of an NCS, some other features may have to be taken into account while designing such control systems.

As specific objectives, the strategies presented in this document intend to:

- investigate the use of delay information in the structure of the controller, somehow compensating their occurrence;

- use design techniques based on known tools from robust, hybrid and sampled-data control theories;

- outline a more comprehensive design, with respect to the multidisciplinary nature of an NCS.

1.2 RELATED WORKS

The increasing use of NCSs by the industry over the past years has also represented a continuous growth of interest of the academic community on the subject; see, for instance, the surveys Hespanha, Naghshtabrizi & Xu (2007), Heemels & Wouw (2010), Gupta & Chow (2010), Zhang, Gao & Kaynak (2013) and references therein.

Until recently, the studies on this subject have been mostly dealing with state-feedback control design and stability analysis, as in Hetel, Daafouz & lung (2007), Izák, Görges & Liu (2010), Moraes et al. (2010) and Cloosterman et al. (2010). Besides, more specifically with respect to the output feedback control synthesis for NCSs, several techniques may also be found in the literature, e.g., designing methods based on the use of state-observers considering continuous-time modeling of the plant and controller, which are mostly based on emulation techniques (MONTESTRUQUE; ANTSAKLIS, 2002; NAGHSHTABRIZI; HESPANHA, 2005; MAHMOUD, 2013).

Alternatively, static output feedback gain has been proposed, for instance, in: Weihua & Minrui (2009) and Yoo, Koo & Won (2010), both based on an emulation approach and with the first one also considering uncertain systems; Zhang, Lam & Xia (2014), based on a discrete-time approach with delay compensation using a set of possible gains; Zhang, Shi & Mehr (2011), also based on a discrete-time polytopic representation; and, Dritsas & Tzes (2007), where an approach based on a discretized model of the continuous-time plant is used, considering an uncertain delay, though the designing method is performed for a nominal situation.

Dynamic output feedback controllers have also been investigated, mostly assuming discrete-time plant models, as in Shi & Yu (2011), Rasool, Huang & Nguang (2012), Mahmoud & Khan (2013), Shi & Yu (2009), Rasool, Huang & Nguang (2011), and emulation approaches (GAO et al., 2010; JIANG et al., 2010), with some of them assuming quantized controllers. Still, it may be of relevant interest to have a more *sampled-data*-like approach, in the sense that the system behavior is studied when the digital control system interacts with a continuous-time plant. In this direction, using approaches based on an exact discretization of the plant, a stability analysis is provided in Donkers et al. (2009), whereas the synthesis of dynamic output feedback compensators is issued in Moraes, Castelan & Moreno (2011) and Moraes, Castelan & Moreno (2012), both based on Bilinear Matrix Inequalities (BMI) conditions.

Integrated control and scheduling design has also attracted some attention recently, mainly focusing on shared resource management and network induced effects compensations (YAN et al., 2011; SAUTER et al., 2013).

In this context, *event/self-triggered* control systems have been widely studied (HEEMELS; JOHANSSON; TABUADA, 2012), generally aiming to reduce the resource utilization, but typically taking into

account only the own particular performance, not looking neither to other systems performances nor to an overall resource utilization. These methods usually need a constant monitoring of the triggering condition.

Strategies considering a time-triggered implementation can also be found in the literature. In Cac & Khang (2014) a co-design strategy using dynamic priority medium access, based on the closed-loop error and control signal, is proposed. The authors also assumed a pole-placement state-feedback control, designed in order to compensate a known constant global delay.

A hybrid priority medium access is likewise proposed by Nguyen & Juanole (2012), but based only on the control signal, along with a PD controller design with an online delay compensation. In Velasco et al. (2004) an online bandwidth allocation strategy is presented, where the original state-space representation of each controlled process is augmented with a new state variable that describes the network dynamics. The state-feedback control law is then designed taking into account the variations in the assigned bandwidth, though without considering the network induced delays.

Also assuming a dynamic bandwidth allocation, in Al-Areqi, Görges & Liu (2011) an online periodic scheduler and state-feedback switched control is proposed, which is performed by a supervisor task that needs all plants measurements, whereas in Ji & Kim (2008) the procedure is performed at each controller based on a performance requirement related to the particular closed-loop error. The later strategy also assumes an adaptive switched controller based on a finite set of parameters used for a PID, and that each resource manager has the knowledge of all currently allocated bandwidth.

1.3 STRUCTURE OF THE THESIS

The structure of the thesis is as follows. Chapter 2 first gives some basic preliminaries on networked control systems, presenting required features and their consequences. Later in the same chapter, the modeling of plants controlled over a communication network is addressed, assuming several behavior patterns for the control system.

In Chapter 3, a synthesis of delay-dependent dynamic output feedback compensator is discussed, taken into account the possibility of acquiring information about the time-varying delays at runtime. An alternative to the compensator design presented in Chapter 3 is discussed in Chapter 4, where the time-varying delay is unknown but

it is assumed that an estimate can be computed and then used as a parameter for a DOFC.

In Chapter 5 an extended version of the compensator synthesis is addressed, where it is assumed that the control system may operate with several different sampling intervals, arbitrarily performing the switching between them at runtime. Although the discussion is presented with respect to the delay-dependent DOFC, a similar strategy can also be used for the DOFC based on delay estimates.

Chapter 6 deals with a more comprehensive control system design, taking into account the multidisciplinary nature of an NCS. A strategy of control and resource management co-design for a networked control systems is depicted, based on a resource utilization constraint and on the parameter-dependent compensators from early chapters. The proposed strategy assumes a resource manager task that has the knowledge of all devices that access the communication network, and thus, it can control the bandwidth distribution among them given some arbitrary conditions.

In Chapter 7 some conclusions and recommendations for future research are discussed. The appendices present some additional information about classical results that were used on the definition of the stability conditions, as well as on the compensator synthesis.

To conclude, the Annex A addresses a work that has been developed during an internship at Centre de Recherche en Automatique de Nancy (CRAN), which deals with a control and scheduling co-design approach for multiple control tasks running in a single processor. A major difference to the problems considered before in this document is the absence of the communication network and, in consequence, of time-varying delays. Hence, the co-design deals only with the sampling interval assignment.

2 NETWORKED CONTROL SYSTEMS: PRELIMINARIES AND MODELLING

As previously mentioned, Networked Control Systems (NCSs) are characterized by the interconnection among control system devices through a communication network (the exchange of information using messages sent through a shared network environment), which may provide benefits, but also some undesired effects that may lead to a performance degradation or even to instability (TANG; YU, 2007). Such undesired effects may comprise: time-varying delays between sampling and actuation instants due to the required time for the messages transmission; varying sampling intervals due to operating mode and/or communication protocol; and packet losses due to corrupted data and physical interference.

To deal with these issues in an industrial environment, due to the critical real-time requirements, the use of reliable communication networks with deterministic Medium Access Control (MAC) protocols are typically used (WITTENMARK; ÅSTRÖM; ÅRZÉN, 2002; HRISTU-VARSAKELIS; LEVINE, 2005). In such environments, packet losses are not likely to happen, and it is possible to guarantee message deadlines through an appropriate scheduling of the packets transmitted through the network (TINDELL; BURNS; WELLINGS, 1995).

It is important to note that, even though the use of a reliable network is able to afford part of the solution to the induced undesired effects, time-varying delays and sampling intervals may still occur. Fortunately, due to the specifications of industrial networks, both remaining issues are typically bounded and these bounds can be computed and used for control and scheduling design. Thus, in this chapter the general features, operating modes and mathematical models for a class of NCSs are described, as well as a brief example of a degradation effect caused by the time-varying delay.

2.1 GENERAL FEATURES AND OPERATING MODE

Some of the possible topologies used in NCSs are shown in Fig. 4. Note that sensor, actuator and controller are represented as independent devices in topologies 1 and 2, differently from the other ones where it is assumed that sensor (topology 3) or actuator (topology 4) has more processing capacity, running also the control task (or either the case

where the controller is physically deployed next to one or another, not being advantageous the use of the network). Note also that, in topology 2 there is only one processor responsible for running all control tasks.
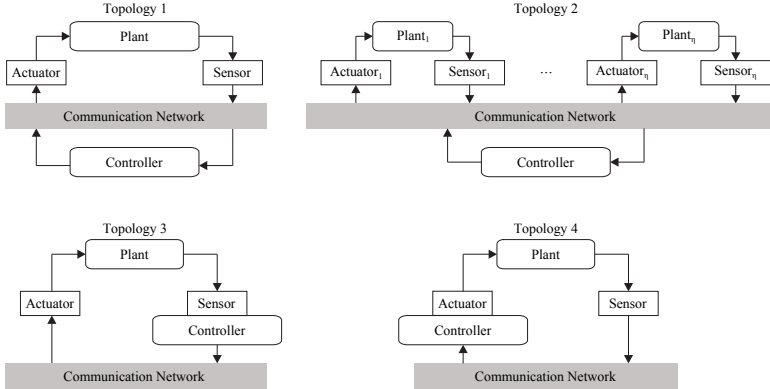
Figure 4 – Typical networked control system topologies.

Although any of these topologies may be used in an actual environment (and also in the strategies presented in this thesis), the most usually found in the literature (i.e., topology 1) is assumed in the course of this document to depict each particular networked control system. This topology is shown with more details in Fig. 5. The system is a hybrid one, once the plant is a continuous-time process and the control system devices are as follow: the sensor is modeled as an analog to digital sampler, the actuator behaves as a zero-order-holder, and the controller is implemented on a digital processor.

Reliable networks and deterministic MAC protocols are used, thus a time limit (*deadline*) can be guaranteed to the control task execution loop, i.e., data transmission and computation time (WITTENMARK; ÅSTRÖM; ÅRZÉN, 2002). Thereby, considering a deadline equal to the sampling interval, it leads to $\tau_k \in [\tau_{\min}, \tau_{\max}]$ $\forall k$, with $0 < \tau_{\min} < \tau_{\max} \leq T$, where τ_k is the time delay related to the k-th interval. This time delay is fundamentally comprised by the sum of three components: $\tau_k = \tau_{sc,k} + \tau_{cc,k} + \tau_{ca,k}$, where $\tau_{sc,k}$ is the sensor-to-controller delay, $\tau_{cc,k}$ is the control computation delay, and $\tau_{ca,k}$ is the control-to-actuator delay

Also in Fig. 5, the delay components with related packet flow (the dotted lines when present) are shown. Additionally, the packet flow from actuator to controller is related to an acknowledge message,
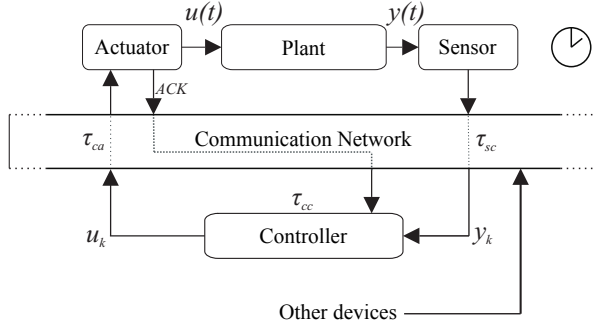
Figure 5 – Networked control system.

namely *ACK*. Recall that, due to the shared communication medium, the delays are time-varying.

When time-stamped messages are used, every sampling and/or actuation instant can be registered and reported to the controller. Thus, the controller may use these values to compute either the actual delay or a delay estimate, that occurred in a given sampling-actuation cycle. In this case, it is important to notice the need of clock synchronization among control system devices (NILSSON, 1998).

Given these specifications, the following general operating modes are considered for the control system devices (HETEL; DAAFOUZ; LUNG, 2007; MORAES et al., 2010):

sensor: the time-driven sensor samples the plant output at regular time intervals T, sending the acquired measurement to the controller. The packet may also include a time-stamp of the sampling instant;

actuator: the actuator is an event-driven zero-order-hold, updating the control signal applied to the plant when new messages sent from the controller are received. The actuator may also sends a message to the controller with the actuation time-stamp, denoted *ACK*;

controller: the controller is event-driven, computing and sending a control signal to the actuator as soon as a new message arrives from the sensor.

By using the described specifications and operating scheme, the controller can use the information provided by the time-stamped messages to compute the actual global delay between sampling and actua-

tion instants (or at least an estimated value). Thus, the time-stamped messages allow the use of the delay information, about the current discrete-time interval, to compute a control signal (delayed by at most one sampling interval, in the case of the actual delay value).

2.1.1 Time-varying Delays

As previously stated, even when reliable communication networks and deterministic MAC protocols are used, time delays may still occur between sampling and actuation instants. Moreover, if the network does not operate based on a policy of allocating time slots, the delay may be time-varying (see Fig. 6), due to waiting time while the network is being used by some other device.
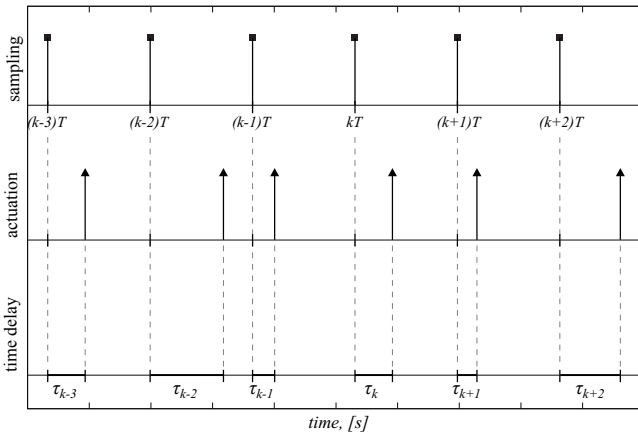
Figure 6 – Time-varying delays between sampling and actuation instants.

The presence of such delays in the closed-loop system may degrade performance, occasionally leading to instability (ZHANG; YU, 2008). For instance, consider a continuous linear time-invariant system, with dynamics given by:

$$\dot{x}(t) = Mx(t) + Nu(t)$$
$$y(t) = Cx(t)$$

where $x(t) \in \Re^n$ is the state vector, $u(t) \in \Re^m$ is the control signal

vector, $y(t) \in \Re^p$ is the output vector and

$$
M = \begin{bmatrix} 1.380 & -0.208 & 6.715 & -5.676 \\ -0.581 & -4.290 & 0 & 0.675 \\ 1.067 & 4.273 & -6.654 & 5.893 \\ 0.048 & 4.273 & 1.343 & -2.104 \end{bmatrix} , \ N = \begin{bmatrix} 0 & 0 \\ 5.679 & 0 \\ 1.136 & -3.146 \\ 1.136 & 0 \end{bmatrix} ,
$$

$$
C = \begin{bmatrix} 1 & 0 & 1 & -1 \\ 0 & 1 & 0 & 0 \end{bmatrix} .
$$

Assume also a discrete time dynamic output feedback compensator, designed without taking into consideration the incidence of time-varying delays (e.g., using a method similar to the one presented in Oliveira, Geromel & Bernussou (2002)):

$$
\zeta_{k+1} = \mathcal{A}\zeta_k + \mathcal{B}y_k
$$
$$
u_k = \mathcal{C}\zeta_k + \mathcal{D}y_k
$$

A sampling interval $T = 32$ms is used, leading to:

$$
\mathcal{A} = \begin{bmatrix} 1.8406 & -4.2316 & -0.5048 & -51.3761 \\ 0.2598 & -0.2111 & -0.1275 & -15.6328 \\ -0.2601 & -2.4998 & 0.3618 & 76.7154 \\ -0.0069 & -0.0113 & 0.0047 & 0.7953 \end{bmatrix} ,
$$

$$
\mathcal{B} = \begin{bmatrix} 102.0608 & 249.3843 \\ 36.0661 & 70.8705 \\ -140.2513 & -297.1810 \\ -1.5667 & -3.2646 \end{bmatrix} ,
$$

$$
\mathcal{C} = \begin{bmatrix} -0.0368 & 0.0801 & 0.0108 & 1.1243 \\ -0.0309 & 0.1849 & -0.0027 & -1.6802 \end{bmatrix} ,
$$

$$
\mathcal{D} = \begin{bmatrix} -2.2987 & -10.5439 \\ 12.7582 & 5.5118 \end{bmatrix} .
$$

The discrete-time closed-loop eigenvalues are: 0.9188, $0.8394 + 0.0488i$, $0.8394 - 0.0488i$, 0.8059, 0.0001, 0, 0 and 0, i.e., it is stable (a simulation of the closed-loop hybrid system without delays is shown in Fig. 7). Yet, when a communication network is used for the interconnection among control devices resulting in time-varying delays, there is a degradation of the system performance, as depicted in Fig. 8. The simulation of the closed-loop NCS with random time-varying delays was performed using the toolbox TrueTime (CERVIN et al., 2003a), with delay bounds: $\tau_{\min} = 1$ms and $\tau_{\max} = T$.
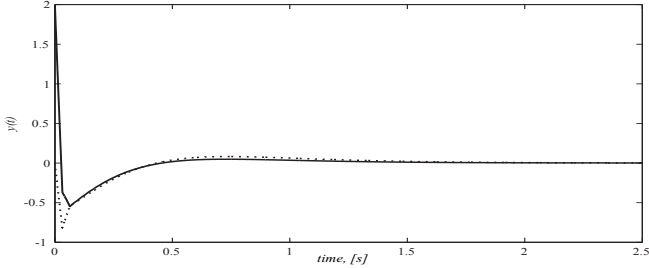
Figure 7 – Plant output without time-varying delays.
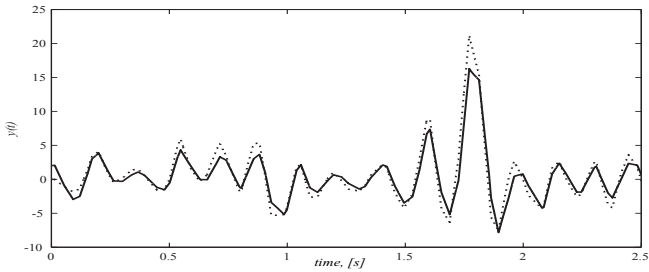
Figure 8 – Plant output with time-varying delays.

2.2 MODELING

First of all, recall that the reliable network is shared among multiple control devices and it uses a deterministic MAC protocol. Also, it is considered a topology where each controller is independent to any other, and therefore each one handles a single plant (see Fig. 5).

The plant is considered to be a continuous linear time-invariant system, with dynamics given by:

$$\begin{aligned} \dot{x}(t) &= Mx(t) + Nu(t) \\ y(t) &= Cx(t) \end{aligned} \tag{2.1}$$

where $x(t) \in \Re^n$ is the state vector, $u(t) \in \Re^m$ is the control signal vector, $y(t) \in \Re^p$ is the output vector, and $M \in \Re^{n \times n}$, $N \in \Re^{n \times m}$ and $C \in \Re^{p \times n}$ are the dynamic matrices.

Once the controller is digital, an exact discrete-time representation of the plant between two consecutive sampling instants, considering a zero-order-hold method, is used to model the system dynamics. Thus,
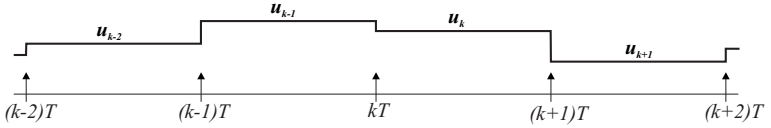
Figure 9 – Classical sampled-data control signal.
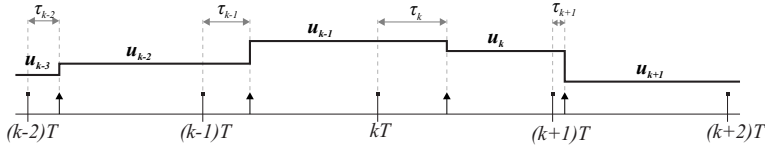
Figure 10 – Effect of time-varying delays on the control signal.

in contrast from the classic discretized model (Fig. 9):

$$x_{k+1} = Ax_k + Bu_k,$$
$$y_k = Cx_k,$$

where $A = e^{MT}$ and $B = \int_0^T e^{Ms} ds \ N$, for an NCS it is required to take into account the effect of time-varying delays on the control signal (see Fig. 10, where the arrows indicate the actuation instants), i.e., for $t \in [kT, (k+1)T]$, $k \in \mathcal{N}$:

$$u(t) = \begin{cases} u_{k-1}, & t \in \big[kT, kT + \tau_k\big) \\ u_k, & t \in \big[kT + \tau_k, (k+1)T\big) \end{cases} \tag{2.2}$$

which leads to (see Åström & Wittenmark (1997) for more details):

$$x_{k+1} = Ax_k + \tilde{\Gamma}(\tau_k)u_{k-1} + \Gamma(\tau_k)u_k$$
$$y_k = Cx_k \tag{2.3}$$

with delay-dependent matrices:

$$\Gamma(\tau_k) = \int_0^{T-\tau_k} e^{Ms} ds \ N,$$

$$\tilde{\Gamma}(\tau_k) = \int_{T-\tau_k}^{T} e^{Ms} ds \ N = B - \Gamma(\tau_k).$$

Notice that the delay dependent matrices in (2.3) are uncertain, once the delay is not constant. These uncertain matrices, $\Gamma(\tau_k)$ and $\tilde{\Gamma}(\tau_k)$, are not suitable for the use with known mathematical tools for analysis and control design. Thus, a reformulation is required.

A possible solution is to represent the uncertain matrices by convex polytopes, as in Cloosterman et al. (2006) where an approach based of the Jordan form is used to reformulate the discrete-time NCS models, or as in (GIELEN; OLARU; LAZAR, 2009) where the Cayley-Hamilton Theorem is used for such reformulation. Another possible method is to describe the uncertainty as a combination of a polytopic bounding with an additional uncertainty, which is described in the following section.

2.2.1 Polytopic Representation with Additional Norm-bounded Uncertainty

Recently, Heemels et al. (2010) presented a comparison review of some overapproximation methods to represent an uncertain discrete-time system, showing that mixed polytope with additional norm-bounded residual uncertainty approaches are generally less conservatives in terms of stability analysis. Among them, the Taylor Series Approximation (TSA) (HETEL; DAAFOUZ; IUNG, 2006) and the Gridding Approach (GA) (DONKERS et al., 2009) provided equivalent results. For both of them, a general equation is given by:

$$\Gamma(\tau_k) = \sum_{i=1}^{N_h} \mu_i(\tau_k)\Gamma_i + \Delta(\tau_k). \tag{2.4}$$

with $\sum_{i=1}^{N_h} \mu_i(\tau_k) = 1$, $\mu_i(\tau_k) \geq 0$.

While in the aforementioned methods the number of vertices is a design parameter, in Dritsas, Nikolakopoulos & Tzes (2007) a particular version of the formulation (2.4) is used, where it is assumed only one vertex based on a mean value of the uncertain matrix. In that case, however, the additional uncertainty has a larger bound, which leads to more conservative results.

Thus, in this thesis, the more general representation with N_h vertices has been chosen to describe the uncertain matrices. Specially, the TSA method is described in the following.

Thereby, rewriting the delay-dependent matix $\Gamma(\tau_k)$ in a Taylor

series expansion, gives (FRANKLIN; POWELL; WORKMAN, 1997):

$$\Gamma(\tau_k) = \int_0^{T-\tau_k} e^{Ms} ds \; N = \sum_{i=1}^{\infty} \frac{M^{i-1}}{i!}(T - \tau_k)^i N.$$

Next, considering an approximation order h:

$$\Gamma(\tau_k) = \sum_{i=1}^{h} \frac{M^{i-1}}{i!}(T - \tau_k)^i N + \Delta(\tau_k), \tag{2.5}$$

then the uncertain matrix can be rewritten as a convex polytope with additional norm-bounded uncertainty (HETEL; DAAFOUZ; IUNG, 2006):

$$\Gamma(\tau_k) = \sum_{i=1}^{N_h} \mu_i(\tau_k)\Gamma_i + \Delta(\tau_k), \tag{2.6}$$

with $\sum_{i=1}^{N_h} \mu_i(\tau_k) = 1$, $\mu_i(\tau_k) \geq 0$, $N_h = h + 1$.

The polytope vertices are given by:

$$\Gamma_i = \begin{bmatrix} \frac{M^{h-1}}{h!} & \cdots & \frac{M}{2!} & I \end{bmatrix} \phi_i N,$$

$\Gamma_i \in \Re^{n \times m}$, $\phi_i \in \Re^{hn \times n}$, $\forall i = 1, \ldots, h+1$, where:

$$\phi_1 = \begin{bmatrix} \underline{\alpha}^h I \\ \vdots \\ \underline{\alpha} I \end{bmatrix}, \quad \phi_2 = \begin{bmatrix} \underline{\alpha}^h I \\ \vdots \\ \bar{\alpha} I \end{bmatrix}, \quad \cdots, \quad \phi_{h+1} = \begin{bmatrix} \bar{\alpha}^h I \\ \vdots \\ \bar{\alpha} I \end{bmatrix},$$

with $\underline{\alpha} = T - \tau_{\max}$ and $\bar{\alpha} = T - \tau_{\min}$.

Since, by hypothesis, $\tau_{\min} < \tau_{\max}$, the weighting factors $\mu_i(\tau_k)$ can be obtained by solving the following nonsingular linear system, where $\alpha(\tau_k) = T - \tau_k$:

$$\begin{bmatrix} 1 & 1 & \cdots & 1 \\ \underline{\alpha} & \bar{\alpha} & \cdots & \bar{\alpha} \\ \vdots & \vdots & \ddots & \vdots \\ \underline{\alpha}^h & \underline{\alpha}^h & \cdots & \bar{\alpha}^h \end{bmatrix} \begin{bmatrix} \mu_1(\tau_k) \\ \mu_2(\tau_k) \\ \vdots \\ \mu_{(h+1)}(\tau_k) \end{bmatrix} = \begin{bmatrix} 1 \\ \alpha(\tau_k) \\ \vdots \\ \alpha^h(\tau_k) \end{bmatrix}.$$

For instance, using LU factorization leads to the following equations

that can be used for online computations:

$$\mu_1(\tau_k) = 1 - \frac{\alpha_k - \underline{\alpha}}{\bar{\alpha} - \underline{\alpha}},$$

$$\mu_i(\tau_k) = \frac{\alpha_k^{i-1} - \underline{\alpha}^{i-1}}{\bar{\alpha}^{i-1} - \underline{\alpha}^{i-1}} - \sum_{j=i+1}^{h+1} \mu_j(\tau_k), \ \ \forall i = 2, \ldots, h,$$

$$\mu_{h+1}(\tau_k) = \frac{\alpha_k^h - \underline{\alpha}^h}{\bar{\alpha}^h - \underline{\alpha}^h}.$$

The residual uncertainty $\Delta(\tau_k) \in \Re^{n \times m}$ is considered to be norm-bounded, i.e.:

$$\big\| \Delta(\tau_k) \big\| \ \leq \ \gamma. \tag{2.7}$$

An upper bound of γ, denoted by $\bar{\gamma}$, can be estimated off-line by applying a gridding approach using (2.5). Thus, by setting $\delta\tau = \frac{\tau_{max} - \tau_{min}}{\varrho}$, where $\varrho > 0$ is the considered number of subintervals in $\tau_\ell \in [\tau_{\min}, \tau_{\max}]$:

$$\tau_\ell = \tau_{\min} + \ell\delta\tau, \ \ \ell = 0, 1, \ldots, \varrho.$$

Then

$$\bar{\gamma} = \sup_{\tau_\ell \in [\tau_{\min}, \tau_{\max}]} \left\| \Gamma(\tau_\ell) - \sum_{i=1}^{h} \frac{M^{i-1}}{i!}(T - \tau_\ell)^i N \right\|. \tag{2.8}$$

This approach, together with the previously stated operating modes of the control system devices, allows to use a controller that can be dependent on the actual delay. Still, it may not be always possible to use time-stamped messages. Thus, a model that considers a delay estimate instead of the actual delay can be used, in which the estimation error may be included on the additional norm-bounded uncertainty.

2.2.2 Model with Delay Estimates

Suppose that is not possible to acquire the actual delay value at runtime, then the previous representation cannot be directly used. Alternatively, if it is possible to estimate the delay, the polytopic representation with additional norm-bounded uncertainty can be adapted. Thus, rewriting the uncertain matrix as a function of the delay estimates, $\hat{\tau}_k \in [0, T]$, gives:

$$\Gamma(\tau_k) = \Gamma(\hat{\tau}_k) + \Delta(\tau_k, \hat{\tau}_k),$$

with $\Gamma(\hat{\tau}_k) = \int_0^{T-\hat{\tau}_k} e^{Ms} ds\, N$, and $\Delta(\tau_k, \hat{\tau}_k)$ an additional uncertainty due to the estimation of the delay. Next, using the TSA leads to:

$$\Gamma(\tau_k) = \left(\sum_{i=1}^{N_h} \mu_i(\hat{\tau}_k) \Gamma_i + \Delta(\hat{\tau}_k) \right) + \Delta(\tau_k, \hat{\tau}_k). \qquad (2.9)$$

with $\sum_{i=1}^{N_h} \mu_i(\hat{\tau}_k) = 1$, $\mu_i(\hat{\tau}_k) \geq 0$.

The polytope vertices of (2.9) are given as before, yet it is important to recall that the delay estimates have to be used, instead of the actual delays, to evaluate the weighting factors when needed. Moreover, the resulting additional uncertainty is now a sum of uncertainties:

$$\Omega(\tau_k, \hat{\tau}_k) = \Delta(\hat{\tau}_k) + \Delta(\tau_k, \hat{\tau}_k).$$

Assuming that the estimation error is bounded $\delta_{\min} \leq \delta_{\tau_k} = \tau_k - \hat{\tau}_k \leq \delta_{\max}$, the overall uncertainty $\Omega(\tau_k, \hat{\tau}_k)$ can also be considered norm-bounded (HETEL et al., 2011):

$$\left\| \Omega(\tau_k, \hat{\tau}_k) \right\| \leq \gamma_\Omega. \qquad (2.10)$$

Thus, given the assumptions done on the bounds of τ_k, $\hat{\tau}_k$ and δ_{τ_k}, it is possible to estimate an upper bound, $\bar{\gamma}_\Omega$, using a gridding approach:

$$\bar{\gamma}_\Omega = \sup_{\substack{\tau_\ell \in [\tau_{\min}, \tau_{\max}] \\ \delta_{\tau_\ell} \in [\delta_{\min}, \delta_{\max}]}} \left\| \Gamma(\tau_\ell) - \sum_{i=1}^{h} \frac{M^{i-1}}{i!} (T - \hat{\tau}_\ell)^i N \right\|. \qquad (2.11)$$

Additionally, some methods for delay estimation can be found in Richard (2003), see also references therein. Specially, in the present work the delay estimation has been performed based on the actual sensor-to-controller delay, allowed through the use of time-stamped messages, added by a nominal control computation time and a nominal controller-to-actuator delay.

2.3 CONCLUSION

In this chapter general features and operating modes of a class of networked control systems have been presented, as well as mathematical models based on an exact discretization of the continuous linear time-invariant model at the sampling instants. It is assumed that the sensor behaves in a time-driven fashion and controller and actuator behave

in an event-driven fashion. Also, it is considered either the use of time-stamped messages or the possibility to estimate the delays at runtime.

In the next chapters, the described models are used for the designing of dynamic output feedback compensators, that are dependent on the actual time-varying delay (Chapter 3) or on a delay estimate (Chapter 4). Moreover, in Chapter 5 an extended model of the system is considered, where the sampling intervals are allowed to switch between pre-specified values. The latter case is also used in a control and scheduling co-design strategy for NCSs (Chapter 6).

3 DELAY-DEPENDENT DYNAMIC OUTPUT FEEDBACK COMPENSATOR

This chapter deals with a control design technique (MORAES; CASTELAN; MORENO, 2013) for the NCS model described in Chapter 2. It is important to emphasize that it is assumed the case of real-time control systems where it is highly desirable that no loss of information should happen. Thereby, in such systems, it is typical to use reliable network environments. In addition, once deterministic communication protocols are used, such a network also allows a correct scheduling of the messages sent over the shared medium access. Thus, only time-varying delays smaller than one sampling interval are considered.

Given this overall behavior, allied to the knowledge of some parameters provided by the usage of the communication network, it is possible to focus on the control synthesis for a particular plant controlled over a network (which has a general physical configuration depicted by topology 1 from Fig. 4 and shown again in Fig. 11).
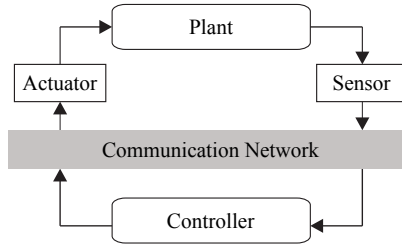
Figure 11 – Networked control system.

Differently from the state-feedback controller presented in Moraes et al. (2010), here, the controller only has access to the output of the plants, since in practice the full state is often not available for feedback. Moreover, the work presented in this chapter also differs from Moraes, Castelan & Moreno (2011) and Moraes, Castelan & Moreno (2012) mainly due to the compensator structure dependency on the time-varying delay parameter and due to the order of the considered compensator, allowing more degrees of freedom in terms of design parameters.

In this context, the aim here is to introduce a method for the synthesis of a full-order discrete-time dynamic output feedback compensator for NCS, based on the discretization of a linear continuous

time-invariant plant. Moreover, it is considered the clock synchroniza-
tion among the control system devices that, in addition to the use of
time-stamped messages, allows to implement a control law dependent
on the time-varying delay. The results are provided in terms of Lin-
ear Matrix Inequalities (LMIs), and some numerical experiments are
proposed to illustrate the applicability of the methodology.

3.1 PROBLEM FORMULATION

The plant model is the same one presented in section 2.2, where
the plant is considered to be a continuous linear time-invariant process,
described by:

$$\dot{x}(t) = Mx(t) + Nu(t)$$
$$y(t) = Cx(t) \tag{3.1}$$

with $x(t) \in \Re^n$, $u(t) \in \Re^m$, $y(t) \in \Re^p$, $M \in \Re^{n \times n}$, $N \in \Re^{n \times m}$ and
$C \in \Re^{p \times n}$, with $p < n$. The controller only has access to the values of
the output of the plant. Recall that this is important in practice, where
usually not all plant states are measurable.

The exact discrete-time representation of system (3.1) is obtained
by considering that the control input is delayed by τ_k, that is, for
$t \in [kT, (k+1)T]$:

$$u(t) = \begin{cases} u_{k-1}, & t \in [kT, kT + \tau_k) \\ u_k, & t \in [kT + \tau_k, (k+1)T) \end{cases}$$

which leads to the following representation (ÅSTRÖM; WITTENMARK,
1997):

$$x_{k+1} = Ax_k + \tilde{\Gamma}(\tau_k)u_{k-1} + \Gamma(\tau_k)u_k$$
$$y_k = Cx_k \tag{3.2}$$

where $A = e^{MT}$, $\Gamma(\tau_k) = \int_0^{T-\tau_k} e^{Ms}ds\ N$, $\tilde{\Gamma}(\tau_k) = \int_{T-\tau_k}^{T} e^{Ms}ds\ N =$
$B - \Gamma(\tau_k)$, with $B = \int_0^T e^{Ms}ds\ N$.

In order to use the actual information about the current time-
varying delay, which is computed after the reception of the ACK message,
it is necessary to apply a control law delayed by at most one sampling
interval. That is to say, the control signal u_k is computed using the
delay τ_{k-1} and applied to the plant at the instant $kT + \tau_k$. Thus, the

discrete-time representation is reformulated defining an extended state vector $\bar{x}_k = \begin{bmatrix} x'_k & u'_{k-1} & u'_k \end{bmatrix}' \in \Re^l$, with $l = n + 2m$, which leads to:

$$\bar{x}_{k+1} = \bar{A}(\tau_k)\bar{x}_k + \bar{B}u_{k+1}$$
$$y_k = \bar{C}\bar{x}_k \tag{3.3}$$

where $\bar{B} = \begin{bmatrix} 0_{m \times n} & 0_m & I_m \end{bmatrix}'$, $\bar{C} = \begin{bmatrix} C & 0_m & 0_m \end{bmatrix}$ and

$$\bar{A}(\tau_k) = \begin{bmatrix} A & B - \Gamma(\tau_k) & \Gamma(\tau_k) \\ 0_{m \times n} & 0_m & I_m \\ 0_{m \times n} & 0_m & 0_m \end{bmatrix}. \tag{3.4}$$

Since (3.3) has uncertain matrices, due to the time-varying delay, it cannot be directly used for control design purpose. Thus, the polytopic representation with additional norm-bounded uncertainty, presented in section 2.2.1, is used:

$$\Gamma(\tau_k) = \sum_{i=1}^{N_h} \mu_i(\tau_k)\Gamma_i + \Delta(\tau_k), \tag{3.5}$$

for which the polytope vertices, Γ_i, and an upper bound

$$\left\| \Delta(\tau_k) \right\| \leq \gamma \tag{3.6}$$

are given as described in section 2.2.1.

In the sequel, it is considered the use of a dynamic output feedback compensator with full-order $l = n + 2m$, that is dependent on the parameter τ_k, given by:

$$\zeta_{k+1} = \mathcal{A}(\tau_k)\zeta_k + \mathcal{B}(\tau_k)y_k$$
$$u_{k+1} = \mathcal{C}(\tau_k)\zeta_k + \mathcal{D}(\tau_k)y_k \tag{3.7}$$

with $\zeta_k \in \Re^l$, $\mathcal{A}(\tau_k) \in \Re^{l \times l}$, $\mathcal{B}(\tau_k) \in \Re^{l \times p}$, $\mathcal{C}(\tau_k) \in \Re^{m \times l}$, $\mathcal{D}(\tau_k) \in \Re^{m \times p}$.

The polytopic structure can also be used on the delay dependent matrices of the compensator (3.7), thus:

$$\begin{bmatrix} \mathcal{A}(\tau_k) & \mathcal{B}(\tau_k) \\ \mathcal{C}(\tau_k) & \mathcal{D}(\tau_k) \end{bmatrix} = \sum_{i=1}^{N_h} \mu_i(\tau_k) \begin{bmatrix} \mathcal{A}_i & \mathcal{B}_i \\ \mathcal{C}_i & \mathcal{D}_i \end{bmatrix},$$

with $\mathcal{A}_i \in \Re^{l \times l}$, $\mathcal{B}_i \in \Re^{l \times p}$, $\mathcal{C}_i \in \Re^{m \times l}$, $\mathcal{D}_i \in \Re^{m \times p}$.

Problem 3.1 *Design a full-order dynamic output feedback compensator, that guarantees asymptotic stability and some time performance for the closed-loop networked control system, i.e., the feedback networked interconnection of system (3.3) with (3.7).*

Similar problems have been considered in Moraes, Castelan & Moreno (2011) and in Moraes, Castelan & Moreno (2012), but using compensators with an order equal to the order of the plant. An inconvenience on those approaches is the use of bilinear matrix inequality conditions for the controller synthesis, whereas here LMI conditions are derived. More details can be found in the cited references.

3.2 CLOSED-LOOP STABILITY

Defining an auxiliary extended variable $z_k = [\bar{x}'_k \quad \zeta'_k]' \in \Re^{2l}$, a closed-loop representation is given by:

$$z_{k+1} = H(\tau_k)z_k + E\Delta(\tau_k)Dz_k \tag{3.8}$$

where $E = \begin{bmatrix} I_n & 0_{n\times m} & 0_{n\times m} & 0_{n\times l} \end{bmatrix}'$, $D = \begin{bmatrix} 0_{m\times n} & -I_m & I_m & 0_{m\times l} \end{bmatrix}$, $H(\tau_k) = \sum_{i=1}^{N_h} \mu_i(\tau_k)H_i$, and

$$H_i = \begin{bmatrix} \bar{A}_i + \bar{B}\mathcal{D}_i\bar{C} & \bar{B}\mathcal{C}_i \\ \mathcal{B}_i\bar{C} & \mathcal{A}_i \end{bmatrix},$$

with, from (3.4) and (3.5):

$$\bar{A}_i = \begin{bmatrix} A & B - \Gamma_i & \Gamma_i \\ 0_{m\times n} & 0_m & I_m \\ 0_{m\times n} & 0_m & 0_m \end{bmatrix}.$$

Considering that τ_{k+1} is independent from τ_k, the induced time-varying delay can be viewed as a bounded and uncertain parameter. Thus, a candidate Parameter Dependent Lyapunov Function (PDLF):

$$V(z_k, \tau_k) = z'_k Q^{-1}(\tau_k)z_k, \tag{3.9}$$

with $Q(\tau_k) = \sum_{i=1}^{N_h} \mu_i(\tau_k)Q_i$, $\sum_{i=1}^{N_h} \mu_i(\tau_k) = 1$, $\mu_i(\tau_k) \geq 0$, $Q_i = Q'_i > 0$, is associated to the closed-loop system (3.8).

Definition 3.2 *The closed-loop system is robustly asymptotically stable, with decay rate α, with respect to the trajectories solutions of system*

(3.8), *if:*

$$\Delta V(z_k, \tau_k) \triangleq V(z_{k+1}, \tau_{k+1}) - e^{-\alpha T}V(z_k, \tau_k) < 0, \qquad (3.10)$$

$\forall z_k \in \Re^{2l}$, $z_k \neq 0$, *and* $\forall \tau_k \in [\tau_{\min}, \tau_{\max}]$.

Notice that the notion of decay rate is mostly used for continuous-time systems, but it also applies to discrete-time systems through the change of variables $\lambda = e^{-\alpha T} \Leftrightarrow \alpha = -\frac{\ln \lambda}{T}$, where $\alpha \in [0, \infty) \Leftrightarrow \lambda \in (0, 1]$, for any $T > 0$ (see Appendix A). Moreover, in the discrete-time literature, the scalar λ is also referred as contractivity coefficient. This relation, between the decay rate and the contractivity coefficient, is basic for designing a discrete-time controller such that the plant output $y(t)$ is guaranteed to satisfy a certain continuous-time performance.

When applied to (3.8), Definition 3.2 leads to:

$$\big(H(\tau_k) + E\Delta(\tau_k)D\big)' Q^{-1}(\tau_{k+1})\big(H(\tau_k) + E\Delta(\tau_k)D\big) - \lambda Q^{-1}(\tau_k) < 0.$$
$$(3.11)$$

Based on the previously described closed-loop representation and Lyapunov stability condition, it is possible to define the following Lemma, which is also based on the use of a known result firstly reported in Petersen (1987) (see Appendix B).

Lemma 3.3 *Let α be a given nonnegative scalar, which implies $\lambda = e^{-\alpha T}$, and $\bar{\gamma}$ computed from (2.8). The closed-loop system (3.8) is robustly asymptotically stable, with a decay rate α, if there exist symmetric positive definite matrices $\tilde{Q}_i \in \Re^{2l \times 2l}$ and a matrix $\tilde{U} \in \Re^{2l \times 2l}$ that verify:*

$$\begin{bmatrix} -\tilde{Q}_j + \bar{\gamma}^2 EE' & H_i\tilde{U} & 0 \\ * & \lambda(\tilde{Q}_i - \tilde{U} - \tilde{U}') & \tilde{U}'D' \\ * & * & -I \end{bmatrix} < 0, \quad \forall i, j = 1, \dots, N_h.$$
$$(3.12)$$

Proof *First, defining $Q_i = \sigma \tilde{Q}_i$ and $U = \sigma \tilde{U}$, with σ being any positive scalar, and by pre- and post-multiplying (3.12) by $\sqrt{\sigma}I_r$, $r = 4l + m$, give:*

$$\begin{bmatrix} -Q_j + \sigma\bar{\gamma}^2 EE' & H_iU & 0 \\ * & \lambda(Q_i - U - U') & U'D' \\ * & * & -\sigma I \end{bmatrix} < 0, \quad \forall i, j = 1, \dots, N_h.$$
$$(3.13)$$

Appropriately performing convex combinations of (3.13), first for i and

after for j, and applying the Schur complement, leads to:

$$\begin{bmatrix} -Q(\tau_{k+1}) + \sigma\bar{\gamma}^2 EE' & H(\tau_k)U \\ * & \lambda\big(Q(\tau_k) - U - U'\big) + \sigma^{-1}U'D'DU \end{bmatrix} < 0.$$

This is equivalent to

$$\begin{bmatrix} -Q(\tau_{k+1}) & H(\tau_k)U \\ * & \lambda\big(Q(\tau_k) - U - U'\big) \end{bmatrix}$$
$$+ \sigma\begin{bmatrix} \bar{\gamma}E \\ 0 \end{bmatrix}\begin{bmatrix} \bar{\gamma}E' & 0 \end{bmatrix} + \sigma^{-1}\begin{bmatrix} 0 \\ U'D' \end{bmatrix}\begin{bmatrix} 0 & DU \end{bmatrix} < 0. \quad (3.14)$$

Since $\Delta(\tau_k)'\Delta(\tau_k) \leq \bar{\gamma}^2 I$, equation (3.14) is equivalent to (see Appendix B):

$$\begin{bmatrix} -Q(\tau_{k+1}) & H(\tau_k)U \\ * & \lambda\big(Q(\tau_k) - U - U'\big) \end{bmatrix}$$
$$+ He\left(\begin{bmatrix} \bar{\gamma}E \\ 0 \end{bmatrix} \bar{\gamma}^{-1}\Delta(\tau_k) \begin{bmatrix} 0 & DU \end{bmatrix} \right) < 0.$$

By the fact that $-U'Q^{-1}U \leq Q - U - U'$, the previous inequality implies

$$\begin{bmatrix} -Q(\tau_{k+1}) & \big(H(\tau_k) + E\Delta(\tau_k)D\big) \\ \big(H(\tau_k) + E\Delta(\tau_k)D\big)' & -\lambda Q^{-1}(\tau_k) \end{bmatrix} < 0$$

that by applying the Schur complement leads to (3.11). □

Notice, from the previous definitions, that the equivalence between inequalities (3.12) and inequalities (3.13) holds for any $\sigma > 0$. Then, there is no loss of generality in using condition (3.12), which is independent of σ, instead of using (3.13) for analyzing the stability of (3.8).

3.3 COMPENSATOR DESIGN

Considering the objective formulated by Problem 3.1, regarding the design of a dynamic output feedback compensator, the condition presented in Lemma 3.3 is not suitable for synthesis purpose. Thus, it can only be used to analyze the stability of the closed-loop system when the values of the compensator matrices are given. Therefore, firstly it is assumed that matrices $\tilde{U}$ and $\tilde{U}^{-1}$ (see Oliveira, Geromel & Bernussou

(2002), Castelan et al. (2010)), are such that:

$$\tilde{U} = \begin{bmatrix} X & (\bullet) \\ Z & (\bullet) \end{bmatrix}, \quad \tilde{U}^{-1} = \begin{bmatrix} Y & (\bullet) \\ W & (\bullet) \end{bmatrix}.$$

Furthermore, it is also assumed the use of an auxiliary matrix Θ:

$$\Theta = \begin{bmatrix} Y & I \\ W & 0 \end{bmatrix},$$

that verify:

$$\Psi = \tilde{U}\Theta = \begin{bmatrix} I & X \\ 0 & Z \end{bmatrix}, \quad \hat{U} = \Theta'\tilde{U}\Theta = \begin{bmatrix} Y' & T' \\ I & X \end{bmatrix},$$

where, by construction:

$$T' = Y'X + W'Z. \tag{3.15}$$

Moreover, the change of variable $\hat{Q}(\tau_k) = \Theta'\tilde{Q}(\tau_k)\Theta$ is used in the following.

Proposition 3.4 *Let α be a given nonnegative scalar, which implies $\lambda = e^{-\alpha T}$, and $\bar{\gamma}$ computed from (2.8). Consider the existence of symmetric positive definite matrices $\hat{Q}_i$, and matrices Y, X, T, $\hat{A}_i$, $\hat{B}_i$, $\hat{C}_i$, $\hat{D}_i$ that verify the LMI conditions:*

$$\begin{bmatrix} -\hat{Q}_j & \Omega_i & 0 & \bar{\gamma}\Theta'E \\ * & \lambda(\hat{Q}_i - \hat{U} - \hat{U}') & \Psi'D' & 0 \\ * & * & -I & 0 \\ * & * & * & -I \end{bmatrix} < 0, \quad \forall i,j = 1,\dots,N_h, \tag{3.16}$$

where $\Omega_i = \begin{bmatrix} Y'\bar{A}_i + \hat{B}_i\bar{C} & \hat{A}_i \\ \bar{A}_i + \bar{B}\hat{D}_i\bar{C} & \bar{A}_iX + \bar{B}\hat{C}_i \end{bmatrix}$. Let W and Z be any two nonsingular matrices such that $W'Z = T' - Y'X$. Then the full-order dynamic output feedback compensator (3.7) with

$$\mathcal{D}_i = \hat{D}_i$$
$$\mathcal{C}_i = (\hat{C}_i - \mathcal{D}_i\bar{C}X)Z^{-1}$$
$$\mathcal{B}_i = (W')^{-1}(\hat{B}_i - Y'\bar{B}\mathcal{D}_i)$$
$$\mathcal{A}_i = (W')^{-1}\big(\hat{A}_i - Y'(\bar{A}_i + \bar{B}\mathcal{D}_i\bar{C})X - Y'\bar{B}\mathcal{C}_iZ - W'\mathcal{B}_i\bar{C}X\big)Z^{-1}$$

is such that (3.8) is robustly asymptotically stable with decay rate α.

Proof *First, it follows from (3.16) that $\hat{U}$ is nonsingular. Then:*

$$rank\left(\begin{bmatrix} I & -Y' \\ 0 & I \end{bmatrix}\begin{bmatrix} Y' & T' \\ I & X \end{bmatrix} = \begin{bmatrix} 0 & T'-Y'X \\ I & X \end{bmatrix}\right) = 2l.$$

This implies that $T' - Y'X$, X and Y are nonsingular. Therefore, by choosing a nonsingular matrix W (or Z) it follows that Z (or W) is also nonsingular. Different choices for computing W and Z are possible, such as applying SVD or LU factorization, or even by fixing W (or Z) and computing Z (or W).

Next, by applying the Schur complement to the upper left term of (3.12) gives:

$$\begin{bmatrix} -\tilde{Q}_j & H_i\tilde{U} & 0 & \bar{\gamma}E \\ * & \lambda(\tilde{Q}_i - \tilde{U} - \tilde{U}') & \tilde{U}'D' & 0 \\ * & * & -I & 0 \\ * & * & * & -I \end{bmatrix} < 0, \quad \forall i,j = 1,\dots,N_h.$$

Thus, by pre- and post-multiplying the resulting inequalities by $diag\{\Theta', \Theta', I, I\}$ and its transpose, respectively, and defining the auxiliary variables

$$\begin{aligned} \hat{D}_i &= \mathcal{D}_i \\ \hat{C}_i &= \mathcal{D}_i\bar{C}X + \mathcal{C}_iZ \\ \hat{B}_i &= Y'\bar{B}\mathcal{D}_i + W'\mathcal{B}_i \\ \hat{A}_i &= Y'(\bar{A}_i + \bar{B}\mathcal{D}_i\bar{C})X + Y'\bar{B}\mathcal{C}_iZ + W'\mathcal{B}_i\bar{C}X + W'\mathcal{A}_iZ \end{aligned}$$

the equivalence between conditions (3.12) and (3.16) has been set. $\square$

3.4 EXAMPLE

For the experiments, the following continuous linear time-invariant plant is considered, also used in Donkers et al. (2009):

$$M = \begin{bmatrix} 1.380 & -0.208 & 6.715 & -5.676 \\ -0.581 & -4.290 & 0 & 0.675 \\ 1.067 & 4.273 & -6.654 & 5.893 \\ 0.048 & 4.273 & 1.343 & -2.104 \end{bmatrix},$$

$$N = \begin{bmatrix} 0 & 0 \\ 5.679 & 0 \\ 1.136 & -3.146 \\ 1.136 & 0 \end{bmatrix}, \ C = \begin{bmatrix} 1 & 0 & 1 & -1 \\ 0 & 1 & 0 & 0 \end{bmatrix},$$

for which some simulation results regarding the effect of the time-varying delay and the use of the proposed synthesis methodology are presented.

The synthesis of the compensator gains are obtained by looking for a feasible solution of LMIs (3.16), using *Yalmip* and *Sedumi* toolboxes, whereas the simulation is performed using the *True-time* toolbox. The time-varying delay is generated by an uniform distribution, using the bounds $\tau_{\min} = 1\text{ms}$ and $\tau_{\max} = T$, yet the delay sequences are the same for each simulation comparison. The approximation order used to write the poltytopic model based on TSA is $h = 2$.

These are the same plant and network conditions used for the motivating example in Section 2.1.1, where it has been shown that using a classical design procedure, the closed-loop system may have the performance degraded due to time-varying delays. Nevertheless, using the approach presented in this chapter, for the same sampling period of $T = 32\text{s}$, it is possible to find a feasible solution which leads to a suitable closed-loop performance (see Fig. 12 and Fig. 13).

For this example, a second analysis is also performed. For a sampling interval of $T = 100\text{ms}$, the decay rate is evaluated, showing that larger values of α allow a performance enhancement in terms of time response of the closed-loop system. Also, the compromise between the design parameter h and some results are addressed.
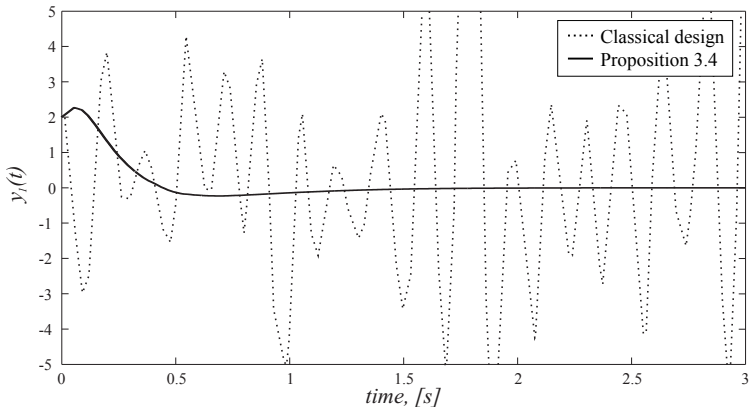
Figure 12 – Performance comparison, $y_1(t)$.
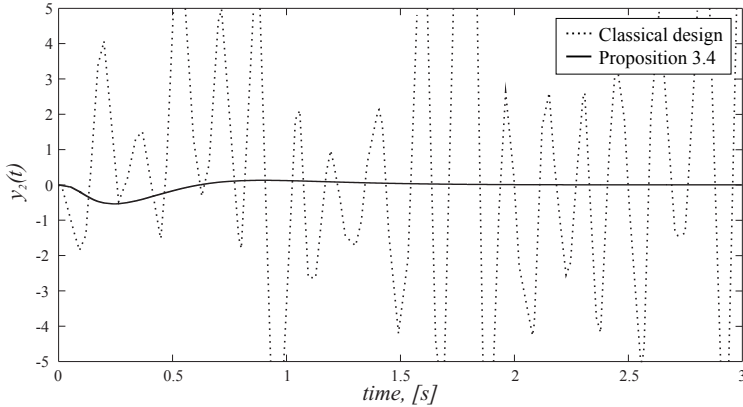
Figure 13 – Performance comparison, $y_2(t)$.

Table 1 – Performance comparison.

contractivity coefficient, λ	decay rate, α	settling time, 1%	control energy	control infinity norm
1.0	0.0000	6.6s	9.04	3.37
0.9	1.0536	4.5s	6.95	3.51
0.8	2.2314	3.3s	5.36	3.70
0.7	3.5667	2.3s	8.40	7.50

In Table 1, it is shown the settling time (1%), the control signal energy and the infinity norm of the control signal, obtained by simulations.

Observe that the results presented in Table 1 confirm the expected enhancement in terms of time convergence, which can be seen from the settling time achieved for each case. Also, a faster convergence to the origin implies in a larger amplitude for the control signal, represented by the infinity norm. With respect to control signal energy, it is not necessarily decreasing with the increasing of α.

Figures 14 and 15 depict the plant outputs for the closed-loop systems with compensators obtained for $\alpha = 3.5667$ and $\alpha = 1.0536$, respectively, whereas Fig. 16 and Fig. 17 depict the control signal dynamics for the corresponding controllers.
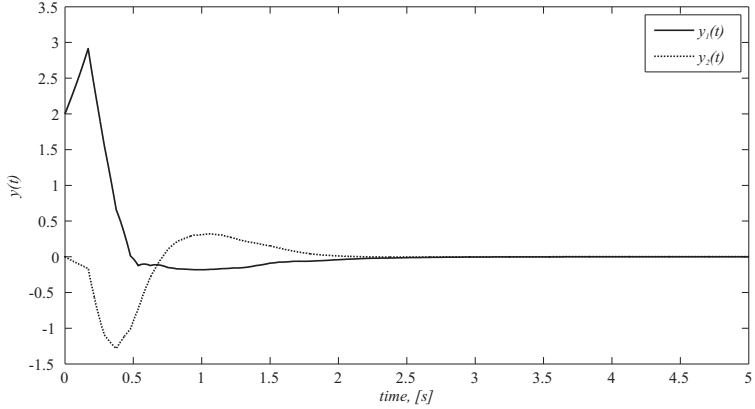
Figure 14 – Plant outputs, $\alpha = 3.5667$.
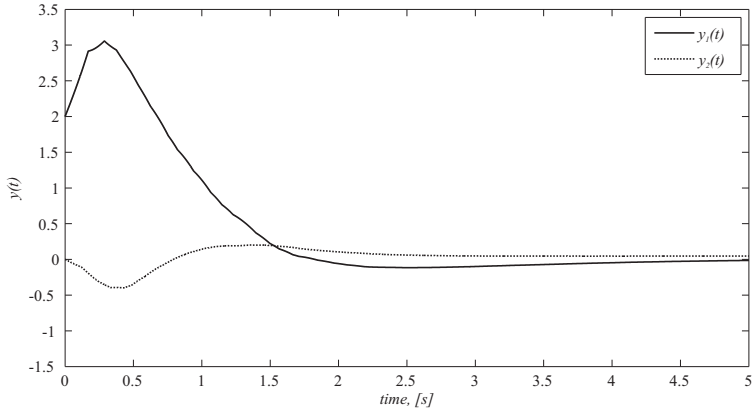
Figure 15 – Plant outputs, $\alpha = 1.0536$.

In Table 2, it is shown the influence of the approximation order h in the results. It can be notice that a larger order of approximation leads to a smaller upper bound $\bar{\gamma}$ for the residual uncertainty (3.6). Besides, the computation of $\bar{\gamma}$ has been performed using a grid with 1000 subintervals. In addition, the largest obtained decay rate α_{sm} for each case, which leads to the smallest $\lambda = \lambda_{sm}$, are also shown in Table 2. Observe that there is no improvement in the λ_{sm} when $h > 3$.
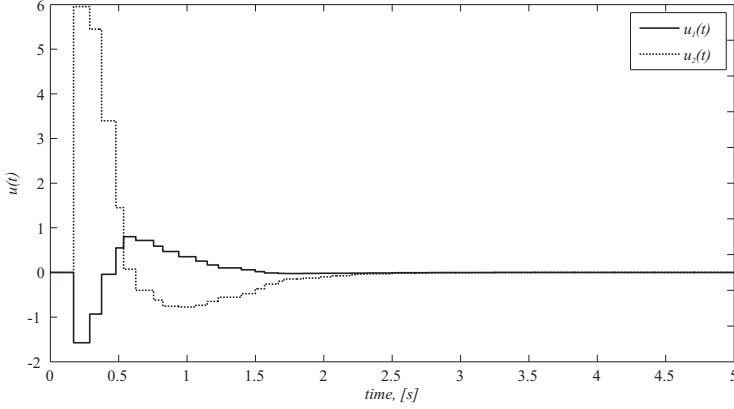
Figure 16 – Control signal, $\alpha = 3.5667$.
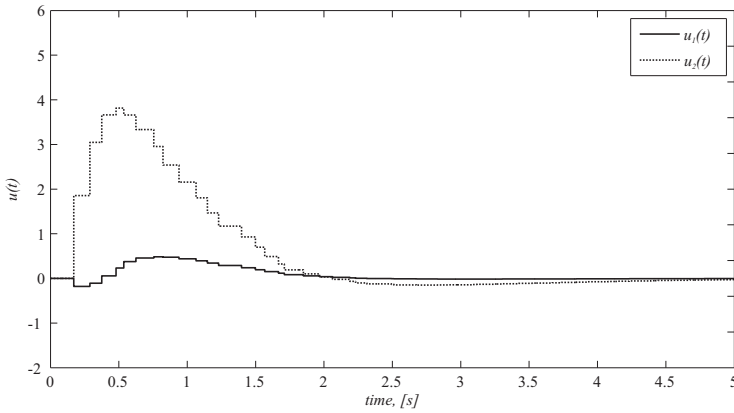
Figure 17 – Control signal, $\alpha = 1.0536$.

Table 2 – Decay rate and additional uncertainty upper bound.

order of approx.	$h = 1$	$h = 2$	$h = 3$	$h = 4$
$\bar{\gamma}$	0.1748	0.0367	0.0074	0.0013
λ_{sm}	0.8602	0.6802	0.5696	0.5696
α_{sm}	1.5059	3.8537	5.6282	5.6282

3.5 CONCLUSION

In this chapter, a result concerning the synthesis of dynamic output feedback compensators for NCS has been presented. The formulation was based on the NCS model presented in Chapter 2. The proposed compensator has full order, compared to the augmented representation of the closed-loop system, and its structure depends on the delay induced by the network. Thus, a network environment that may provide time-stamped messages is assumed, allowing the induced delay to be available at runtime. A similar approach can be used to design a dynamic output feedback compensator based on estimates of the time-varying delays, which is presented in the next chapter.

4 DELAY-DEPENDENT DYNAMIC OUTPUT FEEDBACK COMPENSATOR BASED ON DELAY ESTIMATES

Similar to the result presented in the previous chapter, the stabilization of a networked control system including a global time-varying delay is investigated in this chapter. The time-varying delay is considered to be unknown, but it is assumed that a bounded error estimate is available. The exponential uncertainty induced by the time-varying delay is decomposed into a polytopic representation with an additional uncertain norm-bounded term. Sufficient conditions to design a dynamic output feedback controller depending on an estimate of the time-varying delay are proposed (JUNGERS et al., 2013). The results are also provided in terms of LMI, and an illustration shows how the methodology enlarges the design techniques of the literature.

It is interesting to note that, in the case presented in this chapter, the use of time-stamped messages is not strictly required. Still, if it is possible to the sensor to send such information, it can be somehow used to estimate the full global delay.

4.1 PROBLEM FORMULATION

The plant model is the same one presented in section 2.2, where the plant is considered to be a continuous linear time-invariant process, described by:

$$
\begin{aligned}
\dot{x}(t) &= Mx(t) + Nu(t) \\
y(t) &= Cx(t)
\end{aligned}
\tag{4.1}
$$

with $x(t) \in \Re^n$, $u(t) \in \Re^m$, $y(t) \in \Re^p$, $M \in \Re^{n \times n}$, $N \in \Re^{n \times m}$ and $C \in \Re^{p \times n}$, with $p < n$. Recall that the controller only has access to the values of the output of the plant.

Due to the NCS structure, the continuous-time input $u(t)$ applied to the plant is delayed by a global time-varying delay τ_k which is assumed to be unknown and to verify $0 \le \tau_k \le T$, that is:

$$
u(t) = \begin{cases}
u_{k-1}, & t \in \left[kT , \ kT + \tau_k\right) \\
u_k, & t \in \left[kT + \tau_k , \ (k+1)T\right)
\end{cases}
$$

which leads to the following representation (ÅSTRÖM; WITTENMARK, 1997):

$$x_{k+1} = Ax_k + \tilde{\Gamma}(\tau_k)u_{k-1} + \Gamma(\tau_k)u_k$$
$$y_k = Cx_k \tag{4.2}$$

where

$$A = e^{MT}, \quad B = \int_0^T e^{Ms}ds\ N$$

$$\Gamma(\tau_k) = \int_0^{T-\tau_k} e^{Ms}ds\ N,$$

$$\tilde{\Gamma}(\tau_k) = \int_{T-\tau_k}^T e^{Ms}ds\ N = B - \Gamma(\tau_k).$$

Furthermore, introducing the extended state $\bar{x}_k = \begin{bmatrix} x_k' & u_{k-1}' \end{bmatrix}' \in \Re^{n+m}$:

$$\bar{x}_{k+1} = \bar{A}(\tau_k)\bar{x}_k + \bar{B}(\tau_k)u_k$$
$$y_k = \bar{C}\bar{x}_k \tag{4.3}$$

where

$$\bar{A}(\tau_k) = \begin{bmatrix} A & B - \Gamma(\tau_k) \\ 0_{m \times n} & 0_m \end{bmatrix}, \quad \bar{B}(\tau_k) = \begin{bmatrix} \Gamma(\tau_k) \\ I_m \end{bmatrix}, \quad \bar{C} = \begin{bmatrix} C & 0_{p \times m} \end{bmatrix}.$$

As previously mentioned, the current delay is not exactly known, thus an estimate $\hat{\tau}_k \in [0, T]$ is used, for which $\delta\tau_{\min} \leq \delta\tau = \tau_k - \hat{\tau}_k \leq \delta\tau_{\max}$, where by definition $-T \leq \delta\tau_{\min} \leq \delta\tau_{\max} \leq T$. Then, reformulating (4.3) gives:

$$\bar{x}_{k+1} = \left(\bar{A}(\hat{\tau}_k) + \begin{bmatrix} 0_n & -\Delta(\tau_k, \hat{\tau}_k) \\ 0_{m \times n} & 0_m \end{bmatrix} \right) \bar{x}_k$$
$$+ \left(\bar{B}(\hat{\tau}_k) + \begin{bmatrix} \Delta(\tau_k, \hat{\tau}_k) \\ 0_m \end{bmatrix} \right) u_k, \quad (4.4)$$

where $\Delta(\tau_k, \hat{\tau}_k) = \Gamma(\tau_k) - \Gamma(\hat{\tau}_k)$.

Moreover, the uncertain matrix in (4.3) can be rewritten as a convex polytope with an additional norm-bounded uncertainty, as

described in Section 2.2.2:

$$\Gamma(\tau_k) = \sum_{i=1}^{N_h} \mu_i(\hat{\tau}_k)\Gamma_i + \Omega(\tau_k, \hat{\tau}_k) \ , \quad \left\|\Omega(\tau_k, \hat{\tau}_k)\right\| \ \leq \ \gamma_\Omega. \qquad (4.5)$$

Then, the following problem is considered.

Problem 4.1 *Determine a full-order dynamic output feedback, in the form*

$$\begin{aligned} \zeta_{k+1} &= \mathcal{A}(\hat{\tau}_k)\zeta_k + \mathcal{B}(\hat{\tau}_k)y_k \\ u_k &= \mathcal{C}\zeta_k + \mathcal{D}y_k \end{aligned} \qquad (4.6)$$

with $\zeta_k \in \Re^{n+m}$, which asymptotically stabilizes the system (4.4).

Additionally, the parameter dependent matrices of the compensator (4.6) are also structured as polytopes:

$$\begin{bmatrix} \mathcal{A}(\hat{\tau}_k) & \mathcal{B}(\hat{\tau}_k) \end{bmatrix} = \sum_{i=1}^{N_h} \mu_i(\hat{\tau}_k) \begin{bmatrix} \mathcal{A}_i & \mathcal{B}_i \end{bmatrix}.$$

Remark 4.2 *A slightly different but equivalent notation is used in Jungers et al. (2013). Still, for sake of uniformity of this document, the notation used in this chapter follows the same pattern used in the other ones.*

Despite being possible to use the same overall formulation from the previous chapter, once delay estimates are used, there is no need to consider a control signal delayed by at most one sampling interval. Thus, in (4.6), constant matrices $\mathcal{C}$ and $\mathcal{D}$ are employed, which allows to provide a structure to the dynamic output compensator that is linear with respect to the polytopic weighting parameters.

4.2 CLOSED-LOOP STABILIZATION

Initially, defining an auxiliary extended variable $z_k = [\bar{x}'_k \ \zeta'_k]' \in \Re^{2(n+m)}$, a closed-loop representation is given by:

$$z_{k+1} = H(\hat{\tau}_k)z_k + E\Omega(\tau_k, \hat{\tau}_k)Dz_k \qquad (4.7)$$

where $E = \begin{bmatrix} I_n & 0_{n \times m} & 0_{n \times (n+m)} \end{bmatrix}'$, $D = \begin{bmatrix} 0_{m \times n} & -I_m & 0_{m \times (n+m)} \end{bmatrix} + \begin{bmatrix} \mathcal{D}\bar{C} & \mathcal{C} \end{bmatrix}$, $H(\hat{\tau}_k) = \sum_{i=1}^{N_h} \mu_i(\hat{\tau}_k) H_i$, and

$$H_i = \begin{bmatrix} \bar{A}_i + \bar{B}_i \mathcal{D}\bar{C} & \bar{B}_i \mathcal{C} \\ \mathcal{B}_i \bar{C} & \mathcal{A}_i \end{bmatrix},$$

with, from (4.4) and (4.5):

$$\bar{A}_i = \begin{bmatrix} A & B - \Gamma_i \\ 0_{m \times n} & 0_m \end{bmatrix}, \quad \bar{B}_i = \begin{bmatrix} \Gamma_i \\ I_m \end{bmatrix}.$$

Consider in the following a candidate PDLF:

$$V(z_k, \hat{\tau}_k) = z_k' Q^{-1}(\hat{\tau}_k) z_k, \tag{4.8}$$

with $Q(\hat{\tau}_k) = \sum_{i=1}^{N_h} \mu_i(\hat{\tau}_k) Q_i$, $\sum_{i=1}^{N_h} \mu_i(\hat{\tau}_k) = 1$, $\mu_i(\hat{\tau}_k) \geq 0$, $Q_i = Q_i' > 0$.

Definition 4.3 *The closed-loop system is robustly asymptotically stable, with decay rate α, with respect to the trajectories solutions of system (4.7), if:*

$$\Delta V(z_k, \hat{\tau}_k) \triangleq V(z_{k+1}, \hat{\tau}_{k+1}) - \lambda V(z_k, \hat{\tau}_k) < 0, \tag{4.9}$$

$\forall z_k \in \Re^{2(n+m)}$, $z_k \neq 0$, $\forall \hat{\tau}_k \in [\hat{\tau}_{\min}, \hat{\tau}_{\max}]$, and $\lambda = e^{-\alpha T}$.

When associated to (4.7), Definition 4.3 leads to the following stability condition:

$$\big(H(\hat{\tau}_k) + E\Omega(\tau_k, \hat{\tau}_k) D\big)' Q^{-1}(\tau_{k+1}) \big(H(\hat{\tau}_k) + E\Omega(\tau_k, \hat{\tau}_k) D\big) \\ - \lambda Q^{-1}(\hat{\tau}_k) < 0. \tag{4.10}$$

Finally, a compensator synthesis, similar to the one presented in section 3.3, can be used to solve Problem 4.1.

Proposition 4.4 *Let α be a given scalar $\alpha \in \Re$ and $\bar{\gamma}_\Omega$ computed from (2.11). Consider the existence of symmetric positive definite matrices $\hat{Q}_i$, and matrices Y, X, T, $\hat{A}_i$, $\hat{B}_i$, $\hat{C}$, $\hat{D}$ that verify the LMI conditions:*

$$\begin{bmatrix} -\hat{Q}_j & \Omega_i & 0 & \bar{\gamma}_\Omega \Theta' E \\ * & \lambda(\hat{Q}_i - \hat{U} - \hat{U}') & \Psi' D' & 0 \\ * & * & -I & 0 \\ * & * & * & -I \end{bmatrix} < 0, \quad \forall i, j = 1, \ldots, N_h, \tag{4.11}$$

where

$$\Omega_i = \begin{bmatrix} Y'\bar{A}_i + \hat{B}_i\bar{C} & \hat{A}_i \\ \bar{A}_i + \bar{B}_i\hat{D}\bar{C} & \bar{A}_iX + \bar{B}_i\hat{C} \end{bmatrix}.$$

Let W and Z be any two nonsingular matrices such that

$$W'Z = T' - Y'X. \tag{4.12}$$

Then the full-order dynamic output feedback compensator (4.6) with

$$\mathcal{D} = \hat{D}$$

$$\mathcal{C} = (\hat{C} - \mathcal{D}\bar{C}X)Z^{-1}$$

$$\mathcal{B}_i = (W')^{-1}(\hat{B}_i - Y'\bar{B}_i\mathcal{D})$$

$$\mathcal{A}_i = (W')^{-1}(\hat{A}_i - Y'(\bar{A}_i + \bar{B}_i\mathcal{D}\bar{C})X - Y'\bar{B}_i\mathcal{C}Z - W'\mathcal{B}_i\bar{C}X)Z^{-1}$$

is such that the closed-loop system (4.7) is robustly asymptotically stable with decay rate α.

Proof *Assume the use of an auxiliary matrix $\Theta = \begin{bmatrix} Y & I \\ W & 0 \end{bmatrix}$, and matrices $\tilde{U} = \begin{bmatrix} X & (\bullet) \\ Z & (\bullet) \end{bmatrix}$ and $\tilde{U}^{-1} = \begin{bmatrix} Y & (\bullet) \\ W & (\bullet) \end{bmatrix}$, that verify*

$$\Psi = \tilde{U}\Theta = \begin{bmatrix} I & X \\ 0 & Z \end{bmatrix}, \quad \hat{U} = \Theta'\tilde{U}\Theta = \begin{bmatrix} Y' & T' \\ I & X \end{bmatrix},$$

where, by construction, $T' = Y'X + W'Z$. Assume also the change of variable $\hat{Q}(\hat{\tau}_k) = \Theta'\tilde{Q}(\hat{\tau}_k)\Theta$. Then, by pre- and post-multiplying (4.11) by $diag\{(\Theta')^{-1}, (\Theta')^{-1}, I, I\}$ and its transpose, respectively, defining the additional auxiliary variables

$$\hat{D} = \mathcal{D},$$

$$\hat{C} = \mathcal{D}\bar{C}X + \mathcal{C}Z,$$

$$\hat{B}_i = Y'B_i\mathcal{D} + W'\mathcal{B}_i,$$

$$\hat{A}_i = Y'(\bar{A}_i + \bar{B}_i\mathcal{D}\bar{C})X + Y'\bar{B}_i\mathcal{C}Z + W'\mathcal{B}_i\bar{C}X + W'\mathcal{A}_iZ,$$

and applying the Schur complement, give:

$$\begin{bmatrix} -\tilde{Q}_j + \bar{\gamma}_\Omega^2 EE' & H_i\tilde{U} & 0 \\ * & \lambda(\tilde{Q}_i - \tilde{U} - \tilde{U}') & \tilde{U}'D' \\ * & * & -I \end{bmatrix} < 0, \quad \forall i,j = 1,\ldots,N_h,$$

from which, following similar steps as in the proof of Lemma 3.3, leads to (4.10). □

4.3 EXAMPLE

Consider the plant:

$$M = \begin{bmatrix} 103.5 & 0 \\ 0 & -43.5 \end{bmatrix}, \ N = \begin{bmatrix} 33.6 \\ -5.1 \end{bmatrix}, \ C = \begin{bmatrix} 10 & 1 \end{bmatrix}, \qquad (4.13)$$

with sampling interval $T = 5$ms and bounded time-varying delays $\tau_k \in [0, T]$.

The delay estimates, $\hat{\tau}_k$, are computed based on the actual sensor-to-controller delay, $\tau_{sc,k}$ (obtained through time-stamped messages), added by a nominal constant controller-to-actuator delay, $\hat{\tau}_{ca} = 1.4$ms. In addition, the delay estimates belong to the bounded interval $[0, T]$, and the estimation error is given by $\delta\tau_k = \tau_k - \hat{\tau}_k \in [-\frac{3}{10}T, \frac{3}{10}T]$.

In Hetel et al. (2011) it has been pointed out that the design of a state-feedback controller that is independent from the delay, by applying the design method proposed by Cloosterman et al. (2010), failed for this system. The authors, then, presented a design method for state-feedback controller dependent on delay estimates, which successfully provided a feasible solution. However, such method is not suitable when not all plant states are accessible.

Thereby, using Proposition 4.4 with $h = 1$ and $\lambda = 1$, it is possible to find a feasible solution to the parameter-dependent compensator (4.6). Moreover, with the same parameters for the approximation order and contractivity coefficient, using Proposition 3.4 from the previous chapter also leads to a feasible solution. For each synthesized controller, a simulation is performed with random time-varying delays. It is important to emphasize that the same delay sequence is used for both simulations, which is shown in Fig. 18 along with the delay estimate errors.

In addition, in Fig. 19 and Fig. 20 the plant outputs and the control signals are shown, respectively, where the continuous line is with respect to the system that uses a controller dependent on delay estimates and the dashed line is with respect to the use of a controller dependent on actual delays. It can be noticed that the second one operates with zero control over the first sampling interval, due to a control signal delayed by at most one sampling interval, whereas the controller that is dependent on delay estimates requires less effort from
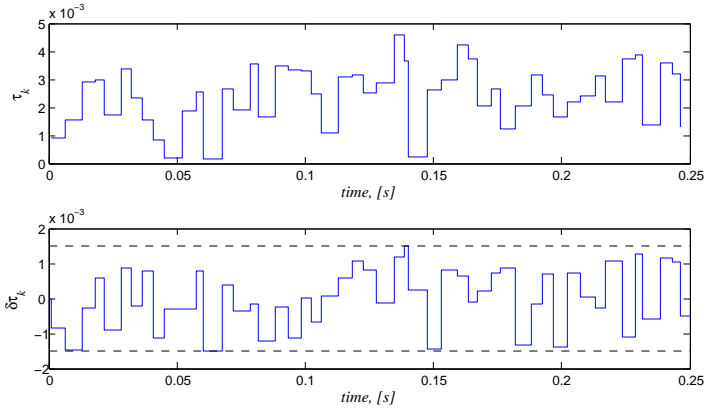
Figure 18 – Time-varying delays and delay estimate errors.
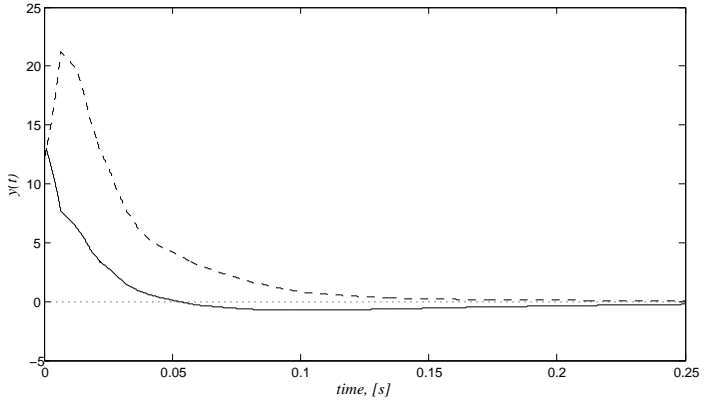
Figure 19 – Plant output.

the actuator in terms of maximum value. Regardless, both closed-loop systems are asymptotically stable, with the controller dependent on actual delays showing a better convergence to the equilibrium.

Furthermore, likewise in the previous chapter, searching for a smaller contractivity coefficient λ_{sm}, which leads to a largest decay rate α_{sm}, gives the results shown in Table 3 for the compensator design based on delay estimates. As expected, here again a larger order of approximation leads to a smaller contractivity coefficient, presumably due to a smaller upper bound for the additional uncertainty.
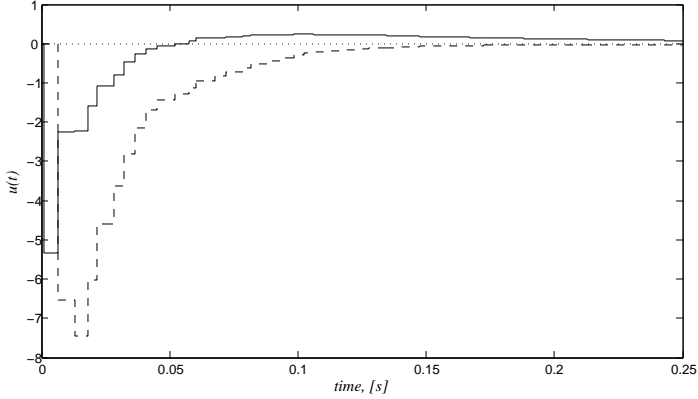
Figure 20 – Control signal.

Table 3 – Contractivity coefficient as a function of h.

	$h = 1$	$h = 2$	$h = 3$	$h = 4$	$h = 5$
$\bar{\gamma}_\Omega$	0.0039	0.0026	0.0024	0.0023	0.0023
λ_{sm}	0.9580	0.8911	0.8790	0.8774	0.8773

Besides, when performing this search using the compensator design based on actual delays, for $h = 1$, gives $\bar{\gamma} = 0.0015$ and consequently a smaller contractivity coefficient compared to the compensator that is dependent on delay estimates, i.e., $\lambda_{sm} = 0.6178$.

4.4 CONCLUSION

The design of a dynamic output feedback controller for a network controlled system based on the knowledge of a time-varying delay estimate has been studied in this chapter. The exponential uncertainty, induced by the time-varying delay, is rewritten as the sum of a polytopic term and an uncertain bounded term. A sufficient condition formulated as LMIs has been provided to design the proposed controller. An application of the designing methodology to an illustrative example has been presented.

5 CONTROL SYNTHESIS FOR NCS WITH SWITCHING SAMPLING INTERVALS

Based on previous results, this chapter deals with the closed-loop stabilization when there might be a need to operate with several different sampling intervals. In the context of networked control systems, such situation may appear in order to preserve the provided QoS, for instance, if bandwidth variation occurs due to network overload. In the literature, this assumption often accompanies the implementation of Resource Managers (RMs) that regulate the network access (e.g., Fig. 21), as in Al-Areqi, Görges & Liu (2011) and Ji & Kim (2008).
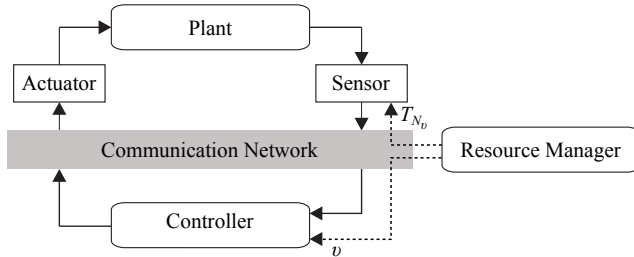
Figure 21 – Networked control system with shared medium access coordinated by a resource manager.

From the control system point of view, the RM has the ability of arbitrarily assigning the current sampling interval, among a finite set of allowable ones. This implies that the closed-loop system behaves as a switching system, in which the switching rule is not a manipulable variable but generated by an heterogeneous input, the RM that acts as a logical decision making algorithm. Such a switching rule is modeled by an *a priori* unknown and induced signal, which then leads to designing control laws that should satisfy any arbitrary switching rule as in, e.g., Daafouz, Riedinger & Iung (2002) and Jungers et al. (2011).

Thus, here the focus is to consider the arbitrary interchangeability among all different possible sampling intervals already in the control synthesis, later allowing the synthesized switching controllers to be used in a co-design strategy. An RM coordinates the communication network, and thus it sends the switching variable to sensor and controller, as depicted by dashed lines in Fig. 21. For simplicity, the method is presented for the case where time-stamped messages are used, as in Chapter 3. Nevertheless, it is also possible to use it for the case presented

in Chapter 4 with minor modifications. An example is presented to illustrate the proposed method.

A similar switching control synthesis can be found in Izák, Görges & Liu (2010), where it is proposed a state-feedback control design, also based on a TSA representation for the uncertain discrete-time system, but without considering the norm-bounded uncertainty in the controller synthesis.

5.1 PROBLEM PRESENTATION

As previously stated, the results in Chapter 3 are used as starting point, thus, a continuous linear time-invariant plant is considered:

$$
\begin{aligned}
\dot{x}(t) &= Mx(t) + Nu(t) \\
y(t) &= Cx(t)
\end{aligned}
\tag{5.1}
$$

with $x(t) \in \Re^n$, $u(t) \in \Re^m$, $y(t) \in \Re^p$, $M \in \Re^{n \times n}$, $N \in \Re^{n \times m}$ and $C \in \Re^{p \times n}$, with $p < n$, as well as the assumption that the controller only has access to the values of the output of the plant. Besides, it is assumed in the sequel that the sensor has the ability to operate with several different sampling intervals, according to the RM demand.

To represent the switching dynamics of the plant in discrete-time, with respect to the sampling instants, consider that the sampling intervals belong to a finite ordered set $\{T_v;\ v = 1, \ldots, N_v\}$, such that $0 < T_1 \leq T_2 \leq \cdots \leq T_{N_v}$. Notice that, at this point, the index v stands for the sensor sampling interval operating mode induced by the RM, that can assume any value in $\{T_v\}$ at instant k. Also, the assumption on the delay bounds is still valid for each particular sampling interval, now being dependent on the operating mode, i.e., $\tau_k \in [\tau_{v,\min}\ ,\ \tau_{v,\max}]$ $\forall k$, with $0 < \tau_{v,\min} < \tau_{v,\max} \leq T_v$.

Then, for $t \in [kT_v, (k+1)T_v]$, $k \in \mathcal{N}$, the control signal

$$
u(t) = \begin{cases} u_{k-1}, & t \in \left[kT_v\ ,\ kT_v + \tau_k\right) \\ u_k, & t \in \left[kT_v + \tau_k\ ,\ (k+1)T_v\right) \end{cases}
$$

leads to the following discrete-time plant with switching dynamics:

$$
\begin{aligned}
x_{k+1} &= A_v x_k + \tilde{\Gamma}_v(\tau_k) u_{k-1} + \Gamma_v(\tau_k) u_k \\
y_k &= C x_k
\end{aligned}
$$

with matrices dependent on the current operating mode v:

$$A_v = e^{MT_v}, \quad B_v = \int_0^{T_v} e^{Ms} ds \ N$$

$$\Gamma_v(\tau_k) = \int_0^{T_v - \tau_k} e^{Ms} ds \ N,$$

$$\tilde{\Gamma}_v(\tau_k) = \int_{T_v - \tau_k}^{T_v} e^{Ms} ds \ N = B_v - \Gamma_v(\tau_k).$$

Similarly as in section 3.1, now consider an extended state $\bar{x}_k = \begin{bmatrix} x_k' & u_{k-1}' & u_k' \end{bmatrix}' \in \Re^l$, $l = n + 2m$. Then, rewriting the switching discrete-time system gives:

$$\begin{aligned} \bar{x}_{k+1} &= \bar{A}_v(\tau_k)\bar{x}_k + \bar{B}u_{k+1} \\ y_k &= \bar{C}\bar{x}_k \end{aligned} \tag{5.2}$$

where $\bar{B} = \begin{bmatrix} 0_{m \times n} & 0_m & I_m \end{bmatrix}'$, $\bar{C} = \begin{bmatrix} C & 0_m & 0_m \end{bmatrix}$, and

$$\bar{A}_v(\tau_k) = \begin{bmatrix} A_v & B_v - \Gamma_v(\tau_k) & \Gamma_v(\tau_k) \\ 0_{m \times n} & 0_m & I_m \\ 0_{m \times n} & 0_m & 0_m \end{bmatrix}. \tag{5.3}$$

Since (5.2) has uncertain matrices, the polytopic representation with additional norm-bounded uncertainty from section 2.2.1 is used:

$$\Gamma_v(\tau_k) = \sum_{i=1}^{N_{h_v}} \mu_{v,i}(\tau_k)\Gamma_{v,i} + \Delta_v(\tau_k), \tag{5.4}$$

for which the $N_{h_v} = h_v + 1$ vertices and the upper bounds for the residual uncertainties

$$\left\| \Delta_v(\tau_k) \right\| \leq \gamma_v$$

are computed, for each operating mode, as presented in section 2.2.1.

Thus, based on the system (5.2), the following problem is considered.

Problem 5.1 *Design dynamic output feedback compensators with full-order $l = n + 2m$, given by:*

$$\begin{aligned} \zeta_{k+1} &= \mathcal{A}_v(\tau_k)\zeta_k + \mathcal{B}_v(\tau_k)y_k \\ u_{k+1} &= \mathcal{C}_v(\tau_k)\zeta_k + \mathcal{D}_v(\tau_k)y_k, \end{aligned} \tag{5.5}$$

for $v \in \{1, \ldots, N_v\}$, such that the corresponding switching closed-loop system is robustly asymptotically stable.

Furthermore, recall that the compensator matrices can also be structured as polytopes, i.e.,

$$\begin{bmatrix} \mathcal{A}_v(\tau_k) & \mathcal{B}_v(\tau_k) \\ \mathcal{C}_v(\tau_k) & \mathcal{D}_v(\tau_k) \end{bmatrix} = \sum_{i=1}^{N_{h_v}} \mu_{v,i}(\tau_k) \begin{bmatrix} \mathcal{A}_{v,i} & \mathcal{B}_{v,i} \\ \mathcal{C}_{v,i} & \mathcal{D}_{v,i} \end{bmatrix}.$$

5.2 SWITCHING CLOSED-LOOP STABILITY

Defining the auxiliary variable $z_k = [\bar{x}_k' \ \zeta_k']' \in \Re^{2l}$, a switching closed-loop representation is given by:

$$z_{k+1} = H_v(\tau_k)z_k + E\Delta_v(\tau_k)Dz_k \tag{5.6}$$

where $E = \begin{bmatrix} I_n & 0_{n \times m} & 0_{n \times m} & 0_{n \times l} \end{bmatrix}'$, $D = \begin{bmatrix} 0_{m \times n} & -I_m & I_m & 0_{m \times l} \end{bmatrix}$, $H_v(\tau_k) = \sum_{i=1}^{N_{h_v}} \mu_{v,i}(\tau_k)H_{v,i}$, and

$$H_{v,i} = \begin{bmatrix} \bar{A}_{v,i} + \bar{B}\mathcal{D}_{v,i}\bar{C} & \bar{B}\mathcal{C}_{v,i} \\ \mathcal{B}_{v,i}\bar{C} & \mathcal{A}_{v,i} \end{bmatrix},$$

with, from (5.3) and (5.4):

$$\bar{A}_{v,i} = \begin{bmatrix} A_v & B_v - \Gamma_{v,i} & \Gamma_{v,i} \\ 0_{m \times n} & 0_m & I_m \\ 0_{m \times n} & 0_m & 0_m \end{bmatrix}.$$

Let us associate a candidate switching and parameter dependent Lyapunov function (SPDLF) to the switching closed-loop system (5.6):

$$V_v(z_k, \tau_k) = z_k'Q_v^{-1}(\tau_k)z_k,$$

with $Q_v(\tau_k) = \sum_{i=1}^{N_{h_v}} \mu_{v,i}(\tau_k)Q_{v,i}$, $\sum_{i=1}^{N_{h_v}} \mu_{v,i}(\tau_k) = 1$, $\mu_{v,i}(\tau_k) \geq 0$, $Q_{v,i} = Q_{v,i}' > 0$.

Definition 5.2 *The switching closed-loop system is robustly asymptotically stable, with contractivity coefficient $\lambda \in (0,1]$, if:*

$$\Delta V_k \triangleq V_{v^+}(z_{k+1}, \tau_{k+1}) - \lambda V_v(z_k, \tau_k) < 0, \tag{5.7}$$

$\forall z_k \in \Re^{2l}$, $z_k \neq 0$, and $\forall \tau_k \in [\tau_{\min}, \tau_{\max}]$.

Notice that v^+ stands for the operating mode activated at the instant $k + 1$. Also, for the purpose of performance measurement, a global minimum decay rate α is assumed in (5.7), once a constant contractivity coefficient λ is used. Hence, the following is assumed:

$$\lambda = e^{-\alpha T_{N_v}} \quad \Longleftrightarrow \quad \alpha = -\frac{\ln \lambda}{T_{N_v}}$$

This means that there is a performance improvement when smaller sampling intervals are used.

Furthermore, applying the Definition 5.2 to the switching closed-loop system (5.6), leads to:

$$\left(H_v(\tau_k) + E\Delta_v(\tau_k)D\right)' Q_{v^+}^{-1}(\tau_{k+1})\left(H_v(\tau_k) + E\Delta_v(\tau_k)D\right)$$
$$- \lambda Q_v^{-1}(\tau_k) < 0, \quad (5.8)$$

from where the following Lemma can be stated.

Lemma 5.3 *Let $\alpha \in \Re^+$ be the minimum admissible decay rate, which implies $\lambda = e^{-\alpha T_{N_v}}$, and the upper bounds $\bar{\gamma}_v$ computed as in (2.8) for each operating mode $v \in \{1, \ldots, N_v\}$. The switching closed-loop system (5.6) is robustly asymptotically stable if there exist symmetric positive definite matrices $\tilde{Q}_{r,i} \in \Re^{2l \times 2l}$, and matrices $\tilde{U}_r \in \Re^{2l \times 2l}$ that verify:*

$$\begin{bmatrix} -\tilde{Q}_{q,j} + \bar{\gamma}_r^2 EE' & H_{r,i}\tilde{U}_r & 0 \\ * & \lambda(\tilde{Q}_{r,i} - \tilde{U}_r - \tilde{U}_r') & \tilde{U}_r'D' \\ * & * & -I \end{bmatrix} < 0, \quad \begin{matrix} \forall r, q = 1, ..., N_v, \\ \forall i, j = 1, ..., N_{h_v}. \end{matrix}$$
$$(5.9)$$

Proof *First, notice that the indices r and q are related to the current operating mode in the k-th and $(k+1)$-th instants, respectively. Thus, evaluating (5.9) gives*

$$\begin{bmatrix} -\tilde{Q}_{v^+,j} + \bar{\gamma}_v^2 EE' & H_{v,i}\tilde{U}_v & 0 \\ * & \lambda(\tilde{Q}_{v,i} - \tilde{U}_v - \tilde{U}_v') & \tilde{U}_v'D' \\ * & * & -I \end{bmatrix} < 0, \ \forall i, j = 1, ..., N_{h_v}.$$

Moreover, the indices i and j are related to the polytope vertices, also in the k-th and $(k+1)$-th instants, respectively, thus following similar

steps as in the proof of Lemma 3.3, the following condition is obtained:

$$\begin{bmatrix} -Q_{v^+}(\tau_{k+1}) + \sigma_v\bar{\gamma}_v^2 EE' & H_v(\tau_k)U_v \\ & \lambda(Q_v(\tau_k) - U_v - U_v') \\ * & +\sigma_v^{-1}U_v'D'DU_v \end{bmatrix} < 0,$$

from which by the use of Petersen's Lemma (see Appendix B), since $\Delta_v(\tau_k)'\Delta_v(\tau_k) \leq \bar{\gamma}_v^2 I$ and by the fact that $-U_v'Q_v^{-1}U_v \leq Q_v - U_v - U_v'$, leads to (5.8). □

5.3 SWITCHING CONTROL SYNTHESIS

To deal with Problem 5.1, some auxiliary matrices are considered in the following:

$$\tilde{U}_v = \begin{bmatrix} X_v & (\bullet) \\ Z_v & (\bullet) \end{bmatrix}, \quad \tilde{U}_v^{-1} = \begin{bmatrix} Y_v & (\bullet) \\ W_v & (\bullet) \end{bmatrix}, \quad \Theta_v = \begin{bmatrix} Y_v & I_v \\ W_v & 0 \end{bmatrix},$$

that verify:

$$\Psi_v = \tilde{U}_v\Theta_v = \begin{bmatrix} I & X_v \\ 0 & Z_v \end{bmatrix}, \quad \hat{U}_v = \Theta_v'\tilde{U}_v\Theta_v = \begin{bmatrix} Y_v' & T_v' \\ I & X_v \end{bmatrix},$$

where, by construction:

$$T_v' = Y_v'X_v + W_v'Z_v. \tag{5.10}$$

Moreover, the change of variable $\hat{Q}_v(\tau_k) = \Theta_v'\tilde{Q}_v(\tau_k)\Theta_v$ is also considered.

Proposition 5.4 *Let $\alpha \in \Re^+$ be the minimum admissible decay rate, which implies $\lambda = e^{-\alpha T_{N_v}}$, and the upper bounds $\bar{\gamma}_v$ computed as in (2.8) for each operating mode $v \in \{1, \ldots, N_v\}$. Consider the existence of symmetric positive definite matrices $\hat{Q}_{r,i}$, and matrices Y_r, X_r, T_r, $\hat{A}_{r,i}$, $\hat{B}_{r,i}$, $\hat{C}_{r,i}$, $\hat{D}_{r,i}$ that verify:*

$$\begin{bmatrix} -\hat{Q}_{q,j} & \Omega_{r,i} & 0 & \bar{\gamma}_r\Theta_r'E \\ * & \lambda(\hat{Q}_{r,i} - \hat{U}_r - \hat{U}_r') & \Psi_r'D' & 0 \\ * & * & -I & 0 \\ * & * & * & -I \end{bmatrix} < 0, \quad \begin{array}{l} \forall r, q = 1, \ldots, N_v, \\ \forall i, j = 1, \ldots, N_{h_v}, \end{array}$$

$$\tag{5.11}$$

where $\Omega_{r,i} = \begin{bmatrix} Y_r'\bar{A}_{r,i} + \hat{B}_{r,i}\bar{C} & \hat{A}_{r,i} \\ \bar{A}_{r,i} + \bar{B}\hat{D}_{r,i}\bar{C} & \bar{A}_{r,i}X_r + \bar{B}\hat{C}_{r,i} \end{bmatrix}$. *Let W_r and Z_r be any nonsingular matrices such that $W_r'Z_r = T_r' - Y_r'X_r$. Then the full-order dynamic output feedback compensators (5.5) with*

$$\mathcal{D}_{r,i} = \hat{D}_{r,i}$$
$$\mathcal{C}_{r,i} = (\hat{C}_{r,i} - \mathcal{D}_{r,i}\bar{C}X_r)Z_r^{-1}$$
$$\mathcal{B}_{r,i} = (W_r')^{-1}(\hat{B}_{r,i} - Y_r'\bar{B}\mathcal{D}_{r,i})$$
$$\mathcal{A}_{r,i} = (W_r')^{-1}\big(\hat{A}_{r,i} - Y_r'(\bar{A}_{r,i} + \bar{B}\mathcal{D}_{r,i}\bar{C})X_r - Y_r'\bar{B}\mathcal{C}_{r,i}Z_r$$
$$\qquad\qquad - W_r'\mathcal{B}_{r,i}\bar{C}X_r\big)Z_r^{-1}$$

is such that the switching closed-loop system (5.6) is robustly asymptotically stable.

Proof *Following similar steps as in the proof of Proposition 3.4, but starting from Lemma 5.3 and the corresponding LMIs set, with auxiliary matrices:*

$$\hat{D}_{r,i} = \mathcal{D}_{r,i}$$
$$\hat{C}_{r,i} = \mathcal{D}_{r,i}\bar{C}X_r + \mathcal{C}_{r,i}Z_r$$
$$\hat{B}_{r,i} = Y_r'\bar{B}\mathcal{D}_{r,i} + W_r'\mathcal{B}_{r,i}$$
$$\hat{A}_{r,i} = Y_r'(\bar{A}_{r,i} + \bar{B}\mathcal{D}_{r,i}\bar{C})X_r + Y_r'\bar{B}\mathcal{C}_{r,i}Z_r + W_r'\mathcal{B}_{r,i}\bar{C}X_r + W_r'\mathcal{A}_{r,i}Z_r$$

it is possible to show the equivalence between (5.11) and (5.9). $\qquad\square$

5.4 EXAMPLE

For this example, the following continuous linear time-invariant plant is used:

$$M = \begin{bmatrix} 1.380 & -0.208 & 6.715 & -5.676 \\ -0.581 & -4.290 & 0 & 0.675 \\ 1.067 & 4.273 & -6.654 & 5.893 \\ 0.048 & 4.273 & 1.343 & -2.104 \end{bmatrix}, \ N = \begin{bmatrix} 0 & 0 \\ 5.679 & 0 \\ 1.136 & -3.146 \\ 1.136 & 0 \end{bmatrix}, \ C' = \begin{bmatrix} 1 & 0 \\ 0 & 1 \\ 1 & 0 \\ -1 & 0 \end{bmatrix}.$$

The aim is to investigate the switching between sampling intervals, and its consequences. For that matter, two operating modes are assumed: $T_1 = 10$ms and $T_2 = 60$ms. For both operating modes, the approximation order of the TSA representation is $h = 2$.

Based on the compensator synthesis presented in Chapter 3 and choosing $\lambda = 0.9$, which means a decay rate of $\alpha_1 = 10.53$ for the first operating mode and $\alpha_2 = 1.75$ for the second operating mode, it is possible to individually design two compensators that both lead to stable closed-loop systems when running without switching, as shown in Fig. 22. However, when implemented in a switching fashion, the synthesized compensators do not perform properly, eventually leading to an unstable closed-loop behavior as seen in Fig. 23.
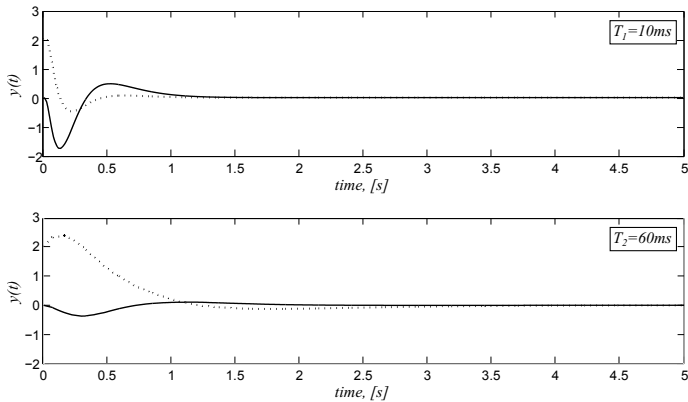
Figure 22 – Systems output for $T_1 = 10$ms and $T_2 = 60$ms.
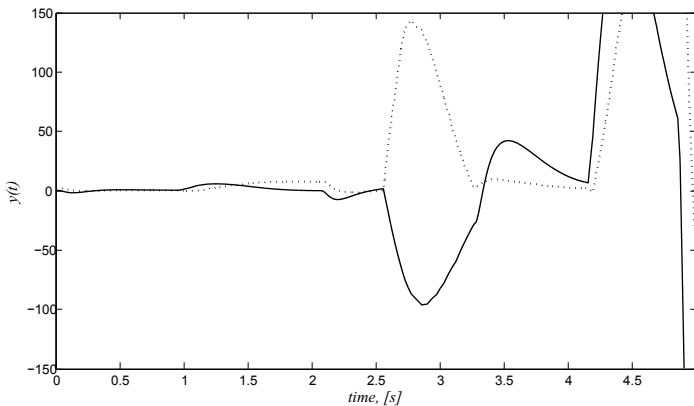
Figure 23 – System output without switching sampling intervals design.
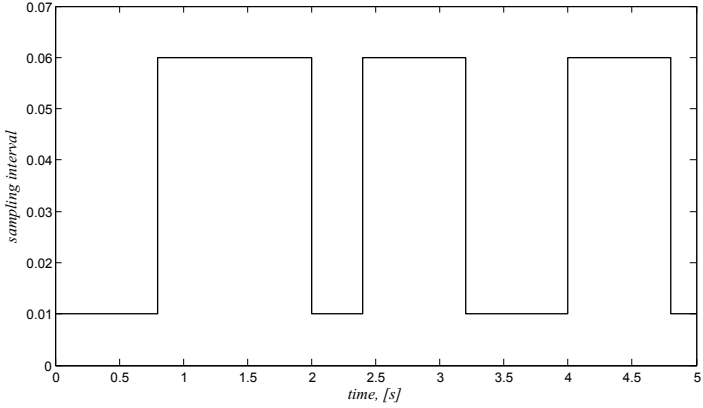
Figure 24 – Switching sampling intervals sequence.
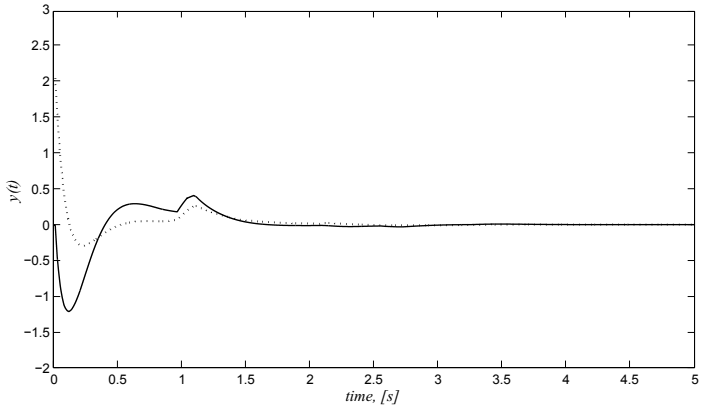
Figure 25 – System outputs with switching sampling intervals design.

On the other hand, when applying the switching design from Proposition 5.4, a feasible solution is reached for the same set of operating modes induced by T_1 and T_2. This means that the obtained compensators may be arbitrarily switched, along with the sampling intervals, preserving closed-loop stability. Indeed, for the same switching sampling intervals sequence used before (which is shown in Fig. 24), as well as the same delay sequence, the closed-loop simulation achieves a better performance, as can be seen in Fig. 25.

5.5 CONCLUSION

A switching compensator design has been discussed in this chapter, where it was considered that the control system may operate with several different sampling intervals. In addition, the switching between two distinct operating modes was allowed to be arbitrarily performed at runtime, in the sense that it may occur once every sampling interval. Sufficient conditions formulated as LMI were used to describe the switching closed-loop stability, which distinguished from the previous results by an additional index related to the switching sampling interval. Despite being presented as en extension to the delay-dependent dynamic output feedback compensator design from Chapter 3, a similar strategy can also be used based on delay estimates. An example has been provided to illustrate the proposed method.

6 A CO-DESIGN STRATEGY FOR NCS

As previously stated, an important characteristic of a Networked Control System is its multidisciplinary scope. Thus, in this chapter a more in-depth co-design strategy for NCS is depicted, considering not only a delay-dependent control design, but also a more comprehensive control system design with respect to the communication network usage and its consequences.

Especially, it has to be noted that the network bandwidth is limited in practice, thus, the shared resource usage has to be accordingly scheduled, so all deadlines can still be met. Furthermore, there might be particular performance requirements for each system that still have to be fulfilled, independently of the communication over network effects, such as time-varying delays. Thus, an integration of controller design and resource allocation is important for NCS (Fig. 26).

Figure 26 – Control and scheduling co-design.

In this context, two main issues appear when dealing with control and scheduling co-design procedures (SALA et al., 2010):

- Given an available resource utilization level, obtain the best possible control performance;

- Given a required control performance, obtain the lowest needed resource utilization level.

Instead of focus in only one of these issues, the idea is to design a system that can deal with both situations, switching between them at runtime given some operating condition (either a network constraint or a plant performance constraint).

Thereby, starting from the delay dependent compensator design methods, a co-design strategy is derived in order to give a more general co-design aspect, other than just using the current delay information at runtime. The main objective of the strategy presented here is with respect to the utilization level of the communication network, controlled

by a supervisor, the Resource Manager (RM), as depicted in Fig. 27. The main objective is to not waste resource, guaranteeing an efficient usage of the network by the real-time control systems and some other manufacturing related devices.
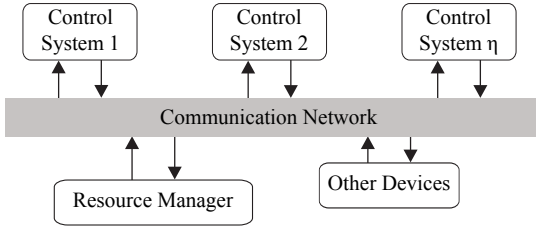
Figure 27 – NCS with shared medium controlled by an RM.

6.1 CO-DESIGN STRATEGY

The overall co-design procedure is partitioned into two parts: an off-line design and an online implementation. The off-line design is mostly based on guaranteeing some performance level for closed-loop systems, through the switching sampling intervals compensator design, while also taking into account the schedulability constraint for the sampling interval assignments.

Switching design is required due to the varying available bandwidth that may happen at runtime. This is briefly shown in Fig. 28, where at κT, after *task 4* had been granted access to the network, the other tasks had their intervals changed from a nominal $\underline{T}_\ell$ to a larger $\bar{T}_\ell$.

The online implementation, in other hand, comprises how to switch between different sampling intervals, once the sampling intervals are not constant. Both parts are presented with more details in the following.

6.1.1 Off-line Design

In an NCS, it is important that all data sent through the shared network meet their deadlines. Thus, a schedulability analysis has to be performed, which directly depends on the MAC protocol that is used.
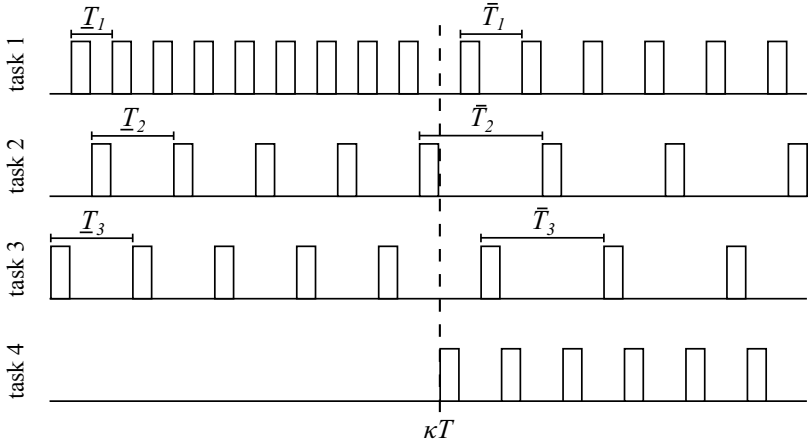
Figure 28 – Varying available bandwidth.

Here, a general case is considered, where a rate monotonic strategy is used for message scheduling (with non preemptive tasks, for it is not possible to pause a packet transmission after it has already began).

Thereby, to guarantee schedulability of a set of η control tasks running with sampling intervals $\underline{T}_\ell$, $\ell = 1, \ldots, \eta$, it is sufficient to verify the following condition (LIU; LAYLAND, 1973):

$$\sum_{\ell=1}^{\eta} \frac{c_\ell}{\underline{T}_\ell} \leq \mathcal{U}_{\max} = \eta(2^{\frac{1}{\eta}} - 1), \tag{6.1}$$

where c_ℓ is the time needed for a control task ℓ to complete its execution loop, and $\mathcal{U}_{\max}$ is the available utilization level of the shared resource when only the control systems have access to the network.

Notice that, guaranteeing condition (6.1) for a set of control tasks running with nominal sampling intervals $\underline{T}_\ell$, also guarantees the schedulability under the same bandwidth utilization bound, $\mathcal{U}_{\max}$, if any control system is switched to operate with a larger sampling interval $\bar{T}_\ell$.

Furthermore, assuming that all control system may have two operating modes and the available bandwidth may vary at runtime, a utilization table can be associated to the bandwidth required by the control systems, $\mathcal{U}_{\text{req}}$, with the respective operating mode combination, such that the overall NCS continues to operate properly.

In Table 4, an example of a utilization table considering two

control systems is depicted. Note that the first combination, $\mathcal{U}_{\text{req,max}}$, is related to all controllers running with nominal sampling interval $\underline{T}_\ell$, i.e., using the maximum available bandwidth. On the other hand, the last combination, $\mathcal{U}_{\text{req,min}}$, is related to all controllers running with their respective larger $\bar{T}_\ell$, i.e., the minimum bandwidth requirement. All other combinations satisfy the relation: $\mathcal{U}_{\text{req,min}} < \mathcal{U}_{\text{req},i} < \mathcal{U}_{\text{req,max}}$.

Table 4 – Utilization table.

$\mathcal{U}_{\text{req}}$	T_1	T_2
$\mathcal{U}_{\text{req,max}} \leq \mathcal{U}_{\text{max}}$	$\underline{T}_1$	$\underline{T}_2$
$\mathcal{U}_{\text{req,2}}$	$\underline{T}_1$	$\bar{T}_2$
$\mathcal{U}_{\text{req,3}}$	$\bar{T}_1$	$\underline{T}_2$
$\mathcal{U}_{\text{req,min}}$	$\bar{T}_1$	$\bar{T}_2$

6.1.1.1 On the Controller Synthesis

With respect to the controllers design, and consequently the switching sampling intervals, it is assumed that each plant ℓ can be described by a continuous and linear time-invariant dynamical system:

$$\mathcal{P}_\ell = \begin{cases} \dot{x}_\ell(t) = M_\ell x_\ell(t) + N_\ell u_\ell(t) \\ y_\ell(t) = C_\ell x_\ell(t) \end{cases} \quad \forall \ell = 1, \ldots, \eta$$

which, by performing an exact discretization between two consecutive sampling instants, leads to:

$$\mathcal{P}_{\ell,v} = \begin{cases} x_{\ell,k+1} = A_{\ell,v_\ell} x_{\ell,k} + \tilde{\Gamma}_{\ell,v_\ell}(\tau_{\ell,k}) u_{\ell,k-1} + \Gamma_{\ell,v_\ell}(\tau_{\ell,k}) u_{\ell,k} \\ y_{\ell,k} = C_\ell x_{\ell,k} \end{cases}$$

$\forall \ell = 1, \ldots, \eta$ and $\forall v_\ell = 1, \ldots, N_{v_i}$.

Thus, a set of switching dynamic output feedback compensators

$$\mathcal{K}_{\ell,v} = \begin{cases} \zeta_{\ell,k+1} = \mathcal{A}_{\ell,v_\ell}(\tau_{\ell,k}) \zeta_{\ell,k} + \mathcal{B}_{\ell,v_\ell}(\tau_{\ell,k}) y_{\ell,k} \\ u_{\ell,k+1} = \mathcal{C}_{\ell,v_\ell}(\tau_{\ell,k}) \zeta_{\ell,k} + \mathcal{D}_{\ell,v_\ell}(\tau_{\ell,k}) y_{\ell,k} \end{cases}$$

$\forall \ell = 1, \ldots, \eta$ and $\forall v_\ell = 1, \ldots, N_{v_\ell}$, is synthesized.

Specially, for each plant, a compensator can be designed for the nominal sampling interval, $\underline{T}_\ell$, and next, using the switching design procedure presented in Chapter 5, perform a search for a second compensator with a larger sampling interval, $\bar{T}_\ell$, such that the desired switching closed-loop performance is guaranteed.

Moreover, with respect to the time-varying delays, observe that the upper bounds may be different for each sampling interval used in the switching compensator design. Actually, this is also related to the preferences used by the control systems to access the shared resource. In this thesis, however, a case where the maximum delay bound is always equal to the sampling interval is assumed, no matter which one is currently being used.

6.1.1.2 Off-line Design Algorithm

Then, based on the delay-dependent compensator design methods previously presented in this thesis, and on condition (6.1), an off-line design procedure can be performed, as depicted in Fig. 29 and briefly described as follows.

1. Choose a set of nominal sampling intervals, such that $\sum_{\ell=1}^{\eta} \frac{c_\ell}{\underline{T}_\ell} = \mathcal{U}_{\max}$, i.e., assuming that only the η control systems have access to the network;

2. Design *nominal controllers* $(\mathcal{K}_{\ell,0})$ for each process ℓ, based on $\underline{T}_\ell$, such that all particular performance requirements are met;

3. Design the switching controllers for each plant (searching for larger sampling intervals $\bar{T}_\ell$), while also guaranteeing switching closed-loop stability;

4. Create a utilization table considering all possible operating mode combinations, with respect to the nominal, $\underline{T}_\ell$, and larger, $\bar{T}_\ell$, sampling intervals of each control task.

Some clarification may be held here. First, with respect to the choice of the nominal sampling intervals, an initial guess might be an equal distribution of the shared resource. Still, this may need some tunning.

In the nominal controller design, one is more interested in a better performance level for each system given some requirements and the
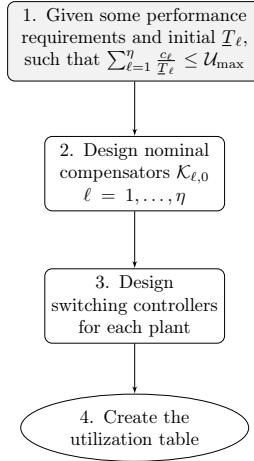
Figure 29 – Off-line co-design procedure.

resource limitation. To perform this, some parameters may have to be adjusted until the desired performance level is achieved, such as decay rate, TSA approximation order, or even sampling interval. In the last case, notice that the schedulability condition (6.1) has to be verified, which means that decreasing the sampling interval of a control system may require to increase some of the other control system sampling intervals.

The second controller design is with respect to the search for a larger sampling interval $\bar{T}_\ell$, or low bandwidth operating mode, thus, typically admitting a performance degradation with respect to the decay rate, as previously commented in Chapter 5. This step aims basically at guaranteeing the switching closed-loop system stability.

Notice that Step 2 and Step 3 may actually be interpreted as a single step, depending on how the switching compensators are designed.

6.1.2 Online Implementation

The online part of the co-design procedure is related to the switching between operating modes, thus, it directly depends on the utilization table created on the off-line design. A RM is handled by a higher priority supervisor task, which coordinates the overall access to the communication channel according to the following rules:

- there are other manufacturing related devices that may, or may not, use the network;
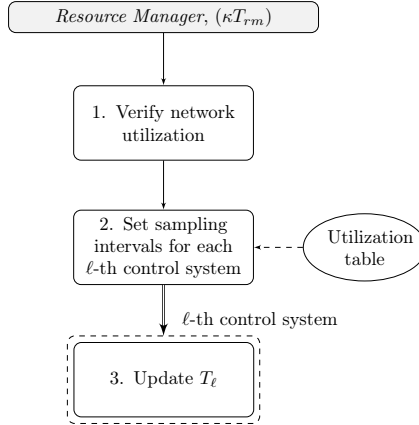
Figure 30 – On-line sampling interval assignment.

- the RM has the knowledge of the utilization level of all tasks, and it is allowed to perform a re-scheduling policy once at every time interval T_{rm};

- the RM aims at avoiding waste of resource, thus it always chooses an overall utilization level as high as possible;

- control system sampling intervals are switched at runtime according to the previously created utilization table;

- every control system operating mode has a sampling interval that is smaller than the RM execution interval, i.e., $T_\ell \leq T_{rm}$, $\forall \ell = 1, \ldots, \eta$.

Thereby, the online procedure can be briefly described as follows (also depicted in Fig. 30):

1. At every instant κT_{rm}, the RM verifies the network utilization, granting or not the medium access to other devices and defining an available bandwidth to the set of NCSs;

2. Based on the utilization table, the RM re-assigns the sampling intervals to the control systems;

3. Each control system updates its sampling interval accordingly.

6.2 EXAMPLE

To illustrate the proposed strategy, a set of three continuous linear time-invariant processes is considered as follows. The first one is a second-order system with dynamic matrices:

$$M_1 = \begin{bmatrix} 0 & 1 \\ 288.24 & 0 \end{bmatrix}, \quad N_1 = \begin{bmatrix} 0 \\ -73.53 \end{bmatrix}, \quad C_1 = \begin{bmatrix} 1 & 0 \end{bmatrix},$$

which gives the eigenvalues: 16.9775 and -16.9775. The second one has its dynamics described by:

$$M_2 = \begin{bmatrix} 1.380 & -0.208 & 6.715 & -5.676 \\ -0.581 & -4.290 & 0 & 0.675 \\ 1.067 & 4.273 & -6.654 & 5.893 \\ 0.048 & 4.273 & 1.343 & -2.104 \end{bmatrix},$$

$$N_2 = \begin{bmatrix} 0 & 0 \\ 5.679 & 0 \\ 1.136 & -3.146 \\ 1.136 & 0 \end{bmatrix}, \quad C_2 = \begin{bmatrix} 1 & 0 & 1 & -1 \\ 0 & 1 & 0 & 0 \end{bmatrix},$$

and has the eigenvalues: 1.99, 0.0585, -5.0484 and -8.6681. Finally, the third one is given by a first-order model with dynamic matrices:

$$M_3 = \frac{5}{100}, \quad N_3 = \frac{1}{1000}, \quad C_3 = 1.$$

A CAN network is used for simulation, with a rate monotonic medium access control algorithm. The data transfer speed is 250Kbps, which for a packet size of 108bits and computation time $\tau_{cc} = 0.5$ms gives a minimum delay $\tau_{min} \approx 1.4$ms. The maximum delay is always assumed to be equal to the current sampling interval and the execution time for each control task is $c_\ell \approx 2.65$ms, $\forall \ell = 1, \ldots, \eta$. Furthermore, for the online simulation, it is assumed that the resource manager runs once every $T_{rm} = 0.5$s.

From the sufficient schedulability condition (6.1), the shared resource utilization bound for when only the set of control systems is using the network is $\mathcal{U}_{max} = 0.7797$. Thus, in order to fulfil this requirement, the off-line design is started with an equal distribution of the bandwidth, which means a nominal sampling interval equal to 10.2ms for each control system. After some tunning, looking for more convenient sampling intervals as well as suitable individual performances,

the following nominal sampling intervals and contractivity coefficients are established:

$$\underline{T}_1 = 8\text{ms}, \quad \underline{T}_2 = 10\text{ms}, \quad \underline{T}_3 = 15\text{ms},$$
$$\lambda_1 = 0.95, \quad \lambda_2 = 0.90, \quad \lambda_3 = 0.96,$$

which gives a utilization of $\mathcal{U}_{\text{req,max}} = 0.7729$.

Then, using the switching control synthesis presented in Chapter 5, delay dependent compensators are designed for each plant ℓ, with the following larger sampling intervals:

$$\bar{T}_1 = 24\text{ms}, \quad \bar{T}_2 = 60\text{ms}, \quad \bar{T}_3 = 60\text{ms}.$$

Notice that the parameter λ_ℓ is the same for both operating modes of plant ℓ, and that the minimum utilization level required for the set of control systems is $\mathcal{U}_{\text{min}} \approx 0.20$. Moreover, for this example, the search for a larger sampling interval $\bar{T}_\ell$ has been performed considering multiples of the nominal sampling interval $\underline{T}_\ell$.

Two simulations are performed, both running for 5s but considering two distinct variation of the resource availability. In the first one, the available bandwidth for the control systems varies according to the graphic shown in Fig. 31.

Observe that only at 4.5s the full bandwidth capacity is made available to the set of NCS. Still, the closed-loop systems are all stables and reach the equilibrium, even after some perturbations (square pulse for plants 1 and 2, and a step for plant 3) have been added to the states of the plants after time $t = 2$s, as depicted in Fig. 32, Fig. 33 and Fig. 34. In addition, notice that the dashed vertical lines indicate when the respective sampling intervals were switched.

For the second simulation, the variation of the resource availability is depicted in Fig. 35, whereas the system outputs are depicted in Fig. 36, Fig. 37 and Fig. 38. For this case, notice that between 2.5s and 3.5s only the minimum utilization level required by the set of control systems is available, yet the closed-loop systems have appropriate performances.

6.3 CONCLUSION

An integrated control design and resource management strategy was studied in this chapter, taking into account a possible varying amount of bandwidth, available to the control systems. The proposed
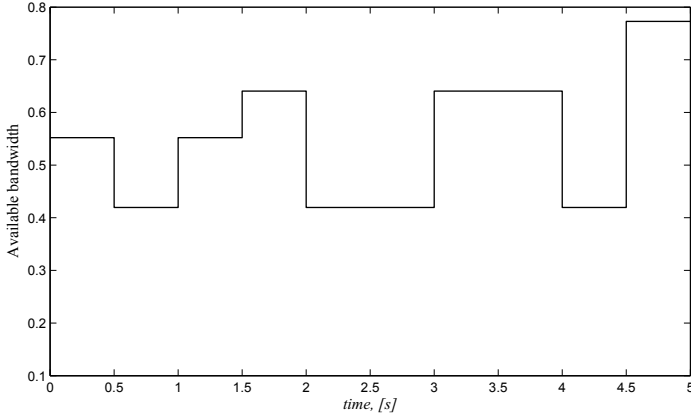
Figure 31 – Available bandwidth for the control systems.
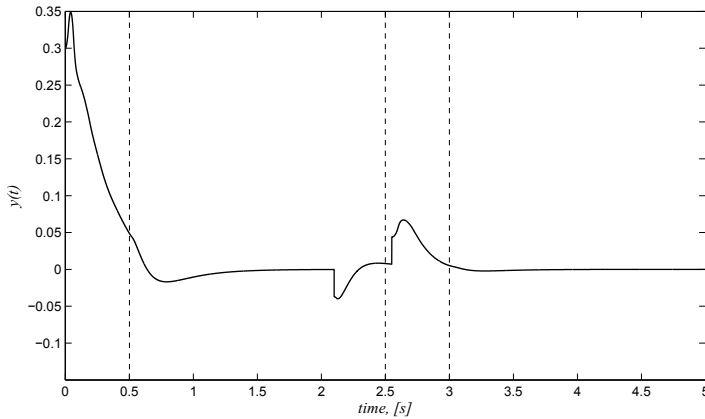
Figure 32 – Output of system 1.

strategy assumes a resource manager that has the knowledge of all devices that access the communication network, and thus, it can control the bandwidth distribution among all of them, given some arbitrary conditions. For instance, it has been considered that other manufacturing related devices may use the communication channel, which is then regulated by the RM, allowing or not the access.

The overall design procedure was divided in two parts. First, the off-line design, mainly based on the switching compensators design for each particular plant, respecting a shared resource constraint due to
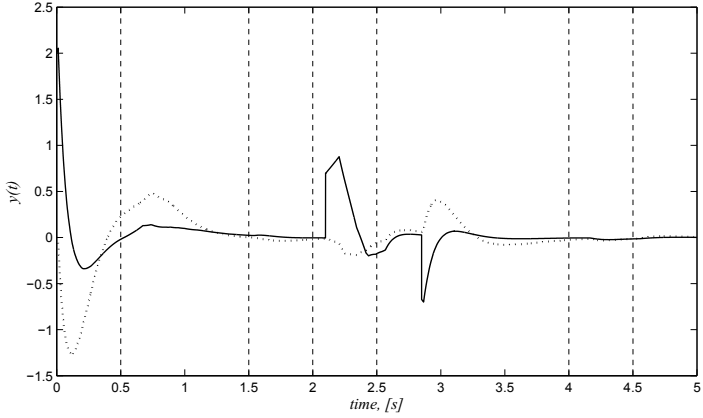
Figure 33 – Output of system 2.
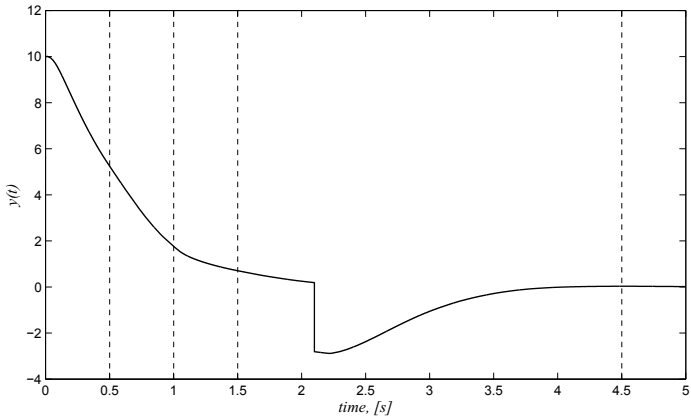
Figure 34 – Output of system 3.

the limited available bandwidth. Second, the on-line implementation governed by the resource manager, which investigates how each control switches between modes. A simulation experiment with three control systems sharing a single network has been provided, illustrating the proposed approach.
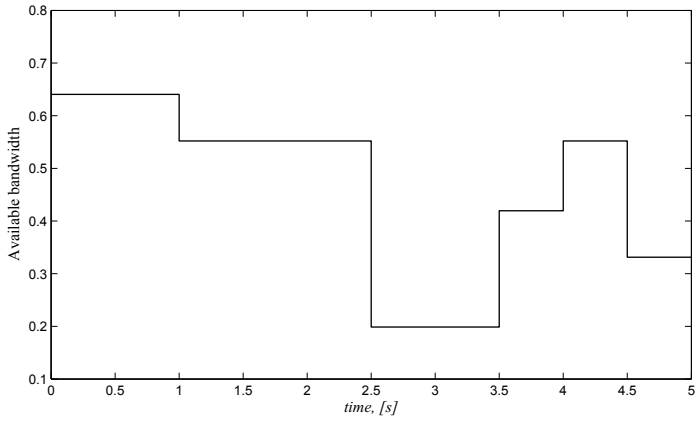
Figure 35 – Available bandwidth for the control systems.
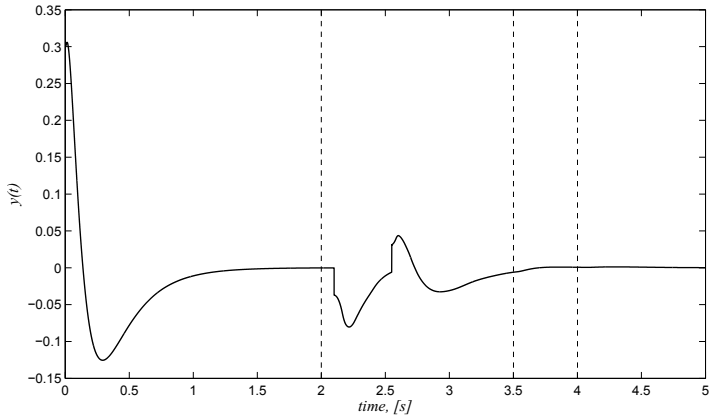
Figure 36 – Output of system 1.
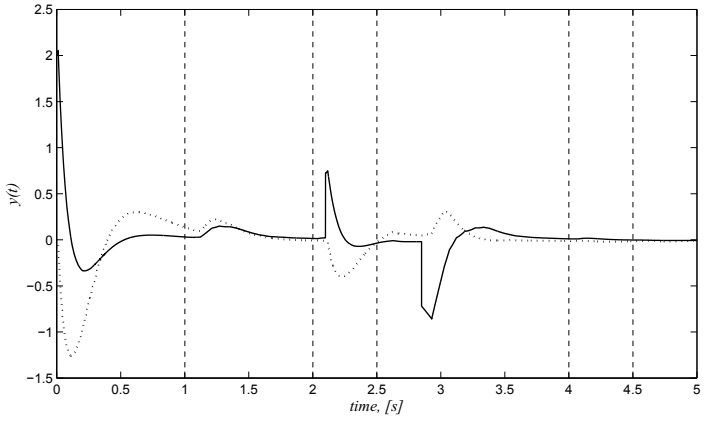
Figure 37 – Output of system 2.
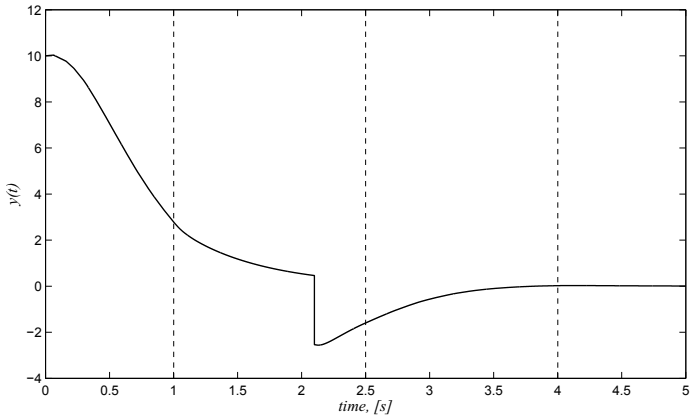
Figure 38 – Output of system 3.

7 CONCLUSION

In this thesis, novel approaches for parameter-dependent output feedback compensator design for a class of networked control systems have been issued. The proposed strategies are based either on the actual time-varying delay or on a delay estimate, which can be evaluated at runtime in both cases. Moreover two general cases have been addressed, first assuming only a single plant controlled over a network, and later extending to a more comprehensive design procedure, considering a set of plants and controllers sharing a limited communication resource. Examples were provided over the document, in order to illustrate the proposed techniques.

At first, in Chapter 2, features and mathematical models were presented for class of NCS, as well as a brief illustration of a possible effect of time-varying delays on the closed-loop system. It is important to remark that the mathematical models were derived based on an exact discretization of the plant at the sampling instants, resulting in a convex polytopic representation with additional norm-bounded uncertainty, due to delay dependency on the system dynamics.

Next, in Chapter 3 and Chapter 4, synthesis of parameter-dependent dynamic output feedback compensator are discussed, taken into account the possibility to acquire information about the time-varying delays at runtime, either the actual time-varying delay or a delay estimate, respectively. In both cases, a single plant was assumed to be controlled over a network, that could provide the required QoS.

In Chapter 5 the control synthesis were extended for the case where the control system may have several operating modes, with different sampling intervals arbitrarily performing the switching between them at runtime. The method was presented with respect to the controller design from Chapter 3. Nevertheless, a similar strategy based on delay estimates can also be derived, with minor modifications.

Later, in Chapter 6, the proposed switching control synthesis was used in the off-line part of a more comprehensive NCS design. A schedulability test for the communication network usage was also introduced in the control and resource management co-design procedure, in order to provide the required QoS. An online operating mode was also depicted, based on a maximization of the resource utilization and controlled by a resource manager task.

7.1 CONTRIBUTIONS OF THE THESIS

Prior to this document, the contributions of the research carried over this PhD include the following journal articles:

- Moraes, Castelan & Moreno (2013). Full-Order Dynamic Output Feedback Compensator For Time-Stamped Networked Control Systems. *Journal of Control, Automation and Electrical Systems*, volume 24, pp. 22–32, which comprises the control synthesis methodology presented in Chapter 3;

- Jungers, Moraes, Castelan & Moreno (2013). A Dynamic Output Feedback Controller for NCS based on Delay Estimates. *Automatica*, volume 49, pp. 788–792, which comprises the control synthesis methodology presented in Chapter 4;

and also the following papers, published in conference proceedings:

- Moraes, Castelan & Moreno (2012). Dynamic Output Feedback Compensator for Time-stamped Networked Control System. In: *Proceedings of XIX Congresso Brasileiro de Automática*, Campina Grande - PB, Brazil, pp. 3782–3787;

- Moraes, Castelan & Moreno (2011). Síntese de Compensador Dinâmico de Saída para Sistemas Controlados via Rede. In: *Proceedings of the X Simpósio Brasileiro de Automação Inteligente*, São João del Rei - MG, Brazil, pp. 516–521.

- Moraes, Jungers, Moreno & Castelan (2014). Sampling Period Assignment: A Cooperative Design Approach. In: *Proceedings of the 53rd IEEE Conference on Decision and Control*, Los Angeles - CA, USA, which comprises a work developed throughout the internship at Centre de Recherche en Automatique de Nancy - CRAN, under supervision of former researcher Marc Jungers.

7.2 PERSPECTIVES

Among some possible extensions to the work presented in this thesis, the following research directions can be mentioned:

- Investigate switching rules coordinated by a resource manager, along with the related operating procedures, possibly based on the bandwidth utilization;

- Inspect the feasibility of switching rules coordinated locally by the control systems, possibly based on the control performance, taking into account the task set schedulability as well as the concept of not wasting shared resources;

- Extend the stability conditions and compensator synthesis assuming some nonlinear behavior of the plant and/or control system, such as sector-bounded non-linearities and saturated actuators;

- Analyze the effects of using quantized data and limited data transmission, due to the digital nature of the networked control system devices and communication protocols;

- Analyze and explore the use of the Resource Manager execution interval T_{rm}, possibly by relating it to the concept of dwell-time existing in the stability theory for switching systems.

REFERENCES

AL-AREQI, S.; GÖRGES, D.; LIU, S. Robust control and scheduling codesign for networked embedded control systems. In: *Decision and Control and European Control Conference (CDC-ECC), 2011 50th IEEE Conference on.* [S.l.: s.n.], 2011. p. 3154–3159.

ÅRZÉN, K.-E.; BERNHARDSSON, B.; EKER, J.; CERVIN, A.; NILSSON, K.; PERSSON, P.; SHA, L. Integrated control and scheduling. *Technical Report ISRN LUTFD2/TFRT–7586–SE, Department of Automatic Control*, 1999.

ÅSTRÖM, K. J. *Introduction to stochastic control theory*. New York: Academic press, 1970. (Mathematics in Science and Engineering).

ÅSTRÖM, K. J.; WITTENMARK, B. *Computer-Controlled Systems: Theory and Design*. [S.l.]: Prentice Hall, 1997.

BOUYSSOUNOUSE, B.; SIFAKIS, J. *Embedded Systems Design: The ARTIST Roadmap for Research and Development*. [S.l.]: Springer, 2005. (Lecture Notes in Computer Science / Programming and Software Engineering).

BOYD, S.; GHAOUI, L. E.; FERON, E.; BALAKRISHNAN, V. *Linear Matrix Inequalities in System and Control Theory*. Philadelphia, USA: Society for Industrial and Applied Mathematics, 1994.

CAC, N. T.; KHANG, N. V. A Co-Design for CAN-Based Networked Control Systems. *Automation, Control and Intelligent Systems*, v. 2, n. 1, p. 6–15, 2014.

CASTELAN, E. B.; LEITE, V. J. S.; MIRANDA, M. F.; MORAES, V. M. Synthesis of output feedback controllers for a class of nonlinear parameter-varying discrete-time systems subject to actuators limitations. In: *American Control Conference, ACC'10*. Baltimore, USA: [s.n.], 2010. p. 4235–4240.

CERVIN, A.; EKER, J.; BERNHARDSSON, B.; ÅRZÉN, K.-E. Feedback-Feedforward Scheduling of Control Tasks. *Real-Time Systems*, Kluwer Academic Publishers, norwell, MA, USA, v. 23, n. 1/2, p. 25–53, July 2002.

CERVIN, A.; HENRIKSSON, D.; LINCOLN, B.; EKER, J. E.; ÅRZÉN, K.-E. How Does Control Timing Affect Performance? Analysis and Simulation of Timing Using Jitterbug and TrueTime. *IEEE Control Systems Magazine*, v. 23, n. 3, p. 16–30, 2003.

CERVIN, A.; HENRIKSSON, D.; LINCOLN, B.; EKER, J.; ÅRZÉN, K.-E. How Does Control Timing Affect Performance? Analysis and Simulation of Timing Using Jitterbug and TrueTime. *IEEE Control Systems Magazine*, v. 23, n. 3, p. 16–30, June 2003.

CERVIN, A.; VELASCO, M.; MARTÍ, P.; CAMACHO, A. Optimal Online Sampling Period Assignment: Theory and Experiments. *Control Systems Technology, IEEE Transactions on*, v. 19, n. 4, p. 902–910, July 2011.

CLOOSTERMAN, M.; WOUW, N. van de; HEEMELS, M.; NIJMEIJER, H. Robust Stability of Networked Control Systems with Time-varying Network-induced Delays. In: *Decision and Control, 2006 45th IEEE Conference on.* [S.l.: s.n.], 2006. p. 4980–4985.

CLOOSTERMAN, M. B. G.; HETEL, L.; WOUW, N. van de; HEEMELS, W.; DAAFOUZ, J.; NIJMEIJER, H. Controller synthesis for networked control systems. *Automatica*, Elsevier, v. 46, n. 10, p. 1584–1594, 2010.

DAAFOUZ, J.; RIEDINGER, P.; IUNG, C. Stability analysis and control synthesis for switched systems: a switched Lyapunov function approach. *Automatic Control, IEEE Transactions on*, v. 47, n. 11, p. 1883–1887, Nov. 2002.

DONKERS, M.; HETEL, L.; HEEMELS, W. P. M. H.; WOUW, N. van de; STEINBUCH, M. Stability Analysis of Networked Control Systems Using a Switched Linear Systems Approach. In: MAJUMDAR, R.; TABUADA, P. (Ed.). *Hybrid Systems: Computation and Control.* [S.l.]: Springer Berlin / Heidelberg, 2009, (Lecture Notes in Computer Science, v. 5469). p. 150–164.

DRITSAS, L.; NIKOLAKOPOULOS, G.; TZES, A. On the modeling of networked controlled systems. In: *Control Automation, 2007. MED '07. Mediterranean Conference on.* Athens, Greece: [s.n.], 2007. p. 1–5.

DRITSAS, L.; TZES, A. Robust Output Feedback Control of Networked Systems. In: *Proceedings of the 9th European Control Conference.* Kos, Greece: [s.n.], 2007. p. 3939–3945.

EKER, J.; HAGANDER, P.; ÅRZÉN, K.-E. A feedback scheduler for real-time controller tasks. *Control Engineering Practice*, v. 8, n. 12, p. 1369–1378, 2000.

ENGWERDA, J. *LQ Dynamic Optimization and Differential Games*. Chichester: Wiley, 2005.

FRANKLIN, G. F.; POWELL, J. D.; WORKMAN, M. L. *Digital Control of Dynamic Systems*. California, USA: Prentice Hall, 1997.

GAO, H.; MENG, X.; CHEN, T.; LAM, J. Stabilization of Networked Control Systems via Dynamic Output-Feedback Controllers. *SIAM Journal on Control and Optimization*, Society for Industrial and Applied Mathematics, Philadelphia, PA, USA, v. 48, n. 5, p. 3643–3658, Mar. 2010.

GIELEN, R.; OLARU, S.; LAZAR, M. On polytopic approximations of systems with time-varying input delays. *Nonlinear Model Predictive Control*, Springer, p. 225–233, 2009.

GUPTA, R. A.; CHOW, M. Y. Networked Control System: Overview and Research Trends. *Industrial Electronics, IEEE Transactions on*, v. 57, n. 7, p. 2527–2535, July 2010.

HEEMELS, W. P. M. H.; JOHANSSON, K. H.; TABUADA, P. An introduction to event-triggered and self-triggered control. In: *Decision and Control (CDC), 2012 IEEE 51st Annual Conference on*. [S.l.: s.n.], 2012. p. 3270–3285.

HEEMELS, W. P. M. H.; WOUW, N. van de. Stability and Stabilization of Networked Control Systems. In: BEMPORAD, A.; HEEMELS, M.; JOHANSSON, M. (Ed.). *Networked Control Systems*. [S.l.]: Springer Berlin / Heidelberg, 2010, (Lecture Notes in Control and Information Sciences, v. 406). p. 203–253.

HEEMELS, W. P. M. H.; WOUW, N. van de; GIELEN, R. H.; DONKERS, M. C. F.; HETEL, L.; OLARU, S.; LAZAR, M.; DAAFOUZ, J.; NICULESCU, S. Comparison of overapproximation methods for stability analysis of networked control systems. In: *Proceedings of the 13th ACM International Conference on Hybrid Systems: Computation and Control*. Stockholm, Sweden: [s.n.], 2010. p. 181–190.

HENRIKSSON, D.; CERVIN, A. Optimal On-line Sampling Period Assignment for Real-Time Control Tasks Based on Plant State

Information. In: *Decision and Control, 2005 and 2005 European Control Conference. CDC-ECC '05. 44th IEEE Conference on.* [S.l.: s.n.], 2005. p. 4469–4474.

HESPANHA, J. P.; NAGHSHTABRIZI, P.; XU, Y. A survey of recent results in networked control systems. *Proceedings of the IEEE*, v. 95, n. 1, p. 138–162, Jan. 2007.

HETEL, L.; DAAFOUZ, J.; IUNG, C. Stabilization of Arbitrary Switched Linear Systems With Unknown Time-Varying Delays. *IEEE Transactions on Automatic Control*, v. 51, n. 10, p. 1668–1674, 2006.

HETEL, L.; DAAFOUZ, J.; LUNG, C. LMI control design for a class of exponential uncertain systems with application to network controlled switched systems. In: *American Control Conference, ACC'07.* New York City, USA: [s.n.], 2007. p. 1401–1406.

HETEL, L.; DAAFOUZ, J.; RICHARD, J. P.; JUNGERS, M. Delay-dependent sampled-data control based on delay estimates. *Systems & Control Letters*, v. 60, n. 2, p. 146–150, 2011.

HRISTU-VARSAKELIS, D.; LEVINE, W. S. *Handbook of networked and embedded control systems.* [S.l.]: Birkhauser, 2005.

IZÁK, M.; GÖRGES, D.; LIU, S. Stabilization of systems with variable and uncertain sampling period and time delay. *Nonlinear Analysis: Hybrid Systems*, Elsevier, v. 4, n. 2, p. 291–305, 2010.

JI, K.; KIM, W. J. Optimal Bandwidth Allocation and QoS-adaptive Control Co-design for Networked Control Systems. *International Journal of Control, Automation, and Systems*, v. 6, n. 4, p. 596–606, 2008.

JIANG, C.; ZOU, D.; ZHANG, Q.; GUO, S. Quantized dynamic output feedback control for networked control systems. *Systems Engineering and Electronics, Journal of*, v. 21, n. 6, p. 1025–1032, Dec. 2010.

JUNGERS, M.; CASTELAN, E. B.; MORAES, V. M.; MORENO, U. F. A dynamic output feedback controller for NCS based on delay estimates. *Automatica*, v. 49, n. 3, p. 788–792, 2013.

JUNGERS, M.; CASTELAN, E. B.; TARBOURIECH, S.; DAAFOUZ, J. Finite $\mathcal{L}_2$-induced gain and λ-contractivity of discrete-time switching systems including modal nonlinearities and actuator saturations. *Nonlinear Analysis: Hybrid Systems*, v. 5, n. 2, p. 289–300, 2011.

KHLEBNIKOV, M. V.; SHCHERBAKOV, P. Petersen's lemma on matrix uncertainty and its generalizations. *Automation and Remote Control*, MAIK Nauka/Interperiodica distributed exclusively by Springer Science+Business Media LLC., v. 69, p. 1932–1945, 2008.

KUHN, H. W.; TUCKER, A. W. Nonlinear programming. In: NEYMAN, J. (Ed.). *Proceedings of the Second Berkeley Symposium on Mathematical Statistics and Probability.* [S.l.]: University of California Press, Berkeley, California, 1951. p. 481–492.

LAILA, D.; NEŠIĆ, D.; ASTOLFI, A. Sampled-data Control of Nonlinear Systems. In: LORÍA, A.; LAMNABHI-LAGARRIGUE, F.; PANTELEY, E. (Ed.). *Advanced Topics in Control Systems Theory.* [S.l.]: Springer Berlin / Heidelberg, 2006, (Lecture Notes in Control and Information Sciences, v. 328). p. 91–137.

LIU, C. L.; LAYLAND, J. W. Scheduling Algorithms for Multiprogramming in a Hard-Real-Time Environment. *J. ACM*, ACM, New York, NY, USA, v. 20, n. 1, p. 46–61, Jan. 1973.

MAHMOUD, M. S. Output-Feedback Control for Networked Systems with Probabilistic Delays. In: *Proceedings of the World Congress on Engineering.* [S.l.: s.n.], 2013. v. 2.

MAHMOUD, M. S.; KHAN, G. D. Dynamic output feedback of networked control systems with partially known Markov chain packet dropouts. *Optimal Control Applications and Methods*, John Wiley & Sons, Ltd, 2013.

MIETTINEN, K. Some Methods for Nonlinear Multi-Objective Optimization. In: ZITZLER, E.; DEB, K.; THIELE, L.; COELLO, C. A. C.; CORNE, D. (Ed.). *Evolutionary Multi-Criterion Optimization, First International Conference, EMO 2001, Zurich, Switzerland, March 2001, Proceedings.* Berlin, Heidelberg: Springer-Verlag, 2001. p. 1–20.

MONTESTRUQUE, L. A.; ANTSAKLIS, P. J. State and output feedback control in model-based networked control systems. In: *Decision and Control, 2002, Proceedings of the 41st IEEE Conference on.* Las Vegas, USA: [s.n.], 2002. v. 2, p. 1620–1625.

MORAES, V. M.; CASTELAN, E. B.; MORENO, U. F. Síntese de Compensador Dinâmico de Saída para Sistemas Controlados via Rede. In: *Proceedings of the X Simpósio Brasileiro de Automação Inteligente - SBAI'11.* São João del Rei, MG, Brasil: [s.n.], 2011.

MORAES, V. M.; CASTELAN, E. B.; MORENO, U. F. Dynamic Output Feedback Compensator for Time-Stamped Networked Control System. In: *Proceedings of the XIX Congresso Brasileiro de Automática - CBA'12*. Campina Grande, PB, Brasil: [s.n.], 2012. p. 3782–3787.

MORAES, V. M.; CASTELAN, E. B.; MORENO, U. F. Full-Order Dynamic Output-Feedback Compensator for Time-Stamped Networked Control Systems. *Journal of Control, Automation and Electrical Systems*, Springer, US, v. 24, n. 1-2, p. 22–32, 2013.

MORAES, V. M.; FOLETTO, T. C.; CASTELAN, E. B.; MORENO, U. F. Realimentação de Estados com Ganhos Variantes para uma Classe de Sistemas de Controle via Rede. In: *Proceedings of the XVIII Congresso Brasileiro de Automática - CBA'10*. Bonito, MS, Brasil: [s.n.], 2010. p. 4669–4676.

MORAES, V. M.; JUNGERS, M.; CASTELAN, E. B.; MORENO, U. F. Sampling Period Assignment: A Cooperative Design Approach. In: *Decision and Control (CDC), 2014 IEEE 53rd Annual Conference on*. Los Angeles, CA, USA: [s.n.], 2014.

MOYNE, J. R.; TILBURY, D. M. The Emergence of Industrial Control Networks for Manufacturing Control, Diagnostics, and Safety Data. *Proceedings of the IEEE*, v. 95, n. 1, p. 29–47, Jan. 2007.

NAGHSHTABRIZI, P.; HESPANHA, J. P. Designing an observer-based controller for a network control system. In: *Decision and Control, 2005 and 2005 European Control Conference. CDC-ECC '05. 44th IEEE Conference on*. [S.l.: s.n.], 2005. p. 848–853.

NGUYEN, X. H.; JUANOLE, G. Design of Networked Control Systems (NCSs) on the basis of interplays between Quality of Control and Quality of Service. In: *In Proceedings of 7th IEEE International Symposium on Industrial Embedded Systems (SIES'12)*. [S.l.: s.n.], 2012. p. 1–9.

NILSSON, J. *Real-time control systems with delay*. Tese (PhD thesis) — Automatic Control Department, Lund Institute of Technology, Lund, Sweden, 1998.

OLIVEIRA, M. C. de; GEROMEL, J. C.; BERNUSSOU, J. Extended H_2 and H_∞ norm characterizations and controller parametrizations for discrete-time systems. *International Journal of Control*, Taylor & Francis, v. 75, n. 9, p. 666–679, 2002.

PETERSEN, I. R. A stabilization algorithm for a class of uncertain linear systems. *Systems & Control Letters*, Elsevier Science Publishers B. V., Amsterdam, The Netherlands, v. 8, n. 4, p. 351–357, Mar. 1987.

RASOOL, F.; HUANG, D.; NGUANG, S. K. Robust output feedback control of discrete-time networked systems with limited information. *Systems & Control Letters*, v. 60, n. 10, p. 845–853, 2011.

RASOOL, F.; HUANG, D.; NGUANG, S. K. Robust H_∞ output feedback control of networked control systems with multiple quantizers. *Journal of the Franklin Institute*, v. 349, n. 3, p. 1153–1173, 2012.

RICHARD, J.-P. Time-delay systems: an overview of some recent advances and open problems. *Automatica*, v. 39, n. 10, p. 1667–1694, 2003.

SALA, A.; ARIÑO, C.; ROMERO, J.; SANCHIS, R. Optimal Selection of Sampling Rate in Multiple H_2 Control Loops. In: *ADVCOMP 2010, The Fourth International Conference on Advanced Engineering Computing and Applications in Sciences*. [S.l.: s.n.], 2010. p. 23–27.

SAUTER, D.; SID, M. A.; ABERKANE, S.; MAQUIN, D. Co-design of safe networked control systems. *Annual Reviews in Control*, v. 37, n. 2, p. 321–332, 2013.

SETO, D.; LEHOCZKY, J. P.; SHA, L.; SHIN, K. G. On task schedulability in real-time control systems. In: *Real-Time Systems Symposium, 1996, 17th IEEE*. [S.l.: s.n.], 1996. p. 13–21.

SHI, Y.; YU, B. Output Feedback Stabilization of Networked Control Systems With Random Delays Modeled by Markov Chains. *Automatic Control, IEEE Transactions on*, v. 54, n. 7, p. 1668–1674, July 2009.

SHI, Y.; YU, B. Robust mixed H_2/H_∞ control of networked control systems with random time delays in both forward and backward communication links. *Automatica*, v. 47, n. 4, p. 754–760, 2011.

TANG, X.; YU, J. Networked Control System: Survey and Directions. In: LI, K.; FEI, M.; IRWIN, G.; MA, S. (Ed.). *Bio-Inspired Computational Intelligence and Applications*. [S.l.]: Springer Berlin / Heidelberg, 2007, (Lecture Notes in Computer Science, v. 4688). p. 473–481.

TINDELL, K.; BURNS, A.; WELLINGS, A. J. Analysis of hard real-time communications. *Real-Time Systems*, Springer, v. 9, n. 2, p. 147–171, 1995.

TORNGREN, M.; HENRIKSSON, D.; ÅRZÉN, K.-E.; CERVIN, A.;
HANZALEK, Z. Tool supporting the co-design of control systems and
their real-time implementation: Current status and future directions.
In: *Computer Aided Control System Design, 2006 IEEE International
Conference on Control Applications, 2006 IEEE International
Symposium on Intelligent Control, 2006 IEEE.* [S.l.: s.n.], 2006. p.
1173–1180.

VELASCO, M.; FUERTES, J. M.; LIN, C.; MARTI, P.; BRANDT, S.
A control approach to bandwidth management in networked control
systems. In: *Industrial Electronics Society, 2004. IECON 2004. 30th
Annual Conference of IEEE.* [S.l.: s.n.], 2004. v. 3, p. 2343–2348.

WEIHUA, D.; MINRUI, F. Dynamic Output Feedback Control of
Uncertain Networked Control Systems. In: *Proceedings of the First
ACM/SIGEVO Summit on Genetic and Evolutionary Computation.*
New York, NY, USA: ACM, 2009. (GEC'09), p. 571–576.

WITTENMARK, B.; ÅSTRÖM, K. J.; ÅRZÉN, K.-E. *Computer
Control: An Overview.* [S.l.], Jan. 2002.

XIA, F.; SUN, Y. Control-Scheduling Codesign: A Perspective on
Integrating Control and Computing. *Dynamics of Continuous, Discrete
and Impulsive Systems*, v. 13, n. S1, p. 1352–1358, 2006.

YAN, H.; WAN, J.; LI, D.; TU, Y.; ZHANG, P. Codesign of networked
control systems: A review from different perspectives. In: *Cyber
Technology in Automation, Control, and Intelligent Systems (CYBER),
2011 IEEE International Conference on.* [S.l.: s.n.], 2011. p. 84–90.

YANG, T. C. Networked control system: a brief survey. *IEE
Proceedings-Control Theory and Applications*, v. 153, n. 4, p. 403–412,
2006.

YOO, Y. J.; KOO, J. H.; WON, S. C. Output feedback controller
design of networked control systems with nonlinearity: An LMI
approach. In: *SICE Annual Conference 2010, Proceedings of.* [S.l.: s.n.],
2010. p. 663–667.

ZHANG, H.; SHI, Y.; MEHR, A. S. Robust Static Output Feedback
Control and Remote PID Design for Networked Motor Systems.
Industrial Electronics, IEEE Transactions on, v. 58, n. 12, p. 5396–5405,
Dec. 2011.

ZHANG, J.; LAM, J.; XIA, Y. Output feedback delay compensation control for networked control systems with random delays. *Information Sciences*, v. 265, n. 0, p. 154–166, 2014.

ZHANG, L.; GAO, H.; KAYNAK, O. Network-Induced Constraints in Networked Control Systems: A Survey. *Industrial Informatics, IEEE Transactions on*, v. 9, n. 1, p. 403–416, Feb. 2013.

ZHANG, W.-A.; YU, L. New approach to stabilisation of networked control systems with time-varying delays. *Control Theory Applications, IET*, v. 2, n. 12, p. 1094–1104, Dec. 2008.

APPENDIX A – Decay Rate

A.1 DECAY RATE

In this thesis, the considered performance requirement for the design of discrete-time compensators is based on a notion of closed-loop decay rate. Such notion comes from a discrete-time interpretation of the continuous-time performance

$$\dot{V}(t) = \frac{dV(t)}{dt} < -\alpha V(t),$$

which, although not in a formal way, can be rewritten as

$$\frac{dV(t)}{V(t)} < -\alpha dt,$$

and when evaluated over any sampling interval

$$\int_{kT}^{(k+1)T} \frac{dV(t)}{V(t)} < \int_{kT}^{(k+1)T} -\alpha dt,$$

gives

$$\ln V\big((k+1)T\big) - \ln V\big(kT\big) < -\alpha\big((k+1)T - kT\big),$$

that leads to

$$\frac{V\big((k+1)T\big)}{V\big(kT\big)} < e^{-\alpha T},$$

and finally

$$\Delta V\big(kT\big) \triangleq V\big((k+1)T\big) - e^{-\alpha T} V\big(kT\big) < 0, \qquad \text{(A.1)}$$

where $\alpha \in \Re$ is the decay rate of the closed-loop system, with respect to the trajectories solutions.

From (A.1), it follows that, for all $k > 0$, there exists $0 < e^{-\alpha_k T} < e^{-\alpha T}$ such that:

$$V\big((k+1)T\big) = e^{-\alpha_k T} V\big(kT\big)$$

Let $\bar{k} > 0$ be any discrete-time instant. By defining

$$\bar{\Lambda} := \max_{1 \leq k \leq \bar{k}} e^{-\alpha_k T},$$

it follows that:

$$V(\bar{k}T) = \left(\prod_{k=1}^{\bar{k}} e^{-\alpha_k T} \right) V(0) \leq \bar{\Lambda}^{\bar{k}} V(0),$$

for any $k = 0, 1, \ldots, \bar{k}$. Thus, by letting $\bar{k} \to \infty$, since $\bar{\Lambda} < e^{-\alpha T}$, it follows from equation (A.1) that any closed-loop trajectory asymptotically converges to the origin with a speedy of convergence which is associated to the decay rate α. Furthermore, we also infer that the bigger is the α, the faster is the asymptotic convergence to the origin.

APPENDIX B – Petersen's Lemma

B.1 PETERSEN'S LEMMA

In order to cope with a norm-bounded term $\boldsymbol{\Delta(\tau_k)}$ in the LMIs, the following Lemma is used (PETERSEN, 1987).

Lemma B.1 *Let* $\boldsymbol{\Phi = \Phi' \in \Re^{n \times n}}$, $\boldsymbol{\Xi \neq 0 \in \Re^{n \times p}}$, $\boldsymbol{\Pi \neq 0 \in \Re^{q \times n}}$, *be matrices of appropriate dimensions. Then for all* $\boldsymbol{\Delta \in \Re^{p \times q}}$, $\boldsymbol{||\Delta|| \leq 1}$, *the inequality*

$$\boldsymbol{\Phi + \Xi\Delta\Pi + \Pi'\Delta'\Xi' \leq 0}$$

holds if and only if there exists $\boldsymbol{\sigma > 0}$ *such that*

$$\boldsymbol{\Phi + \sigma\Xi\Xi' + \sigma^{-1}\Pi'\Pi \leq 0.}$$

Proof *(KHLEBNIKOV; SHCHERBAKOV, 2008) Let the inequality*

$$\boldsymbol{\Phi + \Xi\Delta\Pi + \Pi'\Delta'\Xi' \leq 0}$$

hold for all $\boldsymbol{||\Delta|| \leq 1}$. *This is equivalent to*

$$\boldsymbol{x'\Phi x + 2x'\Xi\Delta\Pi x \leq 0}$$

for all $\boldsymbol{x \in \Re^n}$ *and all* $\boldsymbol{||\Delta|| \leq 1}$. *Denoting* $\boldsymbol{x'\Xi\Delta \doteq y'}$, *the inequality above is rewritten in the form*

$$\boldsymbol{x'\Phi x + 2y'\Pi x \leq 0}$$

for all $\boldsymbol{x \in \Re^n}$ *and* $\boldsymbol{y \in \Re^q}$ *such that*

$$\boldsymbol{y'y = x'\Xi\Delta\Delta'\Xi'x \leq x'\Xi\Xi'x.}$$

Introducing

$$\boldsymbol{z \doteq \begin{pmatrix} x \\ y \end{pmatrix} \in \Re^{n+q}, \quad A_0 \doteq \begin{pmatrix} \Phi & \Pi' \\ \Pi & 0 \end{pmatrix}, \quad A_1 \doteq \begin{pmatrix} -\Xi\Xi' & 0 \\ 0 & I \end{pmatrix}}$$

it is rewritten in the following matrix form: $\boldsymbol{z'A_0z \leq 0}$ *for all* $\boldsymbol{z}$ *such that* $\boldsymbol{z'A_1z \leq 0}$.

By applying the $\boldsymbol{S}$-*procedure with one constraint (e.g., see Boyd et al. (1994)), the fulfilment of this condition is equivalent to the existence*

of $\sigma \geq 0$ such that $A_0 \leq \sigma A_1$, i.e.,

$$\begin{pmatrix} \Phi + \sigma \Xi \Xi' & \Pi' \\ \Pi & -\sigma I \end{pmatrix} \leq 0.$$

Finally, applying the Schur lemma to this non-strict inequality, the equivalent condition is obtained

$$\Phi + \sigma \Xi \Xi' + \sigma^{-1} \Pi' \Pi \leq 0, \qquad \sigma \geq 0.$$

ANNEX A – Sampling Interval Assignment: A Cooperative Design Approach

A.1 SAMPLING INTERVAL ASSIGNMENT: A COOPERATIVE DESIGN APPROACH

The work presented in this annex was carried over the internship at Centre de Recherche en Automatique de Nancy (CRAN) - Nancy, France - under co-supervision of Dr. Marc Jungers, formal researcher at CRAN, and published in the Proceedings of the 53rd IEEE Conference on Decision and Control (MORAES et al., 2014).

A set of non preemptive controller tasks is assumed, running on a limited computational resource platform. The objective is to regularly re-assign new sampling intervals to the tasks, based on their desirable closed-loop performance while also preserving schedulability of the resource. Linear-quadratic controllers are used, resulting on cost functions and feedback gains that depend on the sampling interval. A multi-objective optimization problem subjected to a resource constraint is formulated to cope with this issue.

The global objective function is chosen as a weighted sum of all plants performances, translating the multi-objective optimization problem into a single-objective one, which provides an additional degree of freedom and leads to a set of solutions denoted as Pareto efficient. To handle this additional weight vector variable, we assume a Nash bargaining cooperative game.

An upper level task performs the computation and update of the sampling intervals and input signals, to be used on a finite-horizon control strategy. A numerical example is provided to illustrate the approach.

A.2 INTRODUCTION

Controllers implemented over computing platforms are more and more common nowadays. In this kind of systems, the computational resource is usually limited and shared among several control tasks. Therefore, it might be desirable to combine some characteristics of control theory and real-time scheduling theory, the so-called co-design, providing an appropriate performance level for each loop.

In this matter, two issues of interest are often investigated in the literature (SALA et al., 2010): *i)* Given a performance level requirement, obtain the lowest level of resource utilization needed; *ii)* Given an allowable resource utilization level, obtain the best possible control performance level.

Some interesting approaches in the first one are the event-triggered and self-triggered methods, in which a triggering mechanism determines when the control input has to be updated (HEEMELS; JOHANSSON; TABUADA, 2012), and consequently the use of the shared resource.

This work investigates the second issue. In this context, Seto et al. (1996) present a study about the performance optimization for a set of tasks under resource constraints. They consider an off-line approach and a performance index approximated by an exponential function for each loop. Later, their work has been improved into an online approach (EKER; HAGANDER; ÅRZÉN, 2000), where each loop performance was described approximating an LQ-cost as a quadratic function of the sampling interval, but without taking into account the current plant states.

Online sampling interval assignment is also analyzed in Henriksson & Cervin (2005), where the solution is obtained by solving an optimization problem regarding the expected future performance of the control loops, taking into account the current states values and the expected noise. By using this strategy, resources can be accordingly distributed with respect to the system performance. Furthermore, in Cervin et al. (2011), an algorithm that approximates the solution at run-time, based on a set of possible sampling intervals, for the generic case of convex cost functions on the sampling interval, is presented.

As in (HENRIKSSON; CERVIN, 2005; CERVIN et al., 2011), in the present work, a system where a set of non preemptive control tasks share one processor with limited computational resources is considered, and an online adjustment of the sampling intervals is possible. Although previous works present solutions for this co-design problem, they do not allow the designer to provide more information about how the resource might be distributed among the control loops. Thereby, here the results already presented in the literature are generalized by using a vector of weighting parameters, providing an additional degree of freedom to the assignment of the sampling interval.

The overall problem is actually a multi-criteria minimization problem, since it aims to find the control signal and the sampling interval for each control loop that results in a suitable performance of the entire system. Nevertheless, it is possible to solve it in two steps. First for the control design, based on a quadratic cost function used for each system, and dependent on the sampling interval. Later allowing the sampling intervals to be re-assigned based on the considered performance requirement, subject to a resource allocation constraint.

The performance of each plant is captured in a finite-time hori-

zon quadratic cost function, that should be minimized and takes into account the sampling interval and the current state of the plant. Nevertheless, the global minimization of all performance indicators is usually not possible, and characterizes a multi-objective optimization problem. Thus, in order to obtain a single-objective optimization problem, the global objective function is translated into a weighted sum of the control-loops performances, which leads to a Pareto efficient solution, requiring a decision maker in order to choose a single suitable solution among all possible ones from the optimal set. In the approach presented here, despite the possibility that the weights may be chosen arbitrarily, an iterative procedure issued from a Nash bargaining game is considered. Therefore, an additional task is performed, that may update the sampling interval of the control loops.

A.3 PROBLEM FORMULATION

Consider a real-time system running $\boldsymbol{p}$ controller tasks that share a computing resource, the Central Processing Unit (CPU), and where each task is responsible for sampling, control computation and actuation of a plant. The plants dynamics are given by:

$$\dot{\boldsymbol{x}}_i(\boldsymbol{\tau}) = \boldsymbol{A}_i \boldsymbol{x}_i(\boldsymbol{\tau}) + \boldsymbol{B}_i \boldsymbol{u}_i(\boldsymbol{\tau}) + \boldsymbol{w}_{c,i}(\boldsymbol{\tau}), \ \forall i = 1, \ldots, p \quad \text{(A.1)}$$

where $\boldsymbol{x}_i(\boldsymbol{\tau}) \in \Re^{n_i}$ are the plant state vectors, $\boldsymbol{u}_i(\boldsymbol{\tau}) \in \Re^{m_i}$ are the control signal vectors, $\boldsymbol{A}_i \in \Re^{n_i \times n_i}$ are the dynamic matrices, $\boldsymbol{B}_i \in \Re^{n_i \times m_i}$ are the input matrices, and $\boldsymbol{w}_{c,i}(\boldsymbol{\tau})$ are white noises with incremental variances $\boldsymbol{R}_{c,i}$. Also, assume that the initial state conditions are known and equal to $\boldsymbol{x}_i(\boldsymbol{0}) = \boldsymbol{x}_{0i}$.

The control design is formulated as solving an optimization problem, where the cost function to minimize is the expression of a compromise between several requirements (stability or more precisely remaining in the vicinity of the origin, minimizing the energy of the state and of the control input, in the presence of noise). Thus, the cost function is chosen to be a finite-time horizon quadratic one, defined as:

$$\begin{aligned} \boldsymbol{J}_i(\boldsymbol{x}_{0i}, \boldsymbol{u}_i) = \mathrm{E}\bigg\{ & \int_{\boldsymbol{0}}^{\boldsymbol{T}_{RM}} (\boldsymbol{x}'_i(\boldsymbol{\tau}) \boldsymbol{Q}_{1c,i} \boldsymbol{x}_i(\boldsymbol{\tau}) + 2\boldsymbol{x}'_i(\boldsymbol{\tau}) \boldsymbol{Q}_{12c,i} \boldsymbol{u}_i(\boldsymbol{\tau}) \\ & + \boldsymbol{u}'_i(\boldsymbol{\tau}) \boldsymbol{Q}_{2c,i} \boldsymbol{u}_i(\boldsymbol{\tau})) \mathrm{d}\boldsymbol{\tau} + \boldsymbol{x}'_i(\boldsymbol{T}_{RM}) \boldsymbol{Q}_{0,i} \boldsymbol{x}_i(\boldsymbol{T}_{RM}) \bigg\} \quad \text{(A.2)} \end{aligned}$$

where E{.} stands for the mathematical expectation due to the noise variable. The weighting matrices $\begin{bmatrix} Q_{1c,i} & Q_{12c,i} \\ Q'_{12c,i} & Q_{2c,i} \end{bmatrix} > 0$ and $Q_{0,i} > 0$ are design parameters, with the last one related to the importance given to the final states of the plant, with respect to the considered finite-time horizon, T_{RM}.

The controller tasks behave as digital controllers. Thus, sampling the continuous-time plants (A.1) with intervals T_i, gives the discrete-time systems:

$$x_{i,t+1} = \Phi_i(T_i)x_{i,t} + \Gamma_i(T_i)u_{i,t} + w_{i,t}, \tag{A.3}$$

with $\Phi_i(T_i) = e^{A_i T_i}$, $\Gamma_i(T_i) = \int_0^{T_i} e^{A_i s} B_i \mathrm{d}s$, and also $R_i(T_i) = \mathrm{E}\{w_{i,t}w'_{i,t}\} = \int_0^{T_i} \Phi'_i(s) R_{c,i} \Phi_i(s) \mathrm{d}s$.

Assuming that T_{RM} is a multiple of the sampling intervals, and consequently $N_i = \frac{T_{RM}}{T_i}$ are integers, the sampled version of the cost functions (A.2) are then given by (CERVIN et al., 2011):

$$J_i(x_{0i}, u_i, T_i) = \mathrm{E}\Bigg\{ \sum_{t=0}^{N_i-1} (x'_{i,t}Q_{1,i}(T_i)x_{i,t} + 2x'_{i,t}Q_{12,i}(T_i)u_{i,t}$$

$$+ u'_{i,t}Q_{2,i}(T_i)u_{i,t} + R_{w,i}(T_i)) + x'_{i,N}Q_{0,i}x_{i,N} \Bigg\}, \tag{A.4}$$

with weighting matrices

$$Q_{1,i}(T_i) = \int_0^{T_i} \Phi'_i(s)Q_{1c,i}\Phi_i(s)\mathrm{d}s,$$

$$Q_{12,i}(T_i) = \int_0^{T_i} \Phi'_i(s)(Q_{1c,i}\Gamma_i(s) + Q_{12c,i})\mathrm{d}s,$$

$$Q_{2,i}(T_i) = \int_0^{T_i} (\Gamma'_i(s)Q_{1c,i}\Gamma_i(s) + 2\Gamma'_i Q_{12c,i} + Q_{2c,i})\mathrm{d}s,$$

and $R_{w,i}(T_i) = \mathrm{tr}\Big(Q_{1c,i}\int_0^{T_i} R_i(s)\mathrm{d}s\Big)$ additional cost terms due to the inter-sample noise (ÅSTRÖM, 1970), where $\mathrm{tr}(\cdot)$ stands for the trace of a matrix.

As previously stated, all controller tasks share the same computational resource, thus a schedulability test has to be performed in order to guarantee that all deadlines will be respected. To meet this goal, the

following properties for each task are assumed: the worst case execution time is given by c_i; the period is equal to the sampling interval, as well as the relative deadline; and the task utilization level is given by $U_i = \frac{c_i}{T_i}$.

Hence, considering a deadline monotonic strategy and based on the utilization of the shared resource, the schedulability of the task set can be guaranteed if:

$$\sum_{j=1}^{p} \frac{c_j}{T_j} \leq U_{sp}, \tag{A.5}$$

where U_{sp} is the overall available utilization level.

In the sequel, the problem of a dynamic sampling interval assignment is considered, which can be performed online by a supervisor task, namely Resource Manager (RM). The RM computations take into account the plants individual performances, as well as the sharing resource constraint. Furthermore, the supervisor is assumed to have the knowledge of each player's dynamics and cost functions.

A.4 BASIC CONCEPTS

A.4.1 Pareto efficiency and the bargaining game

To deal with the situation where there are more than one controller task, that we may call players, running on the same processor, due to the shared resource, a policy used to minimize the cost function from one player, may have a negative effect on another player's performance. Thus, a multi-objective optimization procedure must be taken in account.

Let $J(T) = [J_1(T_1), \ldots, J_p(T_p)]'$ be a vector with all p cost functions, and $T = [T_1, \ldots, T_p]'$, a vector with the sampling intervals. Due to the presence of multiple cost functions, it is not possible to define an optimal solution. It is required to consider compromises and equilibria, which can be determined thanks to game theory (ENGWERDA, 2005).

Among several possibilities, the notion of Pareto efficiency is considered here. A solution point is Pareto efficient if it is not possible to move from that point and improve at least one objective function without detriment to any other objective function. That is, a point T^* is Pareto efficient if and only if there does not exist any other point, T, such that $J(T) \leq J(T^*)$, and $J_i(T) < J_i(T^*)$ for at least one

function.

Generally, there is not a unique Pareto efficient point T^*. The outcome $(J_1(T_1^*), \ldots, J_p(T_p^*))$ associated with a Pareto efficient point T^* is called the Pareto payoff. The set of all Pareto payoffs defines the Pareto frontier, which is depicted in the criteria space and is denoted as the P_f curve in the sequel and in Fig A.1.

Let define the simplex $\mathcal{B} = \{\beta = [\beta_1, \ldots, \beta_p] \mid \beta_i \geq 0$ and $\sum_{i=1}^{p} \beta_i = 1\}$. For any $\beta \in \mathcal{B}$, $T^* \in \arg\min_T \sum_{i=1}^{p} \beta_i J_i(T)$ is Pareto efficient. The reciprocal is true only if the cost functions $J_i(T)$ are convex with respect to T. That is, when $J_i(T)$ are convex, if T^* is Pareto efficient, there exists $\beta^* \in \mathcal{B}$ such that $T^* \in \arg\min_T \sum_{i=1}^{p} \beta_i J_i(T)$. In the convex case, the latter implication is an elegant way to parameterize the Pareto frontier. Thereby, the Pareto frontier translates the multi-objective optimization problem into a single-objective one, by using a parameterized objective function.

A.4.2 Nash bargaining game

It is important to note that, for applications, it is often necessary to incorporate some decision rule in order to determine a single suitable Pareto efficient point to be used. This means that from each player's set of possible outcomes, only one has to be cooperatively chosen. The question is which outcome might the players possibly cooperatively choose. This dealing is carried out by a decision making process (MIETTINEN, 2001). More specifically, in this work a Nash bargaining game approach is considered.

The Nash bargaining rule deals with the idea in which players, through cooperation, can achieve better outcomes than the one which becomes effective when they do not cooperate. The non-cooperative outcome is called disagreement point, and it is given by the point $d(d_1, \ldots, d_p)$.

In Fig. A.1, a sketch of a typical Nash bargaining for a two players game is depicted. The curve P_f is the set of Pareto efficient outcomes of the game (Pareto frontier), the point d is the disagreement point, and the point N_b corresponds to the obtained solution. The asymptotes are related to the utopia point, i.e., when there is a $\beta_i = 1$, while $\beta_j = 0, \forall j \neq i$.

The Nash bargaining rule chooses the point on P_f that maximizes the product of the players gains from disagreement point d. That is,

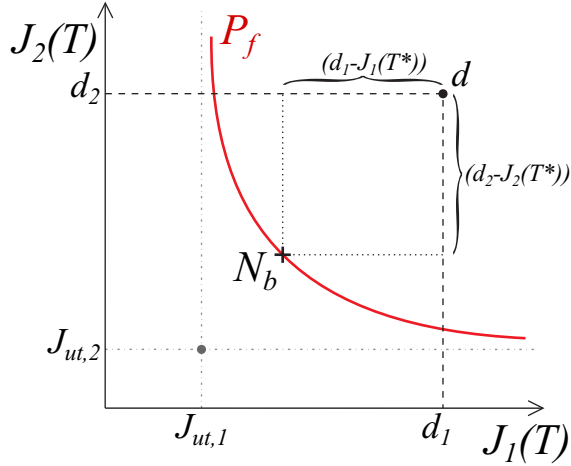Figure A.1 – Nash bargaining solution, two players game.

for $J(T) \in P_f$ with $J_i(T) \leq d_i$:

$$N_b = \arg \max_{J(T) \in P_f} \prod_{i=1}^{p} (d_i - J_i(T)). \qquad (A.6)$$

Under the assumption that all cost functions $J_i(T)$ are convex, and since the solution N_b is also located on the Pareto frontier, for some N_b there is also a $\beta^{N_b} \in \mathcal{B}$, and it is given by (ENGWERDA, 2005):

$$\beta_1^{N_b}(d_1 - J_1^{N_b}) = \cdots = \beta_p^{N_b}(d_p - J_p^{N_b}) \qquad (A.7)$$

or equivalently

$$\beta_i^{N_b} = \frac{\prod_{j \neq i}(d_j - J_j^{N_b})}{\sum_{j=1}^{p} \prod_{\ell \neq j}(d_\ell - J_\ell^{N_b})}, \quad i = 1, \ldots, p. \qquad (A.8)$$

As an important remark, notice that the selection of the disagreement point d, depending on the problem to be dealt with, may not be a trivial task. A possible choice might be using, for each d_i, the upper limit for the respective cost function $J_i(T)$, given by physical, operational or even design constraints.

A.5 SAMPLING INTERVAL ASSIGNMENT

Now, associating the schedulability constraint (A.5) to a weighted sum of the performance requirements (A.4), with respect to a k-th instant, gives:

$$\min_{\substack{u_1,\ldots,u_p \\ T_1,\ldots,T_p}} \sum_{i=1}^{p} \beta_i J_i(x_{k,i}, u_i, T_i) \quad \text{s.t.} \sum_{j=1}^{p} \frac{c_j}{T_j} \leq U_{sp}, \qquad \text{(A.9)}$$

where $\sum_{i=1}^{p} \beta_i = 1$, $\beta_i \geq 0$, $i = 1, \ldots, p$, are the weighting parameters.

In the following, this problem is first solved in terms of the control vectors u_i, following by an approach to determine the sampling intervals to be used for each task. The parameters β_i are used to weight the plants performance, and are computed by an iterative algorithm based on a Nash bargaining approach.

A.5.1 Finite-horizon linear quadratic controller

The control law to be used for each plant i is actually dependent only on the i-th plant dynamics. This is solved by computing the finite-horizon linear quadratic controller independently for each plant, as a function of its own sampling interval. Thus, the minimum cost function, for each system, is obtained:

$$J_i^*(x_{i,k}, T_i) = \min_{u_i} \ J_i(x_{i,k}, u_i, T_i),$$

that leads to

$$J_i^*(x_{i,k}, T_i) = x_{i,k}' S_{0,i}(T_i) x_{i,k} + q_{0,i}(T_i), \qquad \text{(A.10)}$$

which is a quadratic function in the current state vector $x_{i,k}$. The positive semidefinite weighting matrix $S_{0,i}(T_i)$ and the additional scalar term due to the disturbances, $q_{0i}(T_i) \geq 0$, are both given by backward induction, from where we have, for each instant $t = 0, \ldots, N_i - 1$:

$$\begin{aligned}
S_{t,i}(T_i) = {} & \Phi_i'(T_i) S_{t+1,i}(T_i) \Phi_i(T_i) + Q_{1,i}(T_i) \\
& - \left(\Phi_i'(T_i) S_{t+1,i}(T_i) \Gamma_i(T_i) + Q_{12,i}(T_i) \right) \\
& \times \left(\Gamma_i'(T_i) S_{t+1,i}(T_i) \Gamma_i(T_i) + Q_{2,i}(T_i) \right)^{-1} \\
& \times \left(\Gamma_i'(T_i) S_{t+1,i}(T_i) \Phi_i(T) + Q_{12,i}'(T_i) \right)
\end{aligned}$$

and

$$q_{t,i}(T_i) = \mathrm{tr}\big(S_{t+1,i}(T_i)R_i(T_i)\big) + R_{w,i}(T_i) + q_{t+1,i}(T_i).$$

The cost function at $t = N_i$, is assumed to be given by

$$J_i^*(x_{i,N_i}) = x_{i,N_i}' S_{N_i,i} x_{i,N_i},$$

with $q_{N_i,i} = 0$ and $S_{N_i,i} = Q_{0,i}$. Furthermore, as $\Phi_i(T_i)$, $\Gamma_i(T_i)$, $Q_{1,i}(T_i)$, $Q_{12,i}(T_i)$ and $Q_{2,i}(T_i)$ depend on the sampling interval T_i, this implies a solution $S_{0,i}(T_i)$ that also depends on the sampling interval.

Finally, the obtained controller is time-varying, and depends on both, the sampling interval and the state of the plant, and is given by

$$u_{i,t} = -\big(\Gamma_i'(T_i)S_{t+1,i}(T_i)\Gamma_i(T_i) + Q_{2,i}(T_i)\big)^{-1}$$
$$\times \big(\Gamma_i'(T_i)S_{t+1,i}(T_i)\Phi_i(T_i) + Q_{12,i}'(T_i)\big)x_{i,t}$$
$$u_{i,t} = K_{i,t}(T_i)x_{i,t}$$

A.5.2 Resource allocation

Notice that the objective in (A.9) has become the minimization of a weighted sum of the cost functions (A.10):

$$\min_{T_1,\ldots,T_p} \sum_{i=1}^{p} \beta_i J_i^*(x_{k,i}, T_i) \quad \text{s.t.} \sum_{j=1}^{p} \frac{c_j}{T_j} \leq U_{sp}. \tag{A.11}$$

The optimization problem (A.11) is convex thanks to the convexity of the cost functions J_i. Moreover, if the cost functions can be described in the form

$$J_i^*(x_{k,i}, T_i) = \alpha_i + \gamma_i T_i, \tag{A.12}$$

with γ_i, $T_i > 0$, $i = 1, \ldots, p$, then it is possible to find an explicit solution for the optimization problem (A.11).

In general, however, the cost functions are not always described as (A.12). Nevertheless, it is possible to approximate the cost functions by linearizing them around the current sampling intervals, T_i^0. Then, it is possible to solve (A.11) iteratively as follows.

First, let the cost functions, $g_i(T_i) = J_i^*(x_{k,i}, T_i)$, be decom-

posed into a first order approximation:

$$g_i(T_i) = g_i(T_i^0) + \dot{g}_i(T_i^0)(T_i - T_i^0) + \theta_i \qquad \text{(A.13)}$$

where $\dot{g}_i$ is the first order derivative of g_i with respect to the current sampling interval T_i^0, and θ_i corresponds to a remainder.

Note that if the plants are sampled reasonably fast, the term θ_i might be small enough, and thus it can be neglected. Thereby, assuming a limited development for the equation (A.13), the cost functions (A.10) can be approximated by affine functions of T_i:

$$J_i^*(x_{k,i}, T_i) \approx \alpha_i + \gamma_i T_i. \qquad \text{(A.14)}$$

Also, as stated in (CERVIN et al., 2002), the constant α_i can be disregarded, since it is sufficient to estimate the slope of the cost functions. Thereby:

$$\gamma_i = \dot{g}_i(T_i^0) = x_{k,i}' \frac{\partial S_{0,i}(T_i^0)}{\partial T_i} x_{k,i} + \frac{\partial q_{0,i}(T_i^0)}{\partial T_i}. \qquad \text{(A.15)}$$

Second, new sampling intervals are computed using the affine functions (A.14), to find a solution to the optimization problem (A.11). For ease of notation, consider a vector $T = [T_1, \ldots, T_p]'$ and functions $J_\beta(T) = \sum_{i=1}^p \beta_i J_i^*(x_{k,i}, T_i)$ and $f(T) = \sum_{j=1}^p \frac{c_j}{T_j} - U_{sp}$. Hence, the optimization problem (A.11) can be rewritten as

$$\min_T J_\beta(T) \quad \text{s.t. } f(T) \leq 0. \qquad \text{(A.16)}$$

Since (A.16) is a constrained optimization problem, applying Karush-Kuhn-Tucker conditions (KUHN; TUCKER, 1951) leads to the equivalent unconstrained problem:

$$\min_T \quad J_\beta(T) + \lambda f(T), \qquad \text{(A.17)}$$

where the scalar $\lambda \geq 0$ is the Lagrangian multiplier. Then, supposing a T^* that minimizes (A.17):

$$\nabla J_\beta(T^*) + \lambda \nabla f(T^*) = 0, \qquad \text{(A.18)}$$

which after some manipulations gives, for $i = 1, \ldots, p$:

$$T_i^* = \sqrt{\frac{c_i}{\beta_i \gamma_i}} \sum_{j=1}^p \frac{\sqrt{c_j \beta_j \gamma_j}}{U_{sp}}. \tag{A.19}$$

Finally, these two steps may be repeated to improve the solution. Observe that the involved derivatives must be computed off-line and stored in the memory.

A.5.3 Nash bargaining algorithm

Here, an algorithm to compute the N_b-solution is briefly outlined. As often occurs in applications, the Pareto frontier can be very flat and the solution of this kind of problem is not straight-forward, even if there is a convex surface. However, the existence of relations (A.8) facilitates the approach. Thus, the following steps may be used for an iterative computation of the weighting parameters:

Step 0 Set tuning parameters Δ, δ_1, $\delta_2 \in (0, 1)$ and $\epsilon > 0$.

Step 1 Set the disagreement point $d(d_1, \ldots, d_p)$.

Step 2 Set initial weighting parameters β_i^0, $i = 1, \ldots, p$, such that $\sum_{i=1}^p \beta_i = 1$. For example, $\beta_i^0 = \frac{1}{p}$.

Step 3 Compute $T_i(\beta_i^0)$.

Step 4 Verify wether $J_i(T_i(\beta_i^0)) \leq d_i$, $i = 1, \ldots, p$. If not, then there is an l for which $J_l(T_l(\beta_l^0)) > d_l$. In that case update $\beta_l^0 := \beta_l^0 + \Delta$, $\beta_i^0 := \beta_i^0 - \frac{\Delta}{p-1}$, for $i \neq l$ and return to Step 3.

Step 5 For $i = 1, \ldots, n$, compute

$$\tilde{\beta}_i = \frac{\prod_{j \neq i}(d_j - J_j(T_j(\beta_j^0)))}{\sum_{j=1}^p \prod_{\ell \neq j}(d_\ell - J_\ell(T_\ell(\beta_\ell^0)))}.$$

Step 6 If $|\tilde{\beta}_i - \beta_i^0| < \epsilon$, $i = 1, \ldots, p$, then finish the algorithm and set $\beta_i^* = \tilde{\beta}_i$. Else $\beta_i^0 := \delta_1 \beta_i^0 + \delta_2 \tilde{\beta}_i$, and return to Step 3.

The tuning parameters used in the previous steps may be, to a certain level, chosen arbitrarily. In *Step 4*, Δ corresponds to an updating parameter used in case of failure of the condition described in

the referred step. In *Step 6*, ϵ is used as a precision parameter between two consecutive iterations. Also in *Step 6*, the updating parameters $\boldsymbol{\delta_1}$ and $\boldsymbol{\delta_2}$ must be chosen in order to prevent too large steps in the update process, which might result in values β_i^0 for which the inequalities $J_i(T_i(\beta_i^0)) \leq d_i$ are no longer satisfied. Furthermore, this algorithm shows to have a fast convergence, as suggested in (ENGWERDA, 2005) and also verified in our simulation experiments.

A.5.4 Online resource management

Based on the proceedings previously described, a general procedure for the online sampling interval computation may be stated, as follows.

a) Plant states $\boldsymbol{x_i(\tau)}$ are sampled every $\boldsymbol{T_{RM}}$, and then used as initial conditions $\boldsymbol{x_{k,i}}$ for the current finite-time horizon.

b) The values of $\boldsymbol{\gamma_i}$ (A.15) are updated using the current states $\boldsymbol{x_{k,i}}$ and sampling intervals $\boldsymbol{T_i^0}$.

c) Decision making takes place to find weighting parameters $\boldsymbol{\beta_i}$.

d) New sampling intervals to be applied to each plant are computed from (A.19).

e) The new sampling intervals are updated over the controller task set.

Note that this procedure may be repeated from Step b to Step d to improve the results.

A.6 EXAMPLE

To illustrate the approach, in this section an example comprised of two cruise control systems is used. A discussion about the obtained results with respect to the choice of disagreement point is provided.

The purpose of the cruise control system is to maintain constant the vehicle speed despite external disturbances. Thus, for this example, a simplified first order model of a vehicle dynamics is considered:

$$\dot{x}_i(\tau) = \dot{v}_i(\tau) = \frac{-5}{100}v_i(\tau) + \frac{1}{1000}u_i(\tau) + w_i(\tau),$$

with $\boldsymbol{w_i(\tau)}$ a white noises with incremental variance $\boldsymbol{R_{ci} = 1}$.

Table A.1 – Sampling interval sequence for $d_1 = d_2 = 3.5 \times 10^4$.

	plant **1**	plant **2**
$k_0, (0.0s)$	$\beta_1 = 0.3615, T_1 = 0.4100$	$\beta_2 = 0.6385, T_2 = 0.1711$
$k_1, (1.5s)$	$\beta_1 = 0.5004, T_1 = 0.2405$	$\beta_2 = 0.4996, T_2 = 0.2423$
$k_2, (3.0s)$	$\beta_1 = 0.5196, T_1 = 0.2116$	$\beta_2 = 0.4804, T_2 = 0.2811$
$k_3, (4.5s)$	$\beta_1 = 0.5001, T_1 = 0.2411$	$\beta_2 = 0.4999, T_2 = 0.2417$

Sampling the plants with intervals T_i leads to the discrete-time systems:

$$v_i(t+1) = e^{\frac{-T_i}{20}} v_i(t) + \frac{1}{50}\left(1 - e^{\frac{-T_i}{20}}\right) u_i(t) + w_i(t).$$

For further analysis, different initial condition for each plant, $x_1(0) = 2.7$ and $x_2(0) = -10$, are assumed.

The RM runs once every $1.5s$ (at the instants $k_r = rT_{RM}$), for simplicity, on a dedicated processor unit. We assume $c_i = 0.1s$ for both control tasks. Furthermore, we consider a rate monotonic scheduling algorithm, which gives an available utilization level $U_{sp} = 2(2^{\frac{1}{2}} - 1) \approx 0.828$ (LIU; LAYLAND, 1973).

The linear quadratic controllers are designed with $Q_{1ci} = 10^4$, $Q_{12ci} = 0$, $Q_{2ci} = 10^{-4}$ and $Q_{0i} = Q_1(T_i)$ as weighting matrices for the cost functions. Note that Q_{0i} is chosen in order to keep constant the quadratic relation of the plant state, for each system i, throughout the finite-time horizon cost function (A.4).

The *overall iterative process* described in Section A.5.4 is considered, which converges independently of the initial guess used for T_i. As a matter of clarification, in the first run, the algorithm is started using an equal distribution of the computational resource ($T_i^0 = 0.2414$), and for the subsequent ones the current value of the sampling intervals are used. The simulations are performed using the toolbox TrueTime (CERVIN et al., 2003b).

As specified in the procedure presented in Section A.5.3, the Nash bargaining strategy requires the designer to set a disagreement point d. In the case hare, it is arbitrarily chosen as $d_1 = d_2 = 3.5 \times 10^4$, which has lead to the weighting parameters and sampling intervals shown in Table A.1. The corresponding Pareto frontiers and Nash bargaining solutions are shown in Fig. A.2, and the plants outputs in Fig. A.3.

At the beginning of the simulation, as there is a larger difference

between both plant outputs, the solution found through the sampling interval assignment procedure gives a relative preference to the system that is farther from the equilibrium point. On the second RM run, as both system trajectories are close to their respective equilibrium, the solution of the bargaining tends to an equal distribution of the shared resource. At $k_2 = 3.0s$, like in the first run, there is again one system output that is farther from equilibrium than the other one, thus the resource manager accordingly assigns new sampling intervals to deal with the disturbance.
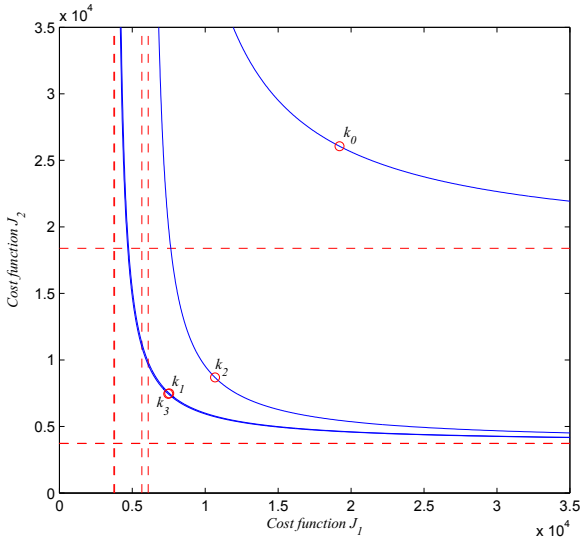

Figure A.2 – Pareto frontiers and Nash bargaining solution.

A.6.1 On the choice of the disagreement point

As an alternative to a fixed disagreement point as used before, two alternatives to dynamically compute the point $\boldsymbol{d}$ at each RM run are investigated. The first one uses *disagreement weights* $\underline{\beta}_i$, that lead to $\boldsymbol{d}_i(\underline{\beta}_i) = \boldsymbol{J}_i(\boldsymbol{T}_i(\underline{\beta}_i))$. Notice that these *disagreement weights* do not belong to a simplex, actually $\sum_{i=1}^{p} \underline{\beta}_i < 1$. The second one uses *disagreement sampling intervals* $\bar{\boldsymbol{T}}_i$, that lead to $\boldsymbol{d}_i(\bar{\boldsymbol{T}}_i) = \boldsymbol{J}_i(\bar{\boldsymbol{T}}_i)$. Both choices ensure that $\boldsymbol{d}$ is computed as a *dynamic disagreement cost*. The simulation conditions are the same as used previously.
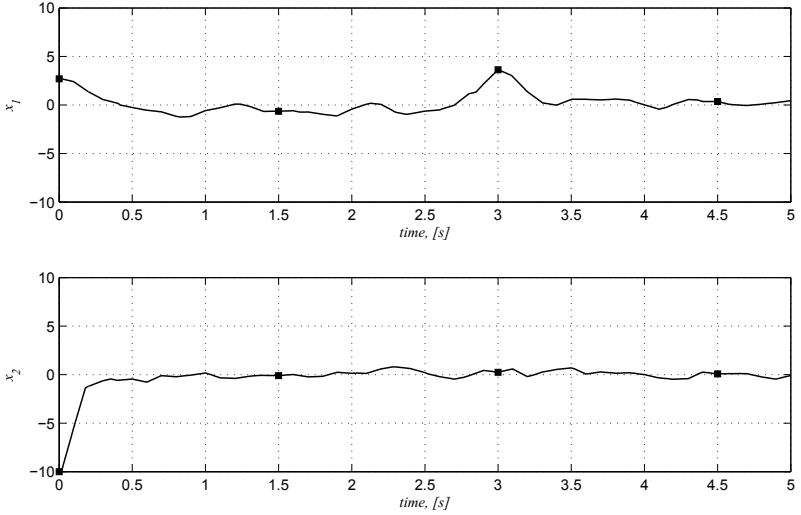
Figure A.3 – System trajectories.

Table A.2 – Agreements based on *disagreement weights*.

	plant **1**	plant **2**
$k_0, (0.0s)$	$d_1 = 5.1340 \times 10^4$ $\beta_1 = 0.5000,\ T_1 = 0.3462$	$d_2 = 6.5325 \times 10^4$ $\beta_2 = 0.5000,\ T_2 = 0.1853$
$k_1, (1.5s)$	$d_1 = 2.0056 \times 10^4$ $\beta_1 = 0.5000,\ T_1 = 0.2410$	$d_2 = 2.0028 \times 10^4$ $\beta_2 = 0.5000,\ T_2 = 0.2419$
$k_2, (3.0s)$	$d_1 = 2.5348 \times 10^4$ $\beta_1 = 0.5000,\ T_1 = 0.2170$	$d_2 = 2.3291 \times 10^4$ $\beta_2 = 0.5000,\ T_2 = 0.2720$
$k_3, (4.5s)$	$d_1 = 2.0016 \times 10^4$ $\beta_1 = 0.5000,\ T_1 = 0.2417$	$d_2 = 0.2411 \times 10^4$ $\beta_2 = 0.5000,\ T_2 = 0.2411$

Consider *disagreement weights* $\beta_i = \mathbf{0.05}$, equal for both plants. This guarantees that there exist $\boldsymbol{J_i(\bar{T}) \leq d_i(\beta_i)}$. The results obtained through the simulation are shown in Table A.2. Notice that using this strategy the weighting parameters are constantly chosen as $\boldsymbol{\beta_1 = \beta_2}$, which is similar to the choice in (HENRIKSSON; CERVIN, 2005).

Consider now *disagreement sampling intervals* $\bar{\boldsymbol{T}}_{\boldsymbol{i}} = \mathbf{1.5s}$, again equal for both plants. The obtained weighting parameters and sampling intervals are shown in Table A.3. In this case, an equal distribution of the available computational resource is obtained for all runs of the RM,

Table A.3 – Agreements based on *disagreement sampling intervals*.

	plant **1**	plant **2**
$k_0, (0.0s)$	$d_1 = 0.6400 \times 10^5$ $\beta_1 = 0.8196, T_1 = 0.2414$	$d_2 = 2.9075 \times 10^5$ $\beta_2 = 0.1804, T_2 = 0.2414$
$k_1, (1.5s)$	$d_1 = 4.7089 \times 10^4$ $\beta_1 = 0.4952, T_1 = 0.2414$	$d_2 = 4.6195 \times 10^4$ $\beta_2 = 0.5048, T_2 = 0.2414$
$k_2, (3.0s)$	$d_1 = 7.4926 \times 10^4$ $\beta_1 = 0.3814, T_1 = 0.2414$	$d_2 = 4.6207 \times 10^4$ $\beta_2 = 0.6186, T_2 = 0.2414$
$k_3, (4.5s)$	$d_1 = 4.6664 \times 10^4$ $\beta_1 = 0.4972, T_1 = 0.2414$	$d_2 = 4.6214 \times 10^4$ $\beta_2 = 0.5028, T_2 = 0.2414$

independently of the current trajectories of the plants.

A.7 DISCUSSION

The online dynamic sampling interval assignment problem, where a set of control tasks runs on the same processor, has been studied. A global weighted cost function was used, providing an additional degree of freedom. Although the weights may be not trivial to define, when accordingly used they can lead to an overall performance that also takes into account a suitable individual performance for each system. In order to obtain a single Pareto efficient solution, a strategy issued from a Nash bargaining game was presented, making use of an iterative procedure. An example has been proposed to illustrate the approach.